Influence of micro-site conditions and environmental gradients on tree-ring based climate reconstructions

Dissertation

zur Erlangung des Grades

"Doktor der Naturwissenschaften"

im Promotionsfach Geographie

am Fachbereich Chemie, Pharmazie und Geowissenschaften

der Johannes Gutenberg-Universität

in Mainz

Elisabeth Düthorn

geb. in Erlangen

Mainz, den 28. September 2015

Mündliche Prüfung

01.12.2015

Für meine Brüder

Summary

Tree-ring chronologies are a powerful natural archive to reconstruct summer temperature variations of the late Holocene with an annual resolution. To develop these long-term proxy records tree-ring series are commonly extended back in time by combining samples from living trees with relict dead material preserved onshore or in lakes. Former studies showed that low frequency variations in such reconstructions can be biased if the relict and recent material is from different origins. A detailed analysis of the influence of various ecological (micro-) habitats representing the recent part is required to estimate potential errors in temperature estimates.

A network analysis of twenty pine and two spruce sites scattered all over Fennoscandia and sampled after a specific micro-site sampling design addresses the question if trees growing at the lakeshore ("wet") are comparable to trees of a dryer micro-site several meters away in the inland ("dry"). Species and micro-site dependent growth dynamics and climate signals are evaluated for two tree-ring parameters: Maximum latewood density (MXD) series are more suitable to represent summer temperatures than ring-width data (TRW) even if both respond positive to summer temperatures. The correlation in the TRW network increases with 0.05 per degree latitude towards north. Micro-site chronologies respond differently to July temperatures with more positive correlations at the lakeshore site. Over 3500 samples show that growth differences between the micro-sites are most pronounced in the first 40 years of tree-growth although this divergence is less obvious in density data. Spatially close sites classified by a cluster analysis enable to spatialize micro-site effects. Two types of micro-site patterns are detected in the boreal forest: higher growth rates at the lakeshore site in the western part and faster juvenile growth at the inland site in Finland. External influences as temperature, precipitation and the carbon content of the soil are responsible for the west-east pattern. Due to the detrending method the long-term trend is affected if the material of the recent and relict part comes from different micro-sites. The application of collective detrending methods, that comprise absolute growth rates, can produce errors in climate reconstructions and results in an underestimation of past temperatures.

The appearance of micro-site effects is a wide-spread phenomenon that takes place all over Fennoscandia. Future research in this key region for dendroclimatology should take this issue into account. Especially the higher climate response at the lakeshore site is interesting to achieve smaller uncertainties when a tree-ring series is transformed to temperature anomalies. For new composite chronologies the main aim should be to minimize potential biases and this includes also micro-site effects.

Zusammenfassung

Jahrringchronologien sind ein einzigartiges natürliches Archiv. Mit ihrer Hilfe lassen sich Temperaturvariationen der letzten tausend Jahre rekonstruieren. Da Bäume eine begrenzte Lebenszeit haben, müssen die Chronologien von lebenden Bäumen mit Totholzproben verknüpft werden. Dadurch wird erreicht, einen möglichst langen Zeitraum abzudecken. Vorherige Studien zeigen, dass die Herkunft und die Vergleichbarkeit des Materials von großer Bedeutung sind. Um festzustellen, ob verschiedene ökologische Milieus eine Auswirkung auf Klimarekonstruktionen haben, bedarf es einer strukturierten und detaillierten Analyse rezenten Materials.

Eine Netzwerkanalyse von zwanzig Kiefern- und zwei Fichtenstandorten aus Fennoskandien soll feststellen, ob es einen eindeutigen Unterschied zwischen Bäumen am Seeufer („nass“) und Bäumen im Inland („trocken“) gibt. Diese kleinräumigen Unterscheidungen werden im Folgenden als „micro-sites“ definiert. Es wurde dazu ein eigens erstelltes Beprobungsschema angewandt, mit dem „micro-site“ und artspezifische Unterschiede im Wachstum und im Klimasignal abgeschätzt werden sollen. Es zeigt sich dabei, dass Chronologien, basierend auf maximaler Spätholzdichte (MXD), die vergangenen Sommertemperaturen besser repräsentieren als Jahrringbreitemessungen (TRW). Ein stetiger Anstieg des Korrelationskoeffizienten zwischen Jahringbreitedaten und Sommertemperaturen um 0,05 mit jedem Grad geographischer Breite unterstreicht die steigende Klimasensitivität der Bäume. Zudem weisen „nasse“ Standorte einen positiveren Zusammenhang mit Julitemperaturen auf als „trockene“. Die Auswertung von mehr als 3500 Proben zeigt, dass die Wachstumsunterschiede zwischen den „nassen“ und „trockenen“ Standorten sich auf die ersten 40 Jahre konzentrieren, bevor sich die Wachstumskurven wieder angleichen. Dieser Effekt ist stärker in TRW als in MXD Zeitreihen zu sehen. Auf Grundlage einer Clusteranalyse kristallisiert sich eine räumliche Aufteilung der „micro-site“ Effekte in Ost und West heraus. Im westlichen Teil des Netzwerkes wächst der nasse Standort besser; im östlichen Bereich sind stärkere Wachstumsraten am trockenen Standort zu beobachten. Verantwortlich für diese Gliederung in Ost und West sind die Verteilung von Temperatur und Niederschlag sowie der Kohlenstoffgehalt im Oberboden. Kollektive Standardisierungsmethoden, die die Wachstumsraten mit einbeziehen, können einen Fehler des Langzeittrends bewirken und somit zu einer Fehleinschätzung von vergangenen Temperaturvariationen führen. Dies tritt vornehmlich dann ein, wenn das rezente Material nicht mit dem alten Material vergleichbar ist und beide von unterschiedlichen ökologischen Standorten kommen.

Zusammenfassend lässt sich sagen, dass die herausgearbeiteten Wachstumsunterschiede von „micro-site“ Effekten weitverbreitet sind und einem eindeutigen Muster folgen. Folglich sollten sich zukünftige Studien dieser Effekte bewusst sein. Neben der ökologischen Vergleichbarkeit können zudem höhere Klimakorrelationen am Ufer erreicht werden. Die Beachtung von „micro-site“ Effekten trägt somit einen großen Teil dazu bei, den Fehler in aussagekräftigen Temperaturrekonstruktionen zu verringern.

Table of contents

Introduction

Climate reconstructions using tree-ring data

It is important to understand the climate of the past and its variations in order to interpret today's climate change and to predict future conditions (Morgan et al. 1994). However, most meteorological records do not even cover the 20th century and there are almost no systematic weather observations before the 19th century. The full range of climate variability and the estimation of recent day´s warming compared to warm periods in the past cannot be assessed by instrumental records. But as many environmental processes depend strongly on the predominant climate it is possible to use proxy archives to reconstruct the climate of the past beyond this time. In this manner millennial long records of past climate originate from several paleoclimatic proxies. The information of past climate variability could be stored in ice cores, marine sediments, loess, speleothems, lake sediments, pollen, corals, tree-rings and historical documents (Bradley 1999).

A very important terrestrial archive are trees as they provide annually resolved information of the late Holocene (Fritts 1976). Even if the mean ring width is a function of many variables, e.g. tree age, site aspects, nutrients, soil and climate, in some regions climate is known to be the main controlling factor for tree growth independent of time and space (Speer 2010). Tree-rings display variations of precipitation (e.g. Trouet et al. 2009, Tejedor et al. 2015) and temperature (e.g. Büntgen et al. 2008, Grudd 2008, Büntgen et al. 2009, Esper et al. 2012c, Trachsel et al. 2012, McCarroll et al. 2013) at different time-scales and contain important information about short-term ecological (Konter et al. 2015) or climatological (Schneider et al. 2014) events. In addition the wide distribution of trees allows an almost global tree-ring network. It should be noted, however, that only trees of the extratropics show a clear annual resolution in their rings due to the cessation of cambial activity in winter times. The scientific field working with the information stored in the trees' annual growth-rings is called dendrochronology (gr: *dendro* – tree; gr: *chronology* – study of time). It links different scientific topics as climatology, ecology, biology, archeology and forestry.

Key principles of dendroclimatology

Tree-ring series illustrate the annually resolved tree growth and from a mathematical point of view these records can be seen as a function of time. In many areas the climate of the vegetation period controls the inter-annual variability of these series. Spatially close trees and sites provide similar growth patterns and the stored sequences of wide and narrow rings can unambiguously be assigned to calendar years. The exact annual dating allows comparisons with other undated records (Speer 2010). The principle behind this method is called "crossdating" and it allows to date floating (i.e. undated) time-series and to combine different types of wood. Next to living trees, relict material from buildings or out of lakes can be used to extend tree-ring time-series back in time.

Detrending is an important statistical tool as it removes age-related growth trends and unwanted noise caused by competition and disturbance. The age trend corresponds to the increasing radius of the stem attended by the increment of a relatively stable annual volume of biomass. This implicates declining ring widths from the pith towards the bark. Next to information about age, this geometrical curve also mirrors the influence of soil composition, competition, the type of forest and site related aspects (Cook 1987).

In dendrochronology two main ideas of standardization can be distinguished. On the one hand individual detrending methods, which are characterized by fitting an adjusted curve to every single tree-ring series, e.g. Spline detrending or Negative Exponential Curve detrending (Cook and Kairiukstis 1990). The collective detrending, on the other hand, is based on the concept of a single representative curve that is used for every single series during standardization (Esper et al. 2002). Thus, it preserves more low-frequency in the resulting chronology compared to an individual approach. A typical collective detrending, the Regional Curve Standardization (RCS; Briffa et al. 1996, Esper et al. 2002, Esper et al. 2003), removes unwanted information with a single curve, the so-called Regional Curve (RC). To produce the RC every time-series is age-aligned by cambial age. This means that the innermost tree-ring is set to a biological age of one. It is assumed that the mean of the age-aligned series displays the typical, common and time-independent growth at a specific site and species (Esper et al. 2003).

Next to all the advantages in preserving low-frequency variability this method also bears some statistical pitfalls depending on the particular structure of the dataset. Tree-ring series containing only slow growing trees (Cook and Peters 1997), trees with a homogeneous age structure (Esper et al. 2003) or material from different ecological settings (Helama et al. 2002) are not suitable for RCS detrending.

Even if the merging of recent and relict material is the basic principle to extend tree-ring series back in time, the potential differences in growth may directly affect long-term trends in tree-ring time series. Especially the origin of the material matters (Büntgen et al. 2005a, Gunnarson et al. 2011, Esper et al. 2012c) so that ecological and elevational differences has to be taken into account. Therefore, the different shaping of Regional Curves is one of the main problems when long-term tree-ring chronologies are standardized with RCS.

Micro-site effects

The term „micro-site“ describes the distinction of spatially close sites based on a diacritic attribute. Here, the distinctive feature is related to the influence of direct water access for trees growing directly at the lakeshore and trees with a certain distance to the lake. For the first time this approach was discussed by Esper et al. (2012c).

The main idea to study these ecological differences is based on the need to combine samples from living trees with dead material preserved in man-made structures or natural archives (e.g. lakes or sediments) to extend tree-ring chronologies back in time. This is a commonly used approach as all millennial tree-ring chronologies from northern Fennoscandia are based on this method (e.g. Eronen et al. 2002, Grudd et al. 2002, Grudd 2008, Esper et al. 2012c, McCarroll et al. 2013, Melvin et al. 2013).

The main idea to study micro-site effects is based on the hypothesis that subfossil material has a certain fingerprint of a relatively wet ecological milieu as it is assumed that these trees at former times stood at the lakeshore. Linderholm et al. (2014) also followed this assumption. In this context, a new sampling design was developed to test the particular singularities of trees from these ecological settings (wet vs. dry). It should be considered that there might be a differences between trees standing at the lakeshore or in the inland. Some special characteristics of lakeshore trees already were described by Naiman and Décamps (1997).

Such comparisons need a clear separation of the investigated sites. As it is described above micro-sites are related to the availability of groundwater and the direct access to the water of the lake, respectively. Most lakeshores in Scandinavia show a small riparian area and an adjacent slope. Due to changes in the hydro-climate in the last centuries the lake levels are fluctuating constantly (Gunnarson et al. 2003). Therefore, the micro-site sampling approach for this studies included the idea of differing lake levels. A clear separation is achieved by integrating trees upslope or on the top of small hills for the inland site. Lakeshore trees are subject to the condition that they might fall into the water at some point of their life.

In this study the main focus is (i) to detect and describe similarities and differences between lakeshore and inland trees and (ii) if these two habitats could be seen as autonomous ecological settings. Furthermore, a highly representative micro-site tree-ring network (iii) helps to understand spatial characteristics of micro-site effects.

State of the art

In northern Fennoscandia several millennial-long tree-ring chronologies are based on the crossdating between relict and recent material (e.g. Eronen et al. 2002, Grudd et al. 2002, Grudd 2008, Esper et al. 2012c, McCarroll et al. 2013, Melvin et al. 2013). However, the combination of material of different ages is responsible for some statistical problems as displayed in Melvin et al. (2013) and Esper et al. (2014). Esper et al. (2012c) tested already the ecological origin of the living material as a potential source of error which is connected to the ideas of Naiman and Décamps (1997) and Glenz et al. (2006). Trees directly standing at the lakeshore and trees a few meters away in the inland were attached to the same subfossil material ("Tail Test"). The resulting chronologies revealed substantial offsets in the most recent part. Similar problems occurred in studies from central Scandinavia where Gunnarson et al. (2011) noticed differences in the absolute TRW growth for trees from different elevations and this impedes the adequate approach of RCS detrending.

The large number of temperature reconstructions with material from northern Fennoscandia is related to the well preserved temperature signal in tree-ring data. But this sensitivity is changing towards lower latitudes. Helama et al. (2005a) described the changing environment in relation to different latitudes in Finland and they summarized the potential of the different areas for various tree-ring studies (e.g. temperature or precipitation reconstructions). Hence, in the southern parts of the boreal forest some studies reveal a sensitivity of the trees to drought (Drobyshev et al. 2011) or precipitation (Helama and Lindholm 2003). In general, by analyzing tree-growth along a gradient (latitudinal, longitudinal or elevational) it is possible to detect regions where trees are more sensitive to particular climate parameters.

For transect and network studies it is approved to include sites of different ecological and climatological settings to have benchmarks and to cover and understand the specific sub-ecosystem. In this context, e.g. altitudinal transects in the Alps help to describe different climate sensitivity patterns in various elevations (Hartl-Meier et al. 2014a, Hartl-Meier et al. 2014b). Moreover, studies on transects supports the identification of sites and altitudes suitable for climate reconstructions (Kienast et al. 1987, Affolter et al. 2010). The alti-latitudinal transect of Rossi et al. (2015) considers the future forest management and the chances of forest productivity. Martin-Benito and Pederson (2015) described the effects on trees relative to latitude in eastern North America and defined precipitation or maximum temperature as main limiting factor according to the latitude.

Study design

The studies presented in this thesis are based on a detailed micro-site tree ring network covering large areas of Fennoscandia. More than 3500 time-series are part of this network to study the influence of micro-site effects. The sampling design followed the idea presented by Esper et al. (2012c) as only trees at the lakeshore and in the upland were sampled. With Scots pine a robust, well distributed and climate sensitive tree species, a fairly known species forms the base for all studies. This species is also suited for the measurement of various tree-parameter (TRW and MXD). By means of multi-parameter approaches, next to inter-annual also intra-annual effects of micro-sites could be analyzed.

European Boreal forest ecosystem

The European forest can be divided into four different bioclimatic forest types. Next to the Temperate (continental and oceanic) and the Mediterranean zone the forest of the northern countries belongs to the Boreal type (Lindner et al. 2010). In Sweden and Finland more than 69% of the country is covered by forest and only 33% of the total land area in Norway. The economic importance of the forest is demonstrated by increasing forested areas in all countries and by the fact that more than 60% of its primary function is wood production (FAO 2010). The main tree species of this ecosystem are *Pinus sylvestris* L. (Scots pine), *Picea abies* (Norway spruce) and *Betula pendula* (Silver birch).

Additionally, in the more southern areas of the boreal forest also *Fagus sylvatica* (European beech) and *Quercus robur* (English oak) occur (Sykes and Prentice 1996).

The relatively undisturbed and continuous forest ecosystem in Fennoscandia is responsible for the large amount of dendroclimatological and dendroecological studies carried out in this area. Ahti et al. (1986) classifies the boreal forest into different subtypes: northern, middle, southern boreal and hemiboreal. Next to Norway spruce, Scots pine can be seen as the dominating tree species (Mátyás et al. 2004). Pines benefit of a high content of resin which hinders and slows down the decomposition of the wooden structures. In combination with the numerous lakes, as relict of glacial period (Tikkanen 2002), Fennoscandia has a unique archive for subfossil material.

Furthermore this region, can adapt to the wide range of climatological settings found in northern Europe. Variations in temperature and precipitation in the boreal forest are related to the latitudinal extension of more than 15°, the influence of the Gulf Stream, the distance to the Atlantic and the Baltic Sea and the orographic barrier of the Scandes (Erhart 1972). In general, tree growth in the north is affected by shorter growing seasons and lower summer temperatures compared to more temperate zones (Kellomaki et al. 1997). Next to the limitation due to temperature also precipitation affects tree growth as in dry years water is known to be a limiting factor in the southern boreal forest (Briceno-Elizondo et al. 2006).

Tree-ring parameters

Annual tree growth is visualized by the alternation of earlywood and latewood (Speer 2010). Earlywood appears brighter as the cells formed in the beginning of the vegetation period have a large lumen which supports water transport from the roots to the leaves. In contrast, latewood is formed in late summer and the cells have a more compact cell lumen relative to the cell walls and serve as a protective barrier (Speer 2010).

Next to the classical approach of measuring ring width (TRW; Fritts 1976) new concepts were created to retain additional information and to better understand tree physiology. Schweingruber et al. (1978) started to measure the density of wood in tree-ring samples and detected that the maximum latewood density (MXD) is highly related to summer temperatures in high altitudes and high latitudes (Schweingruber et al. 1979, Schweingruber et al. 1988). In more recent times this approach was expanded and modified. The so called blue intensity (BI; Rydval et al. 2014, Björklund et al. 2014) offers new scope for developments. Compared to TRW MXD and BI data often provide clearer temperature signals in extreme ecosystems and are less influenced by conditions of the previous year due to nutrition storage (Briffa et al. 2002). However, classical density measurements are expensive and time consuming (Björklund et al. 2014), while BI measurements showed deficits regarding low-frequency variability.

The relationship of tree growth and summer temperature in the northern parts of Fennoscandia is related to the harsh environment and the fact that temperature is the limiting factor for cambial activity. The existence of such restraining external conditions is also responsible for synchronized tree growth among trees from spatially close sites (Fritts 1976). Correlations of tree-ring time series and instrumental data help to determine the influence of the surrounding environment on tree-growth. In northern Fennoscandia especially temperatures during the summer months, are imprinted in tree-ring parameters: While TRW data show highest correlations with July temperatures (Kirchhefer 2001, Grudd et al. 2002), MXD is related to the complete summer season and also the correlations are much higher than for TRW (Briffa et al. 2002, Grudd 2008).

Objectives and aims

This thesis is divided into five main chapters. Each chapter addresses the micro-site topic from a different perspective. The order of the chapters reflects the progress in understanding micro-site dynamics:

CHAPTER I presents the first approach of a systematic analysis of micro-sites. This involves the latitudinal characteristics of micro-site effects (in north and central Sweden) and aims at getting a first idea of the demarcation between wet and dry ecological settings. It is shown that juvenile tree growth at different ecological habitats is directly influenced by continuous water availability.

CHAPTER II includes a micro-site analysis on spruces. The study compares spruces and pines from the same site and shows similar reactions to micro-site conditions for both species. Furthermore, the direct effect on temperature reconstructions was tested and the hidden bias in the standardization approach discussed.

CHAPTER III discusses a potential solution for merging different tree-ring data sets from nearby sites. A structured analysis of recent and relict material was necessary to present a robust and spatially representative summer temperature reconstruction of two long-term tree-ring chronologies (Torneträsk and N-Scan).

CHAPTER IV describes the impact of micro-sites on maximum latewood density (MXD) data and extends the latitudinal gradient analyzed in CHAPTER I at the Finnish site. Moreover, it discusses the effects on forest productivity with regard to increasing precipitation sums due to climate change.

CHAPTER V contains a detailed micro-site network analysis over Fennoscandia. A cluster analysis reveals three different types of tree-ring chronologies. Ecological differences on tree-growth are displayed in an East-West pattern, showing that there are two main types of micro-site effects.

Chapter I: Influence of micro-site conditions on tree-ring climate signals and trends in central and northern Sweden

Elisabeth Düthorn[1], Steffen Holzkämper[2], Mauri Timonen[3], Jan Esper[1]

[1] Department of Geography, Johannes Gutenberg University, Becherweg 21, 55099 Mainz, Germany

[2] Department of Physical Geography and Quaternary Geology, Stockholm University, 10691 Stockholm, Sweden

[3] Finnish Forest Research Institute, Rovaniemi Research Unit, 96301 Rovaniemi, Finland

(Trees – Structure and Function, 2013, published)

Düthorn E., Holzkämper S., Timonen M., Esper J. (2013): Influence of micro-site conditions on tree-ring climate signals and trends in central and northern Sweden. Trees 27: 1395-1404.

1. Introduction

Large-scale temperature reconstructions derived from tree-ring chronologies are important indicators of long-term climate variations over the past centuries to millennia (Briffa et al. 1998, Esper et al. 2002, D'Arrigo et al. 2006, Frank et al. 2007, Christiansen and Ljungqvist 2012). Particularly trees from sites near the northern distribution limit show a strong sensitivity to temperature variations (Esper et al. 2010) and are included the hemispheric reconstructions (Solomon et al. 2007). Among these, tree-ring chronologies from northern Fennoscandia have been used to construct some of the world´s longest continuous tree-ring width (TRW) and maximum latewood density (MXD) chronologies (Schweingruber et al. 1988, Eronen et al. 2002, Grudd et al. 2002, Esper et al. 2012c). Such records are generally developed by combining TRW and MXD measurement series from living trees with either dry dead wood from the ground (or historical buildings; (Büntgen et al. 2006, Büntgen et al. 2007) or with sub-fossil material from lakes (Kultti et al. 2006) or peat bogs (Nicolussi et al. 2009), for example (overview in Esper et al. (2002).

The climate signal inherent to these long tree-ring chronologies is typically assessed by comparison of 20th century TRW (or MXD) measurements – derived from living trees – with instrumental climate data (Fritts 1976). Through this "calibration process", a linear model between tree-ring proxy and a leading climatic variable (e.g. summer temperature in northern environments) is established and subsequently used to transfer a TRW chronology into estimates of temperature variability over the past centuries to millennia (Esper et al. 2005a). This calibration and transfer scheme rests on the assumption that a statistically derived association between living trees and 20th century climate data is equally valid for the pre-instrumental portion of a long chronology derived from historical or sub-fossil wood samples (the principle of "uniformitarianism", e.g. Speer (2010).

In case of the supra-long chronologies from northern Fennoscandia, different wood sources, including sub-fossil material from lakes and dry dead wood from the ground, were combined with samples from living trees to form timeseries spanning the past 7400 years in Swedish Lapland (Grudd et al. 2002) and 7519 years in Finnish Lapland (Eronen et al. 2002). The recent portions of these records are represented by living trees sampled in relatively dry micro-sites in varying distances to the lakes. The coherence of growth characteristics among the relatively wet lakeshore sites, that represent the source habitats of the sub-fossil material of much of the supra-long chronologies, and the relatively dry inland sites remained largely unexplored, however (Esper et al. 2012c).

We here assess the potential influence of varying micro-site conditions on long tree-ring records by analyzing climate signals and growth trends of *Pinus sylvestris* L. trees collected at lakeshores and several meters inland in northern and central Sweden. It is presumed that the central sites, located near Stockholm, contain a predominating drought signal, whereas the northern sites, located near Kiruna, contain a predominating temperature signal (Linderholm et al. 2010). Climate signals of TRW chronologies from six lakeshore and inland micro-sites are evaluated through comparison with regional

instrumental climate data, and growth trends assessed by combining these living tree records with existing relict data from the Torneträsk region in northern Sweden and the Gotland Island located southeast of Stockholm. In this paper, we first provide detail on the sampling regions and micro-sites, as well as the detrending and calibration techniques, then present the results on the common climate signals in northern and central Sweden, followed by a detailed assessment of the climate signals inherent to lakeshore and inland micro-sites. Varying growth trends of these micro-sites are discussed after combining the data with relict material from Torneträsk and Gotland considering different tree-ring detrending techniques.

2. Material and Methods

2.1 Sampling regions and micro-sites

Three hundred eighty five *Pinus sylvestris* L. core samples were collected in northern Sweden 12 km northwest of Kiruna (KIR: 67.95°N, 20.03°E) and in central Sweden 11 km north of Stockholm (STO: 59.44°N, 17.99°E; Fig.I-1). KIR is located about 50 km south of Lake Torneträsk near the northern distribution limit of tree growth where pines and birches (*Betula pubescens)* are the predominating forest species. The area is characterized by a short growing season of only ~120 days with mean annual and July-September (JAS) temperatures of -2.6°C and 10°C, respectively. Due to its position east of the Scandinavian Mountains, in the rain shadow of the prevailing influence of the North Atlantic Oscillation (Linderholm et al. 2010), the northern sampling site receives relatively low summer precipitation sums (~200 mm). The Torneträsk/Kiruna area is situated in the transition zone between the tundra and a humid snow climate with cool summers classified as ET and Dfc, respectively, according to Kottek et al. (2006).

STO is located at Lake Rösjön, ~950 km south of KIR, in a transition zone from boreal to temperate forests predominated by mixed coniferous and deciduous species including pine, spruce (*Picea abies L.*), oak (*Quercus robur*), and beech (*Fagus sylvatica*). Mean annual and JAS temperatures reach 6.6°C and 15.3°C, respectively, and summer precipitation equals ~190 mm. The growing season is ~60 days longer than in the northern sampling area, though much less photosynthetically significant, direct and diffuse, sunlight is received during "nighttime". The Stockholm region is located at the transition between a humid snow climate with warm summers (Dfb) and a warm, temperate and humid climate with warm summers (Cfb) typical for much of Central Europe (Kottek et al. 2006). Overall growth rates are higher at the central STO site (1.19 mm/year) compared to the colder KIR site (0.85 mm/year).

In both sampling sites, KIR and STO, *Pinus sylvestris* was sampled in three distinct micro-sites – lakeshore (A), intermediate (B), and inland (C) – characterized by varying distances to the lakes (Fig. I-1b, c). The micro-sites are oriented along transects starting at the lakeshores, where conditions are wetter and trees have access to groundwater that is largely in balance with the lake levels, towards locally dryer conditions some meters above the lakes. In KIR, the transect reaches from 451 to 471 m asl., tree girths

vary between 0.13 and 1.37 m, and tree heights range from 3 to 13 m. In STO, the transect reaches from 20 to 60 m asl., tree girths vary between 0.2 and 1.85 m, and tree heights range from 2 to 18 m. Transect expositions are west in KIR and southwest in STO. Distances between the single micro-sites are all ≥ 15 m.

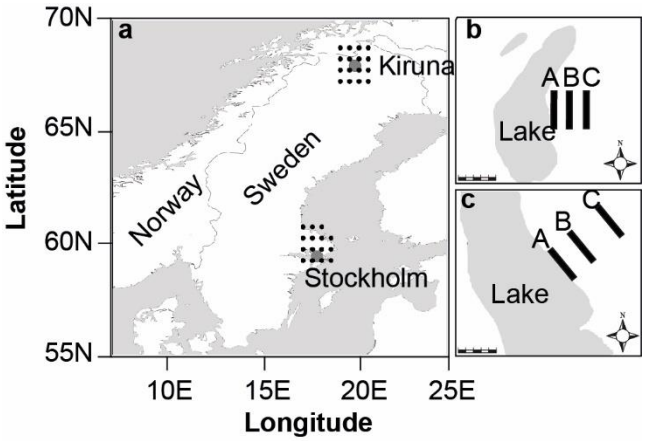

Figure I-1: Map showing the tree-ring sampling sites in northern and central Sweden (a, grey dots) and the lakeshore (A), intermediate (B), and inland micro-sites (b and c) in KIR and STO. Black dots in a indicate the position of the climate data grid points used for calibration of the tree-ring data.

2.2 Tree-ring data and chronology development

To develop well-replicated sub-site chronologies, ~40 Scots pines (mostly two cores per tree) were sampled in each micro-site in KIR and STO (Table 1). Ring widths were measured with an accuracy of 1/100 mm and crosschecked with the programs LinTab and Cofecha (Holmes 1983). Samples were taken in pre-defined plots to ensure representation of micro-site conditions including all age classes (Esper et al. 2012a).

Age trend, that is the decreasing width (and variance) associated with increasing tree girth (Fritts 1976), was removed by *(i)* calculating ratios from negative exponential functions (NegExp) fit to each individual TRW measurement series (Cook and Peters 1997), and *(ii)* removing the trend common to all trees within KIR and STO using the Regional Curve Standardization (RCS) technique (Esper et al. 2003). Every micro-site was detrended with its own regional curve. All measurement series were power transformed prior to index calculation to remove variance changes (i.e., generally more variable juvenile and less variable adult TRW values) inherent to the raw TRW data (Cook and Peters 1997). Sub-site chronologies were developed by averaging the detrended TRW series for each micro-site integrating between 58 and 69 core samples, and removing temporal variance changes that typically arise from changes in interseries correlation and replication (Frank et al. 2007). We additionally averaged all tree-ring data in KIR and STO to assess the common climate forcing at the regional scale (Table 1).

Common variance inherent to the chronologies and the effectiveness of samples to represent theoretically infinite populations were estimated using the interseries correlation (Rbar) and Expressed Population Statistics (EPS) calculated over the 1901-2009 calibration period (Wigley et al. 1984).

Besides calculating site and micro-site chronologies, the living tree data were also combined with relict material from the Torneträsk (Grudd et al. 2002) and Gotland (Esper et al. 2002) regions to assess the influence of growth rate changes – at the micro-site level – on the long-term trends of millennial scale chronologies (Esper et al. 2012c) . While this could effectively also be achieved using artificial data that mirror the properties of TRW data from central and northern Sweden, the combination of living trees representing distinct micro-sites with existing relict samples from a given region, reflects common praxis of developing long-term climate reconstructions in dendrochronology (Tegel et al. 2010). In this approach, the TRW data were detrended using either NegExp or RCS to assess the significance of standardization methodology on the integration of relict and living tree samples.

Table I-1: Sampling site characteristics. Number of measurement series (n) of the Kir and Sto sites, as wells as the lakeshore (KIR-A, STO-A), intermediate (KIR-B, STO-B), and inland (KIR-C, STO-C) micro-sites. Rbar is the interseries correlation, and EPS the expressed population signal, both calculated of the 1901-2009 period.

	KIR	KIR-A	KIR-B	KIR-C
number of samples	195	68	67	60
Rbar (1901-2009)	0.40	0.40	0.39	0.47
EPS (1901-2009)	0.99	0.98	0.98	0.98
mean growth rate (mm/year)	0.85	0.83	0.78	0.97
segmenth length (years)	93.33	83.22	78.21	77.08
	STO	**STO-A**	**STO-B**	**STO-C**
number of samples	190	69	63	58
Rbar (1901-2009)	0.23	0.27	0.41	0.42
EPS (1901-2009)	0.98	0.96	0.98	0.98
mean growth rate (mm/year)	1.19	1.15	1.48	1.00
segmenth length (years)	96.81	119.71	74.92	93.33

2.3 Climate data and calibration

TRW data were calibrated against gridded meteorological data (version CRU TS 3.1 at 0.5° resolution; (Mitchell and Jones 2005) to assess the climate-growth relationships at the site and micro-site scales. The northern KIR chronologies were compared with temperature and precipitation data of 16 grid points averaged over the 67-69°N and 19-21°E area; and the central STO sites using 15 grid points averaged over the 59-61°N and 17-19°E area (see the black dots in Fig. I-1a).

Pearson correlations were calculated among tree-ring chronologies and monthly and seasonally (JAS and MJJAS) averaged climate data over the 1901-2009 common period. 30-year running correlations were computed to assess the temporal variability of climate signals throughout the 20th and early 21st centuries. Correlation significance was estimated using the Standard Error ($SE = (1–r^2)/\sqrt{(1–n)}$) considering first order autocorrelation inherent to the proxy and climate data (Cook and Kairiukstis 1990).

3. Results

3.1 Regional climate signals

Whereas *Pinus sylvestris* growth in northern Sweden is controlled by temperature, the pines in central Sweden are influenced by precipitation (Helama and Lindholm 2003, Drobyshev et al. 2011). Calibration of the well-replicated RCS site chronologies revealed a stronger JJA temperature signal in KIR ($r_{1901-2009} = 0.44$) and a weaker but significant MJJAS precipitation signal in STO ($r_{1901-2009} = 0.36$). The spatial pattern of the temperature signal covers much of northern Fennoscandia (at $r > 0.40$) and extends south towards a line from northern Denmark into western Russia (Fig. I-2; $p < 0.05$). The spatial pattern of the precipitation signal is patchier (Büntgen et al. 2010b) and limited to a region west of the Scandinavian Mountains reaching into Helsinki/St. Petersburg area and south towards Denmark. The seasonal climate signal patterns were similar between the RCS and NegExp detrended micro-site chronologies.

Assessment of the temporal characteristics of these climate signals indicated overall stable associations between the northern and central pine sites and the leading JJA temperature and MJJAS precipitation climatic variables, respectively, though the KIR site shows an increased variability – including exceptionally low and high correlations – towards the late 20th and early 21st centuries (Fig. I-2b). In contrast, correlations with precipitation in the northern site and with temperature in the central site fluctuate around zero, validating that *Pinus sylvestris* at the two sites contain distinctly differing climate signals. The EPS results indicate that both the KIR and STO collections reflect representative samples throughout the 20th century. The interseries correlation (Rbar) is overall higher in KIR (0.40) compared to STO (0.23). KIR Rbar values are increasing back in time, likely due to a growing influence of low sample replications (see Fig. I-2c, and bottom panels in Fig. I-3).

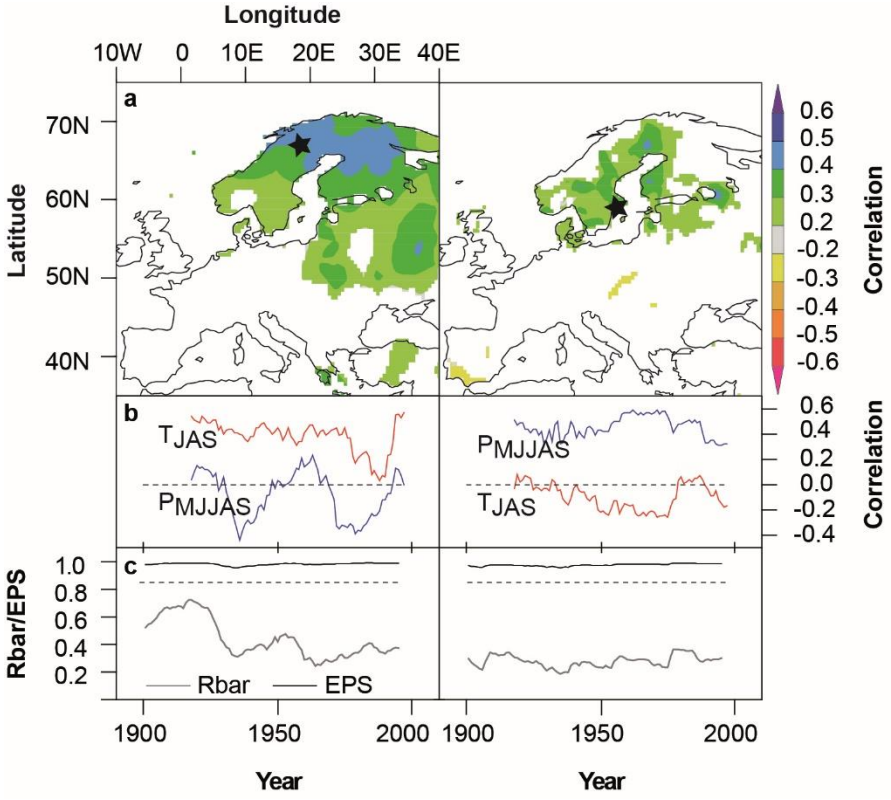

Figure I-2: Tree-ring climate signals in northern and central Sweden. **a**, Spatial correlation patterns ($p < 0.05$) of RCS-detrended TRW chronologies from KIR (left; against JAS temperature) and STO (right; against MJJAS precipitation) with CRU TS3.1 climate data over the 1901-2009 period. **b**, 30-year running correlations with JAS temperatures (red) and MJJAS precipitation (blue) derived from nearby grid points (see Fig. I-1). **c,** 30-year running Rbar and EPS statistics of the RCS detrended KIR and STO chronologies (dashed line indicates the 0.85 value).

3.2 Micro-site coherence and climate signals

Cross-correlations among the micro-site chronologies are substantially lower in STO ($r_{1901\text{-}2009} = 0.53$) compared to KIR ($r_{1901\text{-}2009} = 0.85$) indicating an increased, and differentiating, influence of micro-site conditions in the central sampling area. The Rbar result of the STO-A lakeshore micro-site is also deviating from its intermediate and inland counterparts (STO-B and STO-C), which is likely related to individually differing (at the tree-to-tree level) root access to groundwater (Table I-1). These differences are also reflected in the micro-site chronologies as displayed in Fig. I-3 showing largely synchronous TRW variations between the lakeshore and inland KIR micro-sites, but larger deviations and differing variances between the STO micro-sites. Again all micro-site chronologies analyzed here show EPS values exceeding the commonly accepted 0.85 threshold throughout the 1901-2009 period, similar replication changes, and comparable Rbar results (except for STO-A).

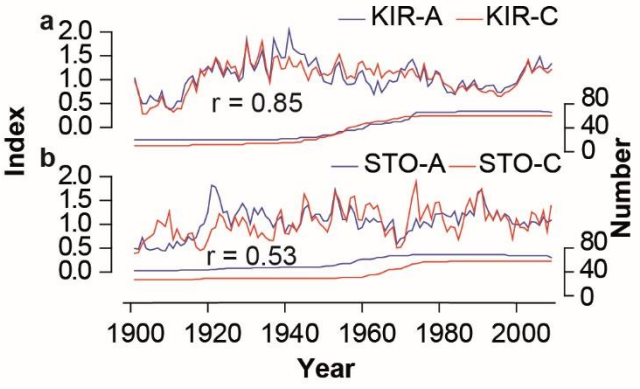

Figure I-3: Lakeshore and inland chronologies. RCS-detrended micro-site chronologies from KIR-A and KIR-C (**a**) and STO-A and STO-C (**b**) over the 1901-2009 period. Bottom panels show the replication curves of the lakeshore (blue) and inland (red) chronologies.

The micro-site climate-growth relationships are largely in line with the results obtained at the site level (see above), i.e. a dominating temperature signal is found in the North, and a less strong, though significant ($p < 0.05$), precipitation signal is found in central Sweden (Fig. I-4). Associated precipitation and temperature signals are insignificant in the North and in the central part, respectively. However, whereas the correlation coefficients are balanced ($r \sim 0.32$) among the STO micro-sites, the temperature signal in the North is decreasing from KIR-A ($r = 0.50$) to KIR-B ($r = 0.44$) to KIR-C ($r = 0.43$). While these differences in KIR micro-site climate signals are again insignificant (note the SE error bars in Fig. I-4), this finding indicates that the sub-fossil Pine stems preserved in northern Swedish lakes contain a slightly stronger temperature signal compared to the dryer, inland trees.

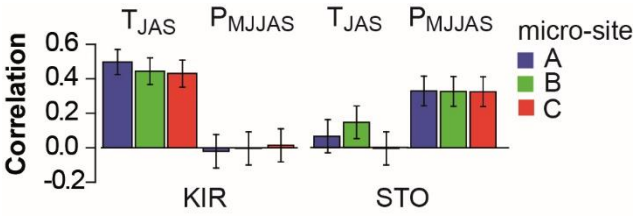

Figure I-4: Tree-ring climate signals. Correlation coefficients derived from calibrating the RCS-detrended lakeshore (A, blue), intermediate (B, green), inland (C, red) micro-site chronologies from KIR (left) and STO (right) against gridded regional JAS temperature data over the 1901-2009 common period. Error bars indicate the SE of the correlation coefficients.

3.3 Micro-site growth trends

Besides the differences in climate signals, the TRW data indicate deviating growth levels and trends between the lakeshore and inland micro-sites (Fig. I-5). Mean growth rates differ by 0.19 mm among the KIR and 0.47 mm among the STO micro-sites (Table I-1). These differences are in part related to the varying segment lengths (that is the mean tree age; Cook et al. (1995) that are comparable among the northern micro-sites but range from ~90 years in STO-C to ~120 years in STO-A.

In both KIR and STO, age trends are overall more balanced and less steep in the lakeshore micro-sites compared to their inland counterparts. Juvenile growth (up to an age of 20-30 years) is more rapid in the inland micro-sites (Helama et al. 2004), followed by a scarped age-trend until cambial ages of ~90 years in KIR-C and ~70 years in STO-C, where these inland growth curves approach levels clearly below the lakeshore micro-sites. Whereas the steep age-trends inherent to the inland micro-sites are likely related to increasing inter-tree competition (and limited access to soil water in the southern site), the subsequent growth increases, up to an age of ~120 years in KIR-C and ~100 year in STO-C, appeared unexpected. Stem wood production of old trees (> 120 years) remains larger at the southern lakeshore site (STO-A) compared to its inland counterpart (STO-C; Fig. I-5).

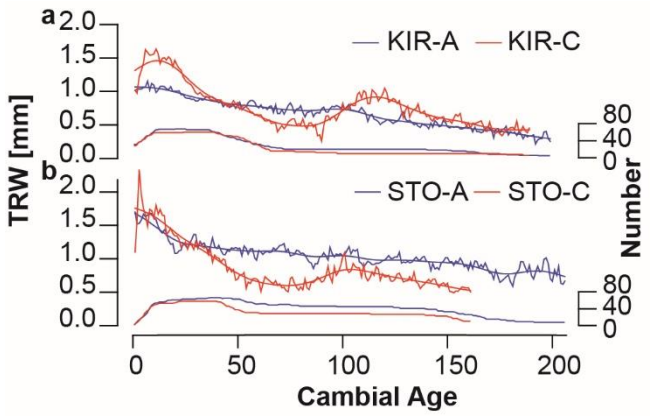

Figure I-5: Growth levels and trends in lakeshore and inland micro-sites. Original and 40-year smoothed Regional Curves (that is the arithmetic mean of the age-aligned TRW data) of the KIR-A and KIR-C (**a**) and STO-A and STO-C (**b**) micro-sites. Bottom panels show the replication curves of the lakeshore (blue) and inland (red) data.

3.4 Effects on long chronologies

Combination and joined detrending of the micro-site datasets together with the relict material from northern and central Sweden enables an assessment of the effects of differing growth rates, inherent to the living tree data, on the long-term trends of millennial scale records. In these experiments, we combined the living tree data from the northern lakeshore and inland micro-sites (KIR-A and KIR-C) with the relict TRW data from the widely cited Torneträsk chronology (Schweingruber et al. 1988, Esper et al. 2002, Grudd et al. 2002) downloaded from the International Tree-Ring Databank: file swed019), and the data from the central lakeshore and inland micro-sites (STO-A and STO-C) with the relict TRW data from Gotland (Esper et al. 2002; file swed022). The resulting (combined) RCS and NegExp detrended chronologies were *(i)* truncated at AD 1146 where the Gotland data reaches a minimum replication of five TRW series, and *(ii)* normalized over the 1146-1859 period covered by only the relict wood samples (Fig. I-6). The chronologies are based on only living tree samples (from the various micro-sites) over the recent 1901-2009 period, and on a mix of living tree and relict wood samples over the 1860-1900 period (see the replication curves at the bottom of Fig. I-6 panels). Data integration of these records are conceptually similar to any millennial scale tree-ring record integrating TRW data from living and relict trees, with the exception that we have full control of the varying micro-site conditions over the recent period of these timeseries (Christiansen and Ljungqvist 2012).

The varying combinations of relict with living tree datasets results in only minor differences, if NegExp detrending is considered, i.e. the blue (lakeshore) and red (inland) recent 'tails' of the millennial scale chronologies display similar variability (Fig. I-6). This conclusion changes considerably, however, if the combined datasets are detrended using RCS. The chronologies not only contain more low frequency variability (as expected; see Esper et al. (2002), but also deviate substantially during the 20th century: (a) the Tor-RCS record is picking up more variability if combined with the inland KIR-C micro-site data (compared to Tor + KIR-A); (b) the Got-RCS record shows much larger recent values if combined with the lakeshore STO-C micro-site data (compared to Got + STO-A).

The foundation for these differing 20th century trends is the varying growth levels of the lakeshore and inland micro-site data in KIR and STO. The overall wider rings in STO-A (see above, Fig. I-5) translate into increased, recent, chronology values after combination and joined RCS-detrending with the relict Got data. Whereas the smoothed 20th century index values of the combined GotA chronology exceeds 3.0 throughout most of the 20th century, the record obtained from combining relict with inland data remains below 2.42 during this period. For the northern Swedish data, the increased variance of the KIR-C inland micro-site (compared to KIR-A) translates into a more variable 20th century 'tail' after combination and joined RCS detrending with Tor. The mid-20th century index values of this record exceed 1.5, whereas the 20th century values of the combined TorA record do not exceed the variance recorded during earlier centuries.

These differences are further emphasized in the 20th century value distributions of the combined RCS chronologies, with the chronology values during the identified, deviating periods (1941-1960 in the northern, and 1990-2009 in the central region) being highlighted in blue and red (Fig. I-7). Whereas the northern RCS chronologies indicate a slight shift towards more positive values when considering the inland micro-site data (20th century mean values change from 0.43 to 0.82; see the black triangles in Fig. I-7), integration of lakeshore instead of inland data results in a substantial shift in the mean value (from 1.27 in GotC to 2.59 in GotA) in the southern Gotland chronology. The northern chronology also indicates differences in the value distributions. Compared to Tor A, the distribution of TorC is negatively skewed towards larger values, but these changes appear overall minor compared to the distributions differences between GotA and GotC. In these latter chronologies, the 1990-2009 mean values change from 1.88 in GotC to 3.73 in GotA.

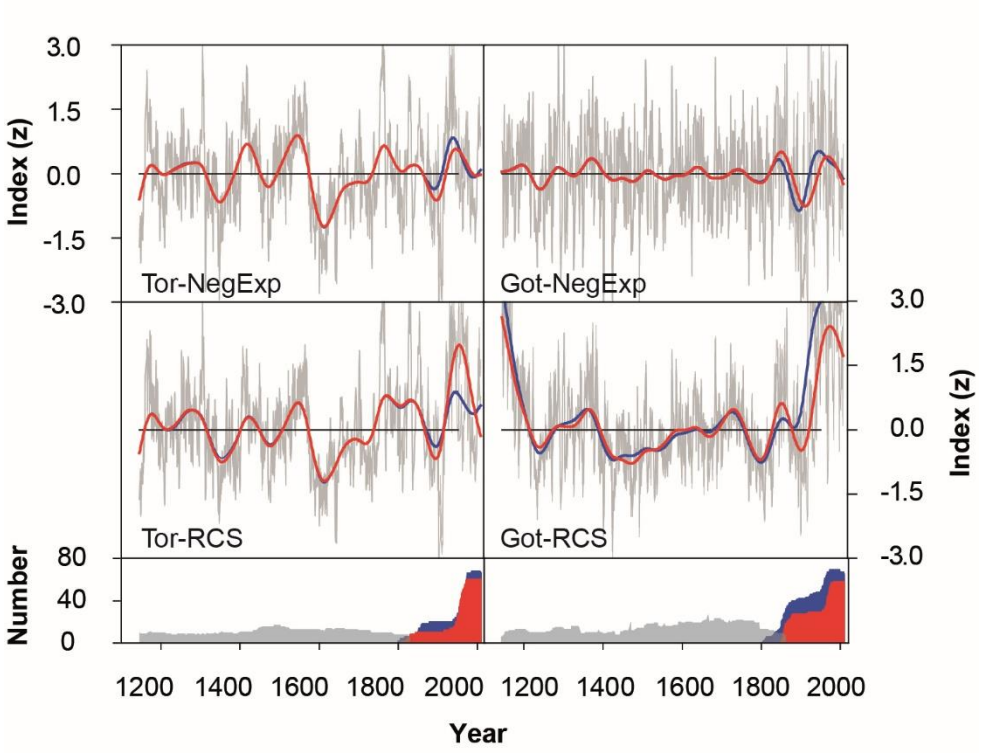

Figure I-6: Influence of micro-site conditions on TRW chronology trends. Millennial scale chronologies derived from combining relict TRW data from Torneträsk (Tor) and Gotland (Got) with living tree data from KIR-A and KIR-C (left panels) and STO-A and STO-C (right panels). Smoothed (100-year low pass filter) composite chronologies integrating living tree lakeshore data (TorA and GotA) are shown in blue; chronologies integrating inland data shown in red (TorC and GotC). Top and middle panels show the NegExp and RCS detrended chronologies, respectively. All records were normalized over the 1146-1859 period covered by only the relict wood samples. Bottom panels show the replication of combined datasets.

4. Discussion

Our high replication micro-site chronologies shed light on the sensitivity of established climate-growth relationships. We identified differences in growth behavior and sensitivity to various climate parameters between the lakeshore and inland micro-sites. These differences arise from varying growth patterns between different micro-sites in one sampling area. While hydrological conditions were expected to be more favorable for tree growth at lakeshores, effective growth rates were higher at the inland sites, in both northern and central Sweden, for the first decades of growth. We assume that the young trees cannot deal with the perhumid conditions surrounding their root system and anaerobic conditions slow down the growth rate at the lakeshore. For a more detailed analysis soil water content and temperature measurements on a micro-site level are required. Also the climate-growth relationships differ between the micro-sites. Even in the high latitude study area, where overall growth conditions are harsh, there are differences, at the micro-site scale, in the response to climate. Similar processes have been revealed in altitudinal micro-site studies (Liang et al. 2010). In central Sweden, the precipitation signal is similar among the micro-sites. The stronger temperature signal recorded towards the lakeshore in the far northern environment is a new aspect that could help to improve long-term reconstructions from such regions.

Our results show that *Pinus sylvestris* growth in northern and central Sweden is controlled by different climate parameters; temperature in the North and precipitation/drought in the central part. The identified relationships offer the possibility to reconstruct temperature and drought variations over longer timescales in these regions. The higher growth rate in the central sampling area is affiliated with an extended growing season period and overall more favorable growing conditions. However, the lower correlations among micro-sites in central Sweden indicates that growth is less affected by external, and unifying, factors compared to the northern micro-site chronologies. This conclusion is supported by the stronger response to climate parameters in northern Sweden, where more TRW variance is explained by summer temperature (compared to the southern sites and precipitation). The northern micro-sites also contain a gradual decrease from higher temperature signals at the lakeshore to weaker signals towards inland, which could be related to short-term drought conditions disturbing the temperature signal in the dryer inland micro-sites. It therefore appears likely that sub-fossil material, from trees originally growing at the lakeshores, and used for developing millennial-length chronologies, contains a stronger climate signal than currently believed. Since the climate-growth relationships differ between the micro-site habitats, we recommend using living trees from only lakeshore sites for calibration purposes of these supra-long chronologies.

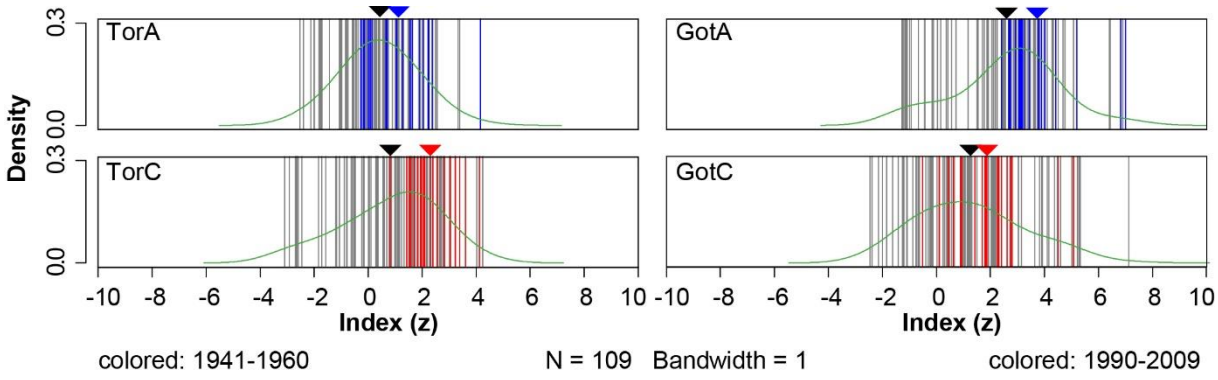

Figure I-7: Influence of micro-site conditions on 20th century chronology values. Distribution of the RCS-detrended chronology values of the combined millennial-length timeseries shown in Fig. I-6. Black lines indicate the 1901-2009 index values; and colored lines of specific 20-year periods (1941-1960 in TorA and TorC; 1990-2009 in GotA and GotC) discussed in the text. Mean values of the longer and shorter periods are indicated with black and colored (blue and red) triangles. Green curves indicate probability density functions derived from kernel estimates (bandwidth = 1).

While varying temperature signals among pine micro-sites can affect the climatically explained variance and uncertainty estimates of combined (living + relict material) chronologies, the plain growth rate differences among micro-sites can affect the long-term course of millennial scale records (Fig. I-7). If an individual detrending scheme (NegExp) is applied to the combined datasets, the differences between relict+lakeshore and relict+inland chronologies are negligible. However, if we apply a detrending method that enables preserving low frequency (centennial scale) variance over the past millennium (Esper et al. 2003), the growth rate differences between lakeshore and inland micro-sites translate into varying long-term trends that can alter conclusions on 20th century warming with respect to the preceding centuries of the past millennium. In the northern study area, the wet micro-site matches the growth curve of the relict wood quite closely, while the inland growth curve trends to differ substantially, during certain periods (0 - 40 and 100 - 160 years), from the Torneträsk relict material (Fig. I-8). In the southern study area, lakeshore micro-site growth is much faster, explaining the severely increased recent trends after combination with the Gotland relict data and RCS detrending. It is thus recommended to study the growth rates and changes with aging, as expressed in the growth curves, when combining living tree data with measurements series from relict material. Our study thereby not only reinforced the importance of analyzing the age structure and growth variations of subsets integrated in millennial scale chronologies, but also emphasized that growth rate (and climate signal) differences at the micro-site scale can affect the conclusion derived from long-term climate reconstructions.

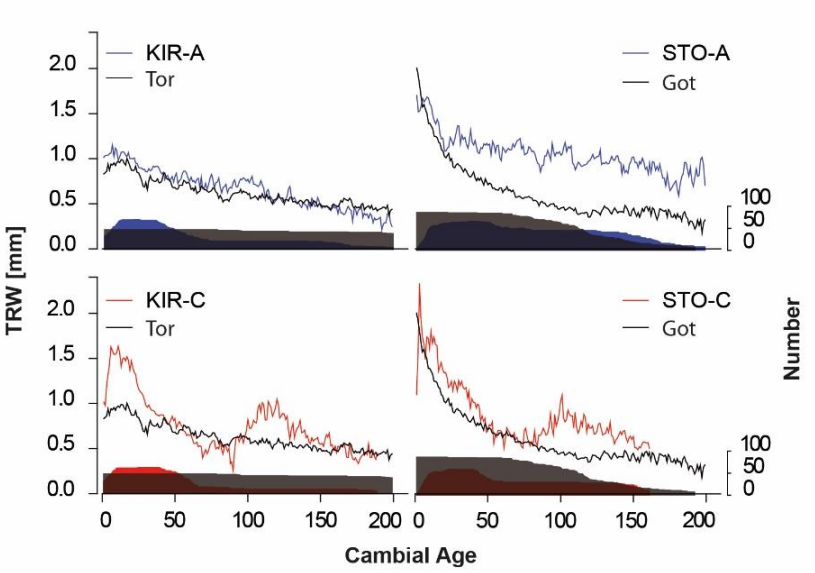

Figure I-8: Growth levels and trends of relict and living tree TRW data. Regional curves of the lakeshore (blue) and inland (red) micro-sites from KIR and STO shown together with the data relict data from Torneträsk and Gotland (black). Lower panel shows the replication.

5. Conclusions

Comparisons of well-replicated micro-site chronologies (lakeshore and several meters inland) from northern and central Sweden showed stronger temperature signals in trees growing directly at the lakeshore, compared to the inland counterparts, in northern Sweden. Besides the differing climate signal strengths, we found varying growth rates (and trends) among the lakeshore and inland microsites in both study regions. These differences appear to be unimportant, if individual detrending techniques (e.g. NegExp), that remove growth rate differences among single measurement series, are applied. Micro-site differences are important, however, when RCS detrending is applied, resulting in differing long-term trends in millennial-length chronologies.

Concerning the discussion on 20th century temperature trends, this study detailed novel approaches to improve existing long-term tree-ring chronologies and derived temperature reconstructions. In line with recommendations to more carefully choose (and combine) living tree with historical wood samples (Tegel et al. 2010), the results presented herein revealed supra-long tree-ring chronologies from northern Fennoscandia should be combined with living tree data from lakeshore micro-sites only. Doing so will not only result in an better assessment of the climate signal retained in these long records, but also improve our understanding of recent climate change with respect to pre-instrumental variations and trends over the past several hundred years to millennia.

Acknowledgements

Supported by the Mainz Geocycles Research Centre. We thank Dana Riechelmann and Florian Benninghoff for help with fieldwork and Lea Schneider for discussion.

References

Briffa K.R., Jones P.D., Schweingruber F.H., Osborn T.J. (1998): Influence of volcanic eruptions on Northern Hemisphere summer temperature over the past 600 years. *Nature* 393: 450-455.

Büntgen U., Bellwald I., Kalbermatten H., Schmidhalter M., Frank D.C., Freund H., Bellwald W., Neuwirth B. et al. (2006): 700 years of settlement and building history in the Lotschental, Switzerland. *Erdkunde* 60: 96-112.

Büntgen U., Frank D.C., Kaczka R.J., Verstege A., Zwijacz-Kozica T., Esper J. (2007): Growth responses to climate in a multi-species tree-ring network in the Western Carpathian Tatra Mountains, Poland and Slovakia. *Tree Physiology* 27: 689-702.

Büntgen U., Franke J., Frank D., Wilson R., Gonzalez-Rouco F., Esper J. (2010b): Assessing the spatial signature of European climate reconstructions. *Climate Research* 41: 125-130.

Christiansen B., Ljungqvist F.C. (2012): The extra-tropical Northern Hemisphere temperature in the last two millennia: reconstructions of low-frequency variability. *Climate of the Past* 8: 765-786.

Cook E.R., Briffa K.R., Meko D.M., Graybill D.A., Funkhouser G. (1995): The Segment Length Curse in Long Tree-Ring Chronology Development for Paleoclimatic Studies. *Holocene* 5: 229-237.

Cook E.R., Kairiukstis L.A. (1990): Methods of dendrochronology. Kluwer Academic Publishers.

Cook E.R., Peters K. (1997): Calculating unbiased tree-ring indices for the study of climatic and environmental change. *Holocene* 7: 361-370.

D'Arrigo R., Wilson R., Jacoby G. (2006): On the long-term context for late twentieth century warming. *Journal of Geophysical Research-Atmospheres* 111.

Drobyshev I., Niklasson M., Linderholm H.W., Seftigen K., Hickler T., Eggertsson O. (2011): Reconstruction of a regional drought index in southern Sweden since AD 1750. *Holocene* 21: 667-679.

Eronen M., Zetterberg P., Briffa K.R., Lindholm M., Merilainen J., Timonen M. (2002): The supra-long Scots pine tree-ring record for Finnish Lapland: Part 1, chronology construction and initial inferences. *Holocene* 12: 673-680.

Esper J., Benz M., Pederson N. (2012a): Influence of wood harvest on tree-ring time-series of Picea abies in a temperate forest. *Forest Ecology and Management* 284: 86-92.

Esper J., Cook E.R., Krusic P.J., Peters K., Schweingruber F.H. (2003): Tests of the RCS method for preserving low-frequency variability in long tree-ring chronologies. *Tree-Ring Research* 59: 81-98.

Esper J., Cook E.R., Schweingruber F.H. (2002): Low-frequency signals in long tree-ring chronologies for reconstructing past temperature variability. *Science* 295: 2250-2253.

Esper J., Frank D., Büntgen U., Verstege A., Hantemirov R.M., Kirdyanov A.V. (2010): Trends and uncertainties in Siberian indicators of 20th century warming. *Global Change Biology* 16: 386-398.

Esper J., Frank D.C., Timonen M., Zorita E., Wilson R.J.S., Luterbacher J., Holzkamper S., Fischer N. et al. (2012c): Orbital forcing of tree-ring data. *Nature Climate Change* 2: 862-866.

Esper J., Frank D.C., Wilson R.J.S., Briffa K.R. (2005a): Effect of scaling and regression on reconstructed temperature amplitude for the past millennium. *Geophysical Research Letters* 32.

Frank D., Esper J., Cook E.R. (2007): Adjustment for proxy number and coherence in a large-scale temperature reconstruction. *Geophysical Research Letters* 34.

Fritts H.C. (1976): Tree rings and climate. Academic Press.

Grudd H., Briffa K.R., Karlen W., Bartholin T.S., Jones P.D., Kromer B. (2002): A 7400-year tree-ring chronology in northern Swedish Lapland: natural climatic variability expressed on annual to millennial timescales. *Holocene* 12: 657-665.

Helama S., Lindholm M. (2003): Droughts and rainfall in south-eastern Finland since AD 874, inferred from Scots pine ring-widths. *Boreal Environment Research* 8: 171-183.

Helama S., Lindholm M., Timonen M., Eronen M. (2004): Detection of climate signal in dendrochronological data analysis: a comparison of tree-ring standardization methods. *Theoretical and Applied Climatology* 79: 239-254.

Holmes R.L. (1983): Computer-assisted quality control in tree-ring dating and measurement. *Tree-Ring Bulletin* 43: 69-78.

Kottek M., Grieser J., Beck C., Rudolf B., Rubel F. (2006): World map of the Koppen-Geiger climate classification updated. *Meteorologische Zeitschrift* 15: 259-263.

Kultti S., Mikkola K., Virtanen T., Timonen M., Eronen M. (2006): Past changes in the Scots pine forest line and climate in Finnish Lapland: a study based on megafossils, lake sediments, and GIS-based vegetation and climate data. *Holocene* 16: 381-391.

Liang E.Y., Wang Y.F., Xu Y., Liu B.M., Shao X. (2010): Growth variation in Abies georgei var. smithii along altitudinal gradients in the Sygera Mountains, southeastern Tibetan Plateau. *Trees* 24: 363-373.

Linderholm H.W., Björklund J.A., Seftigen K., Gunnarson B.E., Grudd H., Jeong J.H., Drobyshev I., Liu Y. (2010): Dendroclimatology in Fennoscandia - from past accomplishments to future potential. *Climate of the Past* 6: 93-114.

Mitchell T.D., Jones P.D. (2005): An improved method of constructing a database of monthly climate observations and associated high-resolution grids. *International Journal of Climatology* 25: 693-712.

Nicolussi K., Kaufmann M., Melvin T.M., van der Plicht J., Schiessling P., Thurner A. (2009): A 9111 year long conifer tree-ring chronology for the European Alps: a base for environmental and climatic investigations. *Holocene* 19: 909-920.

Schweingruber F.H., Bartholin T., Schar E., Briffa K.R. (1988): Radiodensitometric-Dendroclimatological Conifer Chronologies from Lapland (Scandinavia) and the Alps (Switzerland). *Boreas* 17: 559-566.

Solomon S., Intergovernmental Panel on Climate Change., Intergovernmental Panel on Climate Change. Working Group I. (2007): Climate change 2007 : the physical science basis : contribution of Working Group I to the Fourth Assessment Report of the Intergovernmental Panel on Climate Change. Cambridge University Press.

Speer J.H. (2010): Fundamentals of tree-ring research. University of Arizona Press.

Tegel W., Vanmoerkerke J., Büntgen U. (2010): Updating historical tree-ring records for climate reconstruction. *Quaternary Science Reviews* 29: 1957-1959.

Wigley T.M.L., Briffa K.R., Jones P.D. (1984): On the Average Value of Correlated Time-Series, with Applications in Dendroclimatology and Hydrometeorology. *Journal of Climate and Applied Meteorology* 23: 201-213.

Chapter II: On the hidden significance of differing micro-sites on tree-ring based climate reconstructions

Elisabeth Düthorn[1], Lea Schneider[1], Oliver Konter[1], Philipp Schön[1], Mauri Timonen[2], Jan Esper[1]

[1] Department of Geography, Johannes Gutenberg University Becherweg 21, 55099 Mainz, Germany

[2] Finnish Forest Research Institute, Rovaniemi Research Unit 96301 Rovaniemi, Finland

(*Silva Fennica*, 2015, published)

Düthorn E., Schneider L., Konter O., Schön P., Timonen M., Esper J. (2015b): On the hidden significance of differing micro-sites on tree-ring based climate reconstructions. Silva Fennica 49.

1. Introduction

Tree rings are a common proxy to reconstruct past climate variations. At extreme locations, where climate determines tree growth, common variations in tree ring width (TRW) are observed and allow reconstructions of growing-season temperature history, especially referring to TRW measurements from high altitudinal or latitudinal sites (Fritts 1976, Grudd et al. 2002, Helama et al. 2002, Büntgen et al. 2006). In northern Fennoscandia the main species used for such dendrochronological and dendroclimatological studies is Scots pine (*Pinus sylvestris* L.) (Schweingruber et al. 1988, Eronen et al. 2002, Grudd et al. 2002, Büntgen et al. 2011, Gunnarson et al. 2011, Esper et al. 2012c, Melvin et al. 2013). Next to the pines also spruces grow in Northern Fennoscandia although their ecological limit does not extend as far north (Skrøppa 2003). Some spruce populations (*Picea abies* (L.) Karst.) are also included in tree-ring analyses and provide information about past summer temperatures (Gouirand et al. 2008, Büntgen et al. 2011).

In order to extend climate reconstructions beyond maximum tree-age, tree-ring chronologies are complemented with dead wood material (herein "relict material") preserved, for instance, in the numerous lakes of northern Fennoscandia (herein "subfossil material"). Overlapping life spans of these logs with recent material and homogeneous growth patterns, caused by common limiting factors, enable annual dating and combination of these samples with living trees (Fritts 1976). The Regional Curve Standardization (RCS) requires equivalent provenances of dead and living wood samples representing the same ecological and climate setting. Confining such homogeneous sampling sites, however, remains ambiguous. Düthorn et al. (2013) showed that even spatially close populations of *Pinus sylvestris* might comprise different micro-habitats which affect growth-rates and -patterns.

Micro-site effects are not only related to soil moisture content. Similar problems in the standardization process develop when combining samples from different elevations. In Gunnarson et al. (2011) a difference in altitude leads to variations in growth rates that need to be adjusted before the data are combined to mean chronologies. Similar limitations have been addressed in Melvin et al. (2013) when connecting relict and living material and updating the density datasets of Schweingruber (Schweingruber et al. 1988) and Grudd (Grudd 2008). The differences described in Melvin et al. (2013) are not only site related but also due to different methods of maximum latewood density measurements (Esper et al. 2014). Differing growth levels require a separate detrending for each dataset if a common detrending is applied. However, this multiple RCS approach results in a loss of low-frequency climate variability (Briffa and Melvin 2011). Another approach in achieving comparability is made by Tegel et al. (2010). Relict material of heterogeneous origin should not be combined with recent samples from a homogeneous site. Thus, they suggest to select the wood of the living part randomly, e.g. in sawmills, to assure heterogeneity in both datasets. The homogeneity of the different wood sources should be tested using the period of overlap.

Here, we analyze well replicated micro-sites of pines and spruces from northern Finland. Site and species related characteristics are identified by focusing on growth rates and climate sensitivity. In addition, the influence of collective detrending methods on compiled chronologies and temperature reconstructions is tested and discussed with reference to consequences of hidden ecological effects and common pitfalls for TRW-standardization (Esper et al. 2005b, Briffa and Melvin 2011). These effects could have influence on the longer term assessment of Climate Change as paleoclimate records. Our study detects this hidden statistical bias and details ideas to avoid developing erroneous time series

2. Material and Methods

2.1 Tree-ring data

The study area is located at 68.45°N and 27.36°E in northern Finland (Fig. II-1). The sampling design differentiates between trees growing directly at the lakeshore (Fig. II-1: "wet") and trees standing a few meters beyond the lakeshore (Fig. II-1: "dry") (Düthorn et al. 2013). The dataset consists of 50 *Picea abies* and 50 *Pinus sylvestris* per micro-site (spruce_wet/spruce_dry and pine_wet/pine_dry, respectively). After crossdating all tree-ring time series, measured to an accuracy of 1/100mm, we applied a Regional Curve Standardization (RCS) to remove biological age trends while keeping low-frequency information (Briffa et al. 1992, Esper et al. 2003). This method generates a mean growth curve by aligning all TRW-series by cambial age. This "Regional Curve" (RC) represents the local growth behavior and displays the mean age trend of tree growth at a certain site. By dividing every single TRW-series by this RC the biological age effect is removed.

2.2 Climate data

Climate-growth relationships are assessed for different climate parameters. We used the 0.5° x 0.5° CRU TS 3.10 dataset for comparison with precipitation averaged over the 66-70°N and 25-30°E grid-cells (Mitchell and Jones 2005). Over the same area a snow index, based on surface color, is extracted from the Rutgers University Global Snow Lab (Brown et al. 2003). Monthly temperature data for the 20th century are derived from the nearby station Sodankyla. The common period 1931-2011 only covers 81 years since old trees were absent at one of the microsites. The period is defined by the maximum overlap of the micro-site chronologies with a minimum replication of 5 series. For large-scale temperature analysis, the tree ring chronologies were correlated against mean June-July (JJ) values of various grid cells over northern Europe.

2.3 Artificial relict data

A millennial dataset of spruce TRW is not available for northern Fennoscandia. Thus, artificial data had to be created for assessing effects of micro-sites on long-term spruce chronologies. We adjusted the relict part of the subalpine spruce chronology of Büntgen et al. (2005b) to match the properties of a lakeshore site in northern Fennoscandia corresponding to the original habitat of submerged logs. The distant setting of the subalpine relict material results in a mismatch of annual variation in the period of overlap with the fennoscandian living datasets. But more important in assessing a potential long-term bias is to retain the species-specific age-related growth trends. Therefore, we synchronized the regional curve of the subalpine relict spruce data to the spruce_wet dataset by removing the original age trend of the alpine tree ring series by applying RCS detrending. The detrended single series were multiplied with the mean growth rate of the spruce_wet site (Fig. II-5) assuming that trees at the lakeshore show equal mean growth curves like subfossil logs (Düthorn et al. 2013). Consequently, the mean growth rate of the subalpine chronology is similar to the mean growth rate of the lakeshore spruce site. Finally, living and relict material was combined to two long-term spruce chronologies with different recent tails (wet and dry).

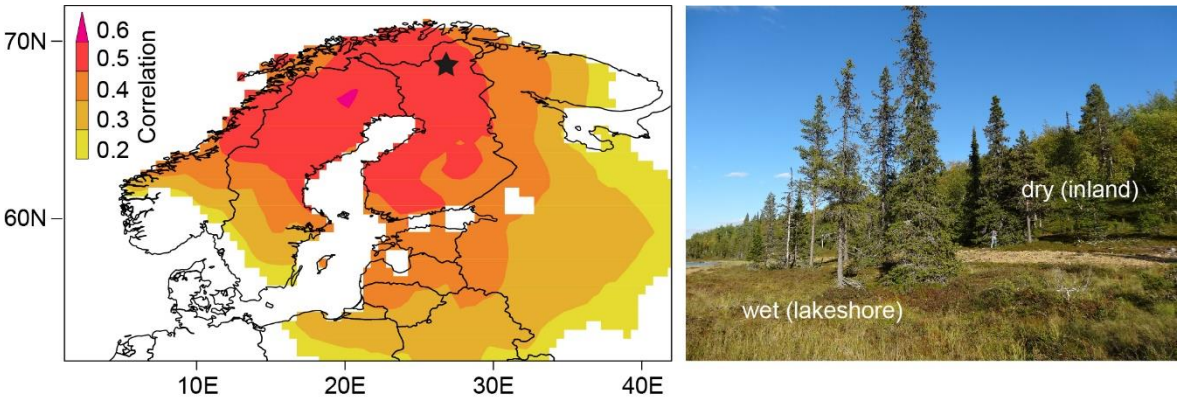

Figure II-1: Sampling area in northern Finland (black star) with the spatial correlation of the spruce chronology with gridded June-July temperatures (CRU TS 3.10, p<5%) over the 1931-2009 period. The picture on the right side shows the micro-site sampling design. Trees growing at the lakeshore (on the inland slope) with more moist (dry) soil conditions are termed “wet” (“dry”).

3. Results

3.1 Variability of micro-site chronologies

Both, wet and dry RCS chronologies display the similar patterns in high and low frequency variations (Fig. II-2) and correlate at r = 0.59 (spruce) and r = 0.68 (pine) for the last 81 years. The consistent shape of these micro-site chronologies shows that annual variations in tree growth at both stands are controlled by a common external driver.

RCS creates a chronology whose mean value is approximately 1.0 and separately processing micro sites with RCS will remove any between-site differences in the mean growth rates of trees. The resulting spruce and pine chronologies allow inter-species comparisons and reveal disparities in growth on long and short terms (Fig. II-2c, r = -0.2). Especially the drop of the pine chronology in the beginning of the 20th century indicates extreme species-specific growth-disturbance.

After this drop and a subsequent steep increase of growth, the trend for the last 90 years is slightly decreasing while the spruces are much more complacent in their low-frequency signal. Both species exhibit an unequal age structure and replication. While the number of spruce trees declines linearly before AD 2000, there are two major steps in the pine chronology replication (1940-1950 and 1980-1990; Fig. II-2d) resulting in a lower mean age of pine individuals in the second half of the 20th century.

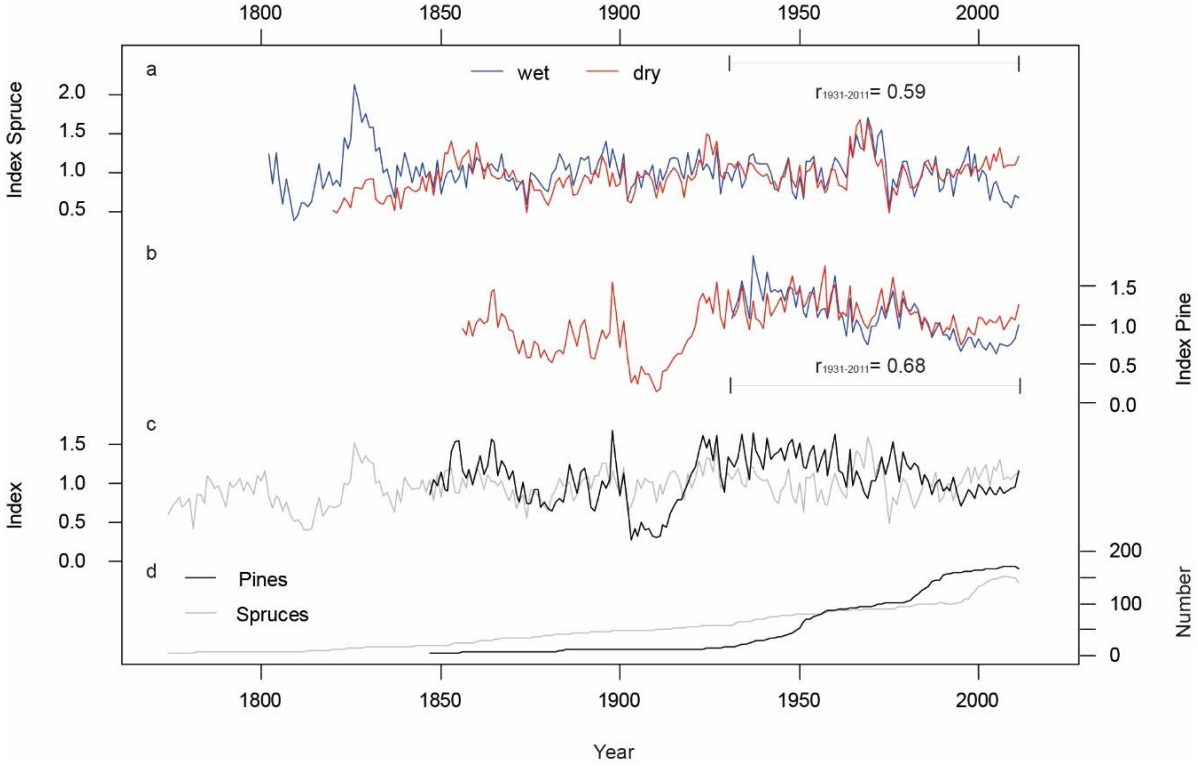

Figure II-2: Micro-site and species specific chronologies after Regional Curve Standardization. a) Spruce chronologies from the wet (blue) and dry (red) micro-sites. b) Same as in a) but for pine. c) Pine (black) and spruce (grey) site chronologies, each including wet and dry trees. d) Numbers of measurement series averaged in the site chronologies. All chronologies were truncated at n < 4.

3.2 Climate growth relationships

The response of the trees to climate is displayed by the high correlation for spruce TRW chronologies with summer temperatures (Fig. II-3). Monthly temperature responses are calculated for the previous and current year using temperature data from Sodankyla over the 1931-2011 common period (Fig. II-3). Strongest climate-growth relationships for spruces on a monthly basis are detected for June (r = 0.49), while the highest seasonal response is found in JJ (r = 0.55) and JJA (r = 0.54). Pines only correlate insignificantly (r = 0.30) with temperatures in July (Fig. II-3), which is also the month of

highest wood production (Schmitt et al. 2004). Also the spruce micro-site chronologies reveal robust June temperature signals, whereas data from both pine micro-sites display slightly negative correlation values in June. Other climate parameters, e.g. precipitation and snow cover, do not show significant influences on microsite- or species-related tree growth.

The impact of the previous year temperature on the current year growth is a well-known feature of TRW data (Briffa et al. 1988, Kozlowski and Pallardy 1996). This memory effect is displayed by strong lag-1 autocorrelations for the chronologies (pine: $ac_{1931\text{-}2011} = 0.61$, spruce: $ac_{1931\text{-}2011} = 0.48$).

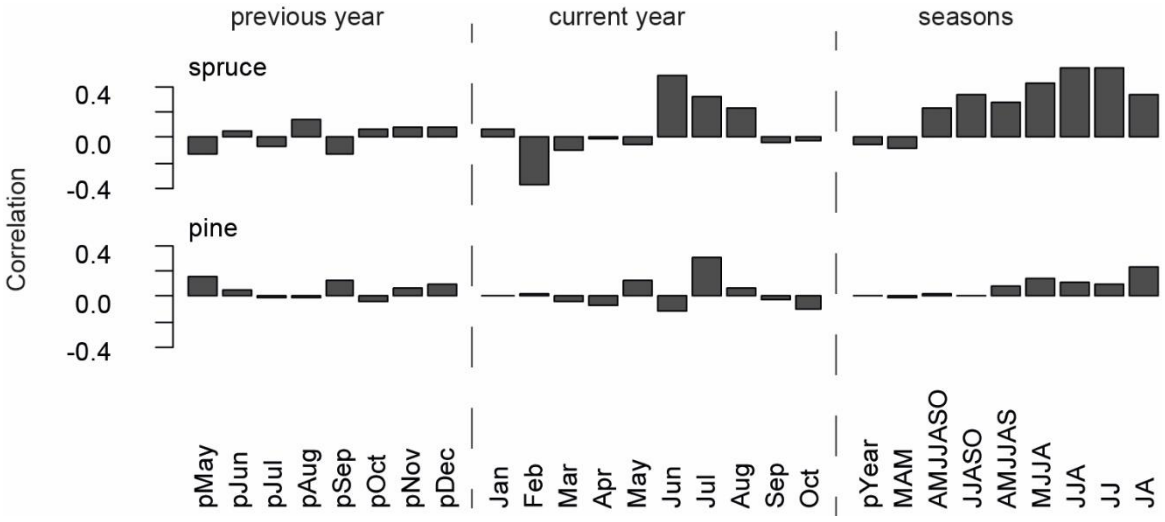

Figure II-3: Correlation of spruce and pine chronologies with temperature data recorded at Sodankyla over the 1931-2011 common period. Correlations are calculated for previous year and current year months, as well as seasonal temperature data.

The differences in the monthly climate response of both species indicates characteristic species-related biological and ecological demands. Figure II-4 shows the regional climograph combining temperature, precipitation and the snow cover index. Between May and October the mean temperature is above 0°C while only the summer temperatures (June-September) rise above the physiologically important threshold of 5°C (Körner 2012) with simultaneously peaking precipitation values, defining the vegetation period. At high latitudes a full snow-cover from November to May is the key constraint for vegetation (Vaganov et al. 1999). In June and October a light snow cover is detected while for the period July-August-September (JAS) no snow is reported. The strong decrease of the snow index between May and June is an indicator for high amounts of melt water, introducing very wet conditions in early summer.

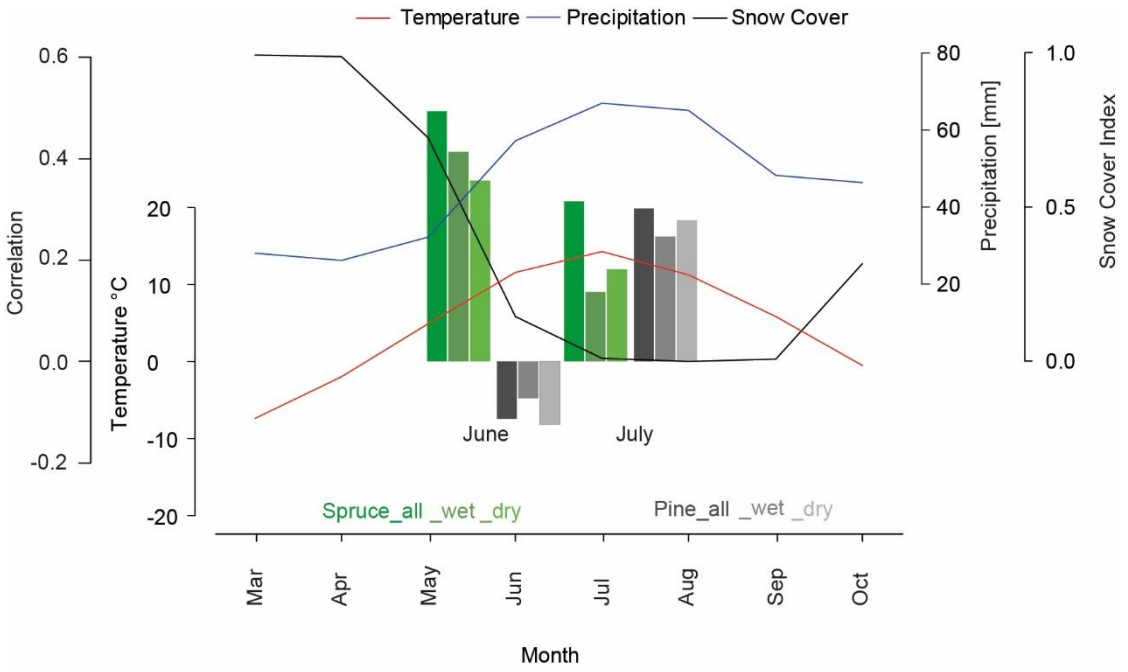

Figure II-4: Monthly mean temperature (red), precipitation (blue) and snow cover (black) for northern Fennoscandia over the 1971-2000 period. Barplot represents correlations of different tree-ring chronologies (site and micro-sites) over the 1931-2011 period with June and July temperatures.

3.3 Growth rate differences

Micro-site effects in pine chronologies are already recognized (Düthorn et al. 2013) but the ecological effects for spruces are unknown so far. Figure II-5 shows the Regional Curves for the wet and dry spruce sites (wet_RC/dry_RC) and a distinct offset between both curves for the first 200 years of growth. At the dry site mean annual increment exceeds 1.5 mm for the first 50 years and declines afterwards linearly to an annual increment of 0.6 mm after 200 years of growth. At the wet site growth does not exceed 1 mm/year, and after 200 years it reaches a mean growth of only 0.4mm/year. We assume that wet, anaerobic soil conditions limit tree growth especially in the juvenile growth phase. This effect is confirmed by the RC´s of the pines analyzed in this study, where also the wet micro-site shows less wood production compared to the dry site. The flat wet_RC mimics characteristics of suppressed growth in closed canopy stands (Helama et al. 2005b).

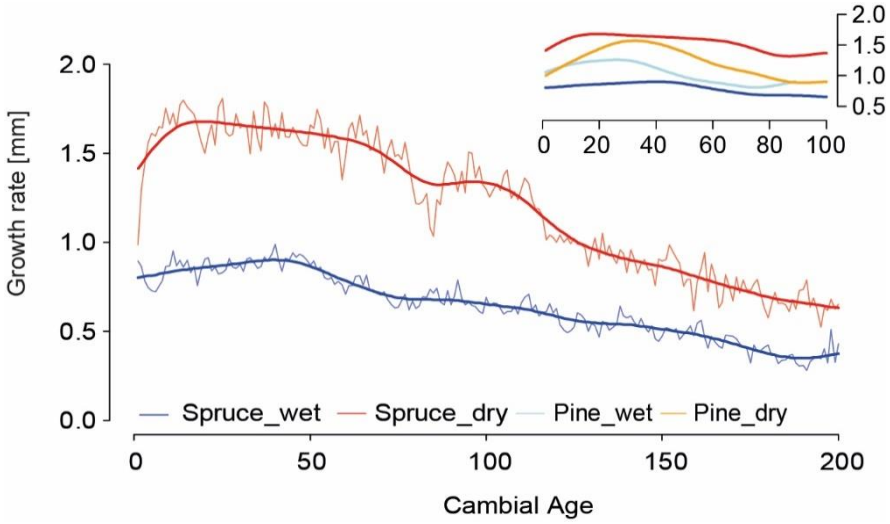

Figure II-5: Age-aligned regional curves and 40-year smoothed mean curves (thick lines) of the spruce micro-site chronologies. Blue (red) represents lakeshore (inland) trees. Regional curves are shown over the first 200 years. Upper panel shows smoothed regional curves of spruce and pine micro-site chronologies for the first 100 years.

3.4 Combined chronologies and tail test

For tests on long-term trends, TRW series from the adjusted "subfossil" data were combined with either TRW series from the wet or dry micro-sites. We applied RCS to both combined datasets (subfossil+wet and subfossil+dry). The overlapping period of relict and living TRW data (Fig. II-6d) is defined by the start of the living spruce chronology (1695) and the last year with data of the relict part (1833). During these 139 years of overlap variance is reduced since growth variations are not coherent for the alpine and fennoscandian region. However, multi-centennial trends bridge this period and are preserved. The final dataset covers the last eight centuries (1163-2011) with a minimum replication of 6 series. The climate-growth relationship of spruce and JJ temperature (r_{spruce} = 0.54) was used to calculate a linear regression model for both long-term chronologies. Finally, the tree-ring indices were transformed into JJ temperature anomalies with respect to the 1961-1990 period (Fig. II-6a and II-6b).

Both reconstructions show synchronized variations and mean values for the most recent period back to 1800. Prior to 1800 the low-frequency trends are very similar but a peculiar level offset is obvious between Fig. II-6a and b. The wet_reconstruction indicates colder (14th and 17th century) and warmer (end of the 13th century and 16th century) periods compared to the 1961-1990 period. The differences vary between +1°C and -1°C. In contrast, the dry_reconstruction generally points to colder conditions prior to 1800, fluctuating around -2°C except for the late 13th century. By scaling both reconstructions over the early period (1163-1694, dashed line in Fig. II-6c) the high coherency between both time series becomes obvious whereas for the most recent period a distinct level offset appears.

No millennial cooling trend is retained in the dry_reconstruction, whereas the wet_reconstruction reveals slightly such a trend (thick dotted line in Fig. II-6a and Fig. II-6b). These differences can be traced back to the higher growth rates in dry stands which are not sufficiently reflected in the RC and thus not eliminated after detrending.

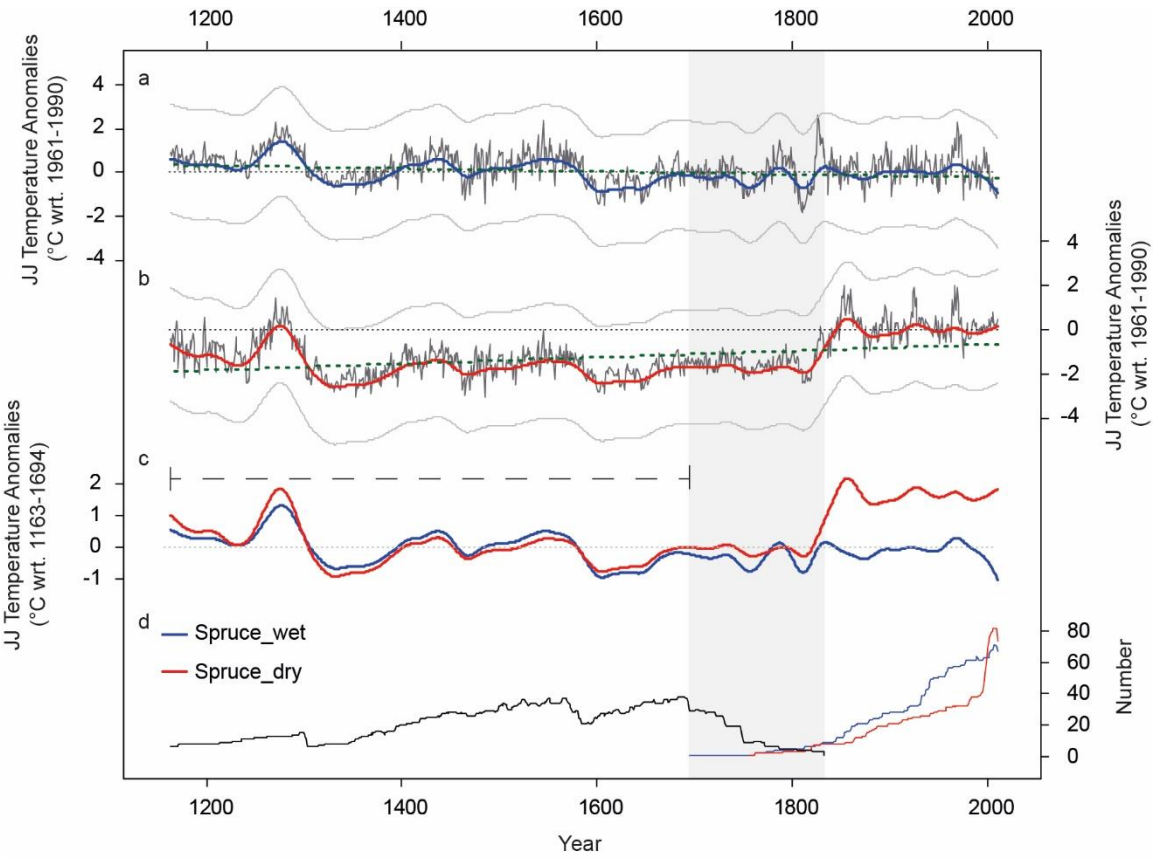

Figure II-6: JJ temperature reconstructions based on long-term spruce chronologies (black). a) Lakeshore wood material (wet) and b) inland (dry) material is used for the living part. The reconstruction extents back to 1163 AD. Low frequency variability of decadal to centennial timescale is displayed by colored lines (50 year spline filter). Green dotted lines show the trend over the last 8 centuries. Uncertainties (+/- standard error) are displayed as error band (grey lines). Thin dotted lines are the 0°C anomaly level. c) Smoothed JJ temperature reconstructions scaled over the 1163-1694 common period (only relict material; black dashed line). d) Replication of relict (black), living_wet (blue) and living_dry (red) tree ring series. Grey area displays the maximum overlap (1695-1833 period) of the different wood sources.

4. Discussion

Tree growth in higher latitudes is directly dependent on the ecological setting at the micro-sites. Independent of the tree species, growth rates are lower for trees growing at the lakeshore. Our results indicate that tree growth at lakeshores is limited and suppressed. Düthorn et al. (2013) assumed that this effect is linked to a high groundwater table and hence anaerobic soil conditions. This effect is stronger for spruce compared to pine.

After removing site-specific growth characteristics spruce and pine chronologies from northern Finland show high intra-species homogeneity resulting from a common and site-independent sensitivity to external factors (i.e. summer temperature for spruce). In contrast to the intra-species homogeneity, no inter-species agreement can be detected. The inter-species discrepancy may indicate that spruce and pine respond different to external influences. But as displayed in Büntgen et al. (2011) and Gouirand et al. (2008) both species are principally sensitive to summer temperatures in these latitudes.

In this study we found a higher sensitivity to summer temperatures for spruces and a weaker response in pines. Our study area is located 8 km southwest from a pine population in Laanila from which a significant and temporally robust summer temperature signal ($r = 0.50$) is reported for TRW (McCarroll et al. 2003). Low correlations with temperature despite related growth patterns among wet and dry sites indicate a more complex growth response at our site. The site-related disturbances, either of climatic, anthropogenic or ecological origin, affect the temperature sensitivity of the pines.

Therefore, the differences need to be associated with differing ecological needs of the species. The indistinct temperature response of pines suggests that this species cannot deal with the moist soil conditions caused by high precipitation sums and melt water runoff and hence sprouts out later when temperatures are higher and soils drier. Spruces in contrast, start growing as early as temperatures rise over the 5°C threshold in June. This species can also deal with light snow cover and sprouts earlier leading to a prolonged vegetation period as expressed in the correlations of the micro-site chronologies against June and July temperatures (barplot in Fig. II-4). Therefore pines are most sensitive to temperatures in July while spruces already respond to June temperatures. Spruces also show a robust temperature signal spanning from June to July and thereby offering the opportunity to retain information about past early growing season temperatures.

The establishment of a long-term TRW or density chronology based on subfossil spruces is hindered by the natural process of wood decomposition. The lower content of resin compared to pines results in a poor conservation and preservation of tree trunks in lakes or lake sediments. The use of "artificial" data for the relict part allows us to point to the effects that micro-sites could have on tree ring chronologies but not to compare it with existing temperature reconstructions of this region, as Torneträsk (Grudd et al. 2002) or Nscan (Esper et al. 2012c). In order to demonstrate that the micro-habitat of living trees matters if recent material is combined with relict wood, we calculated two reconstructions with different recent ends ("wet" and "dry"). The hypothesis that lakeshore trees comprise the same ecological information as subfossil trees, formerly standing at the lakeshore, justifies the assumption that growth rates for the "artificial" part should mimic growth rates of living spruces from the lakeshore. In other words, the sampling design for a living tree site should aim at a close representation of the ecological setting for relict trees in order to avoid problems when collective detrending methods are applied (see "Tail Test"; Düthorn et al. (2013)).

Despite the homogeneity of the short micro-site chronologies the long reconstructions diverge in the most recent part. Although this effect could be misinterpreted as a "hidden" information contained in the micro-sites, it is basically only the result of faster tree growth at the inland site. As RCS is a collective detrending method relict and recent tree ring series were standardized by dividing every single raw series through the same mean growth rate. But the division by an undersized RC for trees from the dry micro-site (wet < dry) and an overestimated growth rate for the relict material creates biases in the chronologies' long term trend reconstructions. In conclusion, the divergence of the temperature reconstructions could be traced back to different growth behavior according to micro-habitats in combination with RCS detrending.

In order to avoid the propagation of these effects into multi-centennial climate-reconstructions, where they can obscure long-term trends (Esper et al. 2012c), a closer look at the sampled material is necessary. The problem of combining living and historical material is also reported in various studies (Tegel et al. 2010, Gunnarson et al. 2011, Melvin et al. 2013) showing that this "hidden" micro-site effect is important in connection with updating and improving long-term chronologies. Beside the effects of sampling strategies on mean chronologies (Nehrbass-Ahles et al. 2014) special care is needed in the selection of statistical methods used to transform tree-ring data into climate reconstructions (Esper et al. 2005b, Esper et al. 2005a, Moberg et al. 2006).

Our study contributes a micro-site assessment for a new species to the existing studies and should help to avoid common pitfalls in developing a long term spruce chronology. Also a higher comparability of the climate signal stored in the trees of the same micro habitat (relict vs. wet) should increase the reliability of long term tree ring chronologies.

5. Conclusion

Millennial-long summer temperature reconstructions are a valuable product of dendroclimatology. Their development, however, requires a thorough assessment of data characteristics and methods as proven by a number of recent studies (Düthorn et al. 2013, Nehrbass-Ahles et al. 2014). This extended micro-site study in northern Finland is designed to expose potential pitfalls in sampling-site selection. Along a lake-inland gradient tree-growth of spruces and pines differs significantly regarding mean annual increment and climate sensitivity. The climate-growth relationship between pines and July temperatures is weak, whereas spruces show a robust June-July signal. The growth rates of both species indicate that lakeshore trees grow significantly slower than trees in the inland do. Even though the micro-site chronologies themselves show high coherence, this site-related effect is responsible for offsets in the mean of long-term chronologies compiled of relict and recent tree-samples, mainly when wood from different ecological provenances is used. Micro-site ecology matters even more for spruce trees than for pines. Consequently, the hidden micro-site effect constrains the spatial comparability of 'Regional' Curves and requires species-independent caution in the development of temperature reconstructions based on a collective detrending method. Due to the importance of RCS detrending regarding the

preservation of low-frequency information, it is necessary to analyze the ecological setting and growth behavior of subsets of wood samples if it is intended to combine these into a single chronology. Next to the recommendations for future studies this effect should also be taken into account while interpreting existing temperature reconstructions.

This study assumes that subfossil wood has a similar growth rate as living lakeshore trees and uses this hypothesis for simulating "artificial" data. Good preserved relict spruce material would offer new possibilities to interpret micro-site effects on long term spruce chronologies.

References

Briffa K.R., Jones P.D., Bartholin T.S., Eckstein D., Schweingruber F.H., Karlen W., Zetterberg P., Eronen M. (1992): Fennoscandian Summers from Ad-500 - Temperature-Changes on Short and Long Timescales. *Climate Dynamics* 7: 111-119.

Briffa K.R., Jones P.D., Pilcher J.R., Hughes M.K. (1988): Reconstructing Summer Temperatures in Northern Fennoscandinavia Back to Ad 1700 Using Tree-Ring Data from Scots Pine. *Arctic and Alpine Research* 20: 385-394.

Briffa K.R., Melvin T.M. (2011): A Closer Look at Regional Curve Standardization of Tree-Ring Records: Justification of the Need, a Warning of Some Pitfalls, and Suggested Improvements in Its Application. In: Hughes, MK, Swetnam, TW, Diaz, HF (eds): Dendroclimatology. Springer Netherlands. 113-145.

Brown R.D., Brasnett B., Robinson D. (2003): Gridded North American monthly snow depth and snow water equivalent for GCM evaluation. *Atmosphere-Ocean* 41: 1-14.

Büntgen U., Bellwald I., Kalbermatten H., Schmidhalter M., Frank D.C., Freund H., Bellwald W., Neuwirth B. et al. (2006): 700 years of settlement and building history in the Lotschental, Switzerland. *Erdkunde* 60: 96-112.

Büntgen U., Frank D.C., Schmidhalter M., Neuwirth B., Seifert M., Esper J. (2005b): Growth/climate response shift in a long subalpine spruce chronology. *Trees-Structure and Function* 20: 99-110.

Büntgen U., Raible C.C., Frank D., Helama S., Cunningham L., Hofer D., Nievergelt D., Verstege A. et al. (2011): Causes and Consequences of Past and Projected Scandinavian Summer Temperatures, 500-2100 AD. *Plos One* 6.

Düthorn E., Holzkämper S., Timonen M., Esper J. (2013): Influence of micro-site conditions on tree-ring climate signals and trends in central and northern Sweden. *Trees* 27: 1395-1404.

Eronen M., Zetterberg P., Briffa K.R., Lindholm M., Merilainen J., Timonen M. (2002): The supra-long Scots pine tree-ring record for Finnish Lapland: Part 1, chronology construction and initial inferences. *Holocene* 12: 673-680.

Esper J., Cook E.R., Krusic P.J., Peters K., Schweingruber F.H. (2003): Tests of the RCS method for preserving low-frequency variability in long tree-ring chronologies. *Tree-Ring Research* 59: 81-98.

Esper J., Düthorn E., Krusic P.J., Timonen M., Büntgen U. (2014): Northern European summer temperature variations over the Common Era from integrated tree-ring density records. *Journal of Quaternary Science*.

Esper J., Frank D.C., Timonen M., Zorita E., Wilson R.J.S., Luterbacher J., Holzkamper S., Fischer N. et al. (2012c): Orbital forcing of tree-ring data. *Nature Climate Change* 2: 862-866.

Esper J., Frank D.C., Wilson R.J.S., Briffa K.R. (2005a): Effect of scaling and regression on reconstructed temperature amplitude for the past millennium. *Geophysical Research Letters* 32.

Esper J., Wilson R.J.S., Frank D.C., Moberg A., Wanner H., Luterbacher J. (2005b): Climate: past ranges and future changes. *Quaternary Science Reviews* 24: 2164-2166.

Fritts H.C. (1976): Tree rings and climate. Academic Press.

Gouirand I., Linderholm H.W., Moberg A., Wohlfarth B. (2008): On the spatiotemporal characteristics of Fennoscandian tree-ring based summer temperature reconstructions. *Theoretical and Applied Climatology* 91: 1-25.

Grudd H. (2008): Tornetrask tree-ring width and density AD 500-2004: a test of climatic sensitivity and a new 1500-year reconstruction of north Fennoscandian summers. *Climate Dynamics* 31: 843-857.

Grudd H., Briffa K.R., Karlen W., Bartholin T.S., Jones P.D., Kromer B. (2002): A 7400-year tree-ring chronology in northern Swedish Lapland: natural climatic variability expressed on annual to millennial timescales. *Holocene* 12: 657-665.

Gunnarson B.E., Linderholm H.W., Moberg A. (2011): Improving a tree-ring reconstruction from west-central Scandinavia: 900 years of warm-season temperatures. *Climate Dynamics* 36: 97-108.

Helama S., Lindholm M., Timonen M., Merilainen J., Eronen M. (2002): The supra-long Scots pine tree-ring record for Finnish Lapland: Part 2, interannual to centennial variability in summer temperatures for 7500 years. *Holocene* 12: 681-687.

Helama S., Timonen M., Lindholm M., Merilainen J., Eronen M. (2005b): Extracting long-period climate fluctuations from tree-ring chronologies over timescales of centuries to millennia. *International Journal of Climatology* 25: 1767-1779.

Körner C. (2012): Alpine Treelines. Springer.

Kozlowski T.T., Pallardy S.G. (1996): Physiology of Woody Plants. Elsevier Science.

McCarroll D., Jalkanen R., Hicks S., Tuovinen M., Gagen M., Pawellek F., Eckstein D., Schmitt U. et al. (2003): Multiproxy dendroclimatology: a pilot study in northern Finland. *Holocene* 13: 829-838.

Melvin T.M., Grudd H., Briffa K.R. (2013): Potential bias in 'updating' tree-ring chronologies using regional curve standardisation: Re-processing 1500 years of Tornetrask density and ring-width data. *Holocene* 23: 364-373.

Mitchell T.D., Jones P.D. (2005): An improved method of constructing a database of monthly climate observations and associated high-resolution grids. *International Journal of Climatology* 25: 693-712.

Moberg A., Sonechkin D.M., Holmgren K., Datsenko N.M., Karlen W., Lauritzen S.E. (2006): Highly variable Northern Hemisphere temperatures reconstructed from low- and high-resolution proxy data (vol 433, pg 613, 2005). *Nature* 439: 1014-1014.

Nehrbass-Ahles C., Babst F., Klesse S., Nötzli M., Bouriaud O., Neukom R., Dobbertin M., Frank D. (2014): The influence of sampling design on tree-ring based quantification of forest growth. *Global Change Biology*: n/a-n/a.

Schmitt U., Jalkanen R., Eckstein D. (2004): Cambium dynamics of Pinus sylvestris and Betula spp. in the northern boreal forest in Finland. *Silva Fennica* 38: 167-178.

Schweingruber F.H., Bartholin T., Schar E., Briffa K.R. (1988): Radiodensitometric-Dendroclimatological Conifer Chronologies from Lapland (Scandinavia) and the Alps (Switzerland). *Boreas* 17: 559-566.

Skrøppa T. (2003): Technical guidelines for genetic conservation and use for Norway spruce Picea abies. *EUFORGEN Technical Guidelines for Genetic Conservation and Use*.

Tegel W., Vanmoerkerke J., Büntgen U. (2010): Updating historical tree-ring records for climate reconstruction. *Quaternary Science Reviews* 29: 1957-1959.

Vaganov E.A., Hughes M.K., Kirdyanov A.V., Schweingruber F.H., Silkin P.P. (1999): Influence of snowfall and melt timing on tree growth in subarctic Eurasia. *Nature* 400: 149-151.

Chapter III: Northern European summer temperature variations over the Common Era from integrated tree-ring density records

Jan Esper,[1] Elisabeth Düthorn,[1] Paul Krusic,[2,3] Mauri Timonen[4] and Ulf Büntgen[5-7]

[1] *Department of Geography, Johannes Gutenberg University, 55099 Mainz, Germany*

[2] *Department of Physical Geography and Quaternary Geology, Stockholm University, 10691 Stockholm, Sweden*

[3] *Navarino Environmental Observatory, Messinia, Greece*

[4] *Finnish Forest Research Institute, Rovaniemi Research Unit, 96301 Rovaniemi, Finland*

[5] *Swiss Federal Research Institute WSL, 8903 Birmensdorf, Switzerland*

[6] *Oeschger Centre for Climate Change Research, University of Bern, 3012 Bern, Switzerland*

[7] *Global Change Research Centre AS CR, v.v.i., Bělidla 986/4a, CZ-60300 Brno, Czech Republic*

(*Journal of Quaternary Science*, 2014)

Esper J., **Düthorn E**., Krusic P.J., Timonen M., Büntgen U. (2014): Northern European summer temperature variations over the Common Era from integrated tree-ring density records. Journal of Quaternary Science.

1. Introduction

Conifer tree-rings are composed of large cells with thin walls formed in the first weeks of the vegetation period, followed by small cells with thick walls formed throughout high and late summer (Moser et al. 2010). This change between earlywood and latewood structure, along with growth dormancy during winter, is the foundation for distinguishing one ring from another and for assigning each ring to a particular calendar year (Fritts 1976). The development of high precision radiography in the 1970s permitted use of X-ray sensitive films to detect changes in the physical properties of wood cell structure and quantify them in form of high-resolution density profiles in units of g/cm^3 (Schweingruber et al. 1978). In one of the first applications of this new technique to palaeoclimatic research, a wood density chronology extending back to AD 441 was developed in the 1980s (Schweingruber et al. 1988), integrating samples from living trees and relict wood of *Pinus sylvestris* from the lake Torneträsk region in northern Sweden (Bartholin and Karlén 1983). The maximum latewood density (MXD), a then novel parameter representing the microscopic area of thickest walls and smallest lumina towards the end of a ring, was found to correlate best with regional instrumental climate data (up to ~ r = 0.8) and subsequently used for reconstructing summer temperatures back to the 5th century AD (Schweingruber et al. 1988, Briffa et al. 1990, Briffa et al. 1992).

This widely recognized reconstruction from Torneträsk (hereafter: Torn) has since been updated repeatedly by the addition of new MXD measurements from living trees, thereby advancing the most recent year of the chronology into the 21st century (Grudd 2008). The latest of these publications (Melvin et al. 2013) deals with removing trend biases that arose from combining the original, analogue measurements developed in the 1980s (Schweingruber et al. 1988) with digital update measurements developed in the 2000s using innovative laboratory technologies (Grudd 2008). Doing so involved changing the mean and variance of the digital measurement series to match the characteristics of the original data, as well as treating the original and update datasets independently in the process of detrending and chronology development (Melvin et al. 2013). The recombined relict and living tree chronologies, to form a temperature reconstruction extending back to AD 441, indicated stronger 20th century warmth than previously reported, but also resulted in a better coherence between the temperature histories derived from MXD and the generally more noisier tree-ring width (TRW) data (Melvin et al. 2013).

This widely recognized reconstruction (hereafter: Torn) has since been updated repeatedly by the addition of new MXD measurements from living trees, thereby advancing the most recent year of the chronology into the 21st century (Grudd 2008). The latest of these publications (Melvin et al. 2013) deals with removing trend biases that arose from combining the original, analogue measurements developed in the 1980s (Schweingruber et al. 1988) with the digital update measurements developed in the 2000s using innovative laboratory technologies (Grudd 2008). Doing so included changing the mean and variance of the new measurement series to match the characteristics of the original data, as well as

treating the original and update datasets independently in the process of detrending and chronology development (Melvin et al. 2013). The recombined relict and living tree chronologies, to form a temperature reconstruction extending back to AD 441, indicated stronger 20th century warmth than previously reported, but also resulted in a better coherence of the temperature histories derived from MXD with the generally more noisier tree-ring width (TRW) data (Melvin et al. 2013).

In addition to the widely cited Torn reconstructions (overview in Büntgen et al. 2011, Büntgen et al. 2012), a new pine MXD record, derived from sub-fossil wood preserved in shallow lakes from Finnish Lapland (Eronen et al. 2002), has been developed providing summer temperature variations back to 138 BC (Esper et al. 2012c; hereafter: N-Scan). The sub-fossil component of this reconstruction originates from an extended region north of 67˚N and was linked to present by samples from living pines growing on lakeshores (Düthorn et al. 2013) in northern Finland and Sweden, including two sites near Torneträsk. N-Scan includes more trees than any other MXD chronology, and has been used to describe a millennial-scale cooling trend related to long-term, orbital insolation changes (Esper et al. 2012c). Subsequent work (Esper et al. 2012b) showed that there still exist substantial differences among the various tree-ring-based climate reconstructions from Fennoscandia, indicating our poor understanding of the pre-instrumental temperature amplitude even in geographically limited regions.

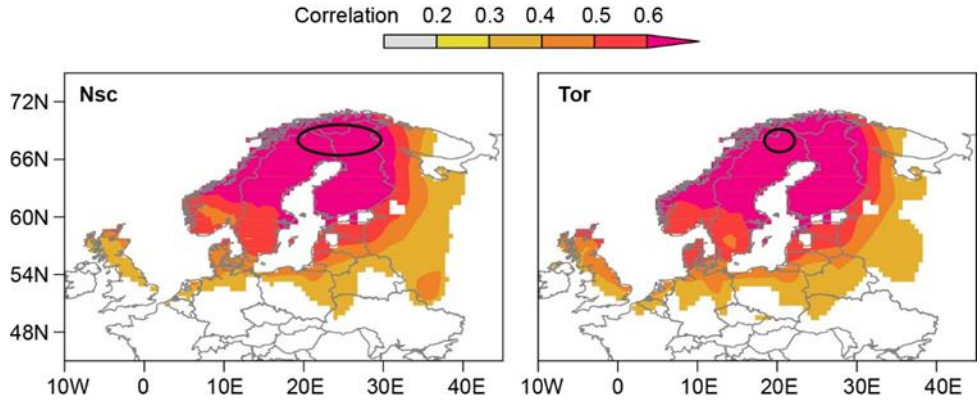

Figure III-1: Correlation fields of the N-Scan and Torn MXD chronologies (black circles) with gridded (0.5° resolution) summer temperatures calculated over the 1901-2006 period.

In an effort to reconcile some of the density data from this region, we here assess the world's two longest MXD based climate reconstructions, Torn (Melvin et al. 2013) and N-Scan (Esper et al. 2012c), and combine portions of both to produce a new summer temperature history for northern Europe from 17 BC to the present. The rationale for combining these data is supported by the chronologies' coherent spatial temperature fields (Fig. III-1), and the desire to mitigate complications in the process of selecting proxy records for the development of large-scale temperature reconstructions (e.g., Esper et al. 2002, D'Arrigo et al. 2006, Mann et al. 2008, Ljungqvist 2010, Ljungqvist et al. 2012).

In this paper we first examine the similarities and differences between the Torn and N-Scan reconstructions, and revisit the challenge of integrating digital and analog MXD data. We describe a manner of selecting coherent MXD data, and use this subsample to produce a new temperature reconstruction for northern Scandinavia spanning the Common Era. We conclude by briefly addressing the long-term cooling trend inherent to our new reconstruction, and demonstrate the value of this record for assessing short-term cooling extremes following large volcanic eruptions.

2. Data and Methods

2.1 Torn and N-Scan MXD data

While the Torn and N-Scan reconstructions are both derived from MXD data and share the same spatial temperature pattern, the records differ in (i) the source of their dead wood samples (lake/sub-fossil and fallen/relict), (ii) the geographical area from which samples were collected, (iii) the number of MXD measurement series and (iv) the X-ray technology used to measure MXD (details in Esper et al. 2012c, Melvin et al. 2013). Whereas the Torn samples all originate from locations surrounding Lake Torneträsk, in the transition zone between the boreal forest and low Arctic tundra, N-Scan integrates samples from 17 lakes and lakeshore sites spread over Finnish Lapland and the Torneträsk region. N-Scan contains substantially more dead wood MXD series (372 subfossil samples) than the Torn chronology (47 fallen/relict samples) making it the most well-replicated and longest MXD chronology in the world.

The 372 N-Scan sub-fossil samples were combined with 215 samples from living trees collected on the shores of four lakes located in northern Finland and Sweden. The 47 Torn log samples were originally combined with 18 samples from living trees collected in 1980 (Schweingruber et al. 1988), then updated with 35 samples from living trees in 2004 (Grudd 2008), and again with an additional 30 living tree samples in 2010 (Melvin et al. 2013). Whereas all 587 N-Scan MXD series were measured at the WSL in Birmensdorf (Switzerland) using a Walesch X-ray densitometer (Schweingruber et al. 1978), the Torn chronology was produced using different technologies in different laboratories: the original 65 Torn MXD series were also measured with a Walesch densitometer in Birmensdorf, but subsequent updates were measured in Stockholm and Kiruna, Sweden, using an ITRAX digital radiographic camera. The 587 MXD series used in (Esper et al. 2012c) are hereafter named E12, the 65 series used in Schweingruber et al. (1988) are named S88 and the 65 updating series used in Melvin et al. (2013) are named M13.

2.2 Reconstruction assessment

Coherence between the Torn and N-Scan reconstructions was assessed using Pearson correlation coefficients calculated over 100-year sliding windows. The procedure was applied to the original reconstructions as well as to first-differenced versions of the two records to evaluate common variation at both high and low frequencies. The interseries correlation (Rbar), a metric based on the correlation among all MXD measurement series in a chronology (Cook and Kairiukstis 1990), was used to estimate the internal coherence of the reconstructions. Rbar was also calculated over 100-year windows shifted along the chronologies. Minimum least square regressions were fitted to the reconstructions to assess the long-term trends inherent to the time series over their common AD 517–2006 period, as well as the AD 517–1900, and the 138 BC to AD 1900 (NScan only) periods.

2.3 Detrending and chronology development

Raw MXD measurement series are characterized by an increase from ~ 0.5 to 0.7 g/cm^3 over the first 30 years of a tree's lifespan, followed by a gradual decrease from ~ 0.7 to 0.6 g/cm^3 through plant maturation (see Fig. III-4A). This age trend has to be removed before averaging MXD series in a mean chronology, otherwise the combination of juvenile and adult MXD values, rather than temperature, determines the changing chronology levels back in time(Bräker 1981). Age trend is here removed using Regional Curve Standardization (RCS; Briffa et al. 1992, Esper et al. 2003), a detrending method capable of retaining the full variance frequency spectrum in the resulting chronologies (Bunde et al. 2013, Franke et al. 2013), from inter-annual to millennial scales (Esper et al. 2012c). Additional methods that have been suggested in conjunction with RCS (Melvin and Briffa 2008) revealed no detectable difference (Supporting information, Fig. III-S1).

RCS involves (i) an alignment of all MXD measurement series by biological age, (ii) calculating a mean time series of the age-aligned data, (iii) smoothing this mean curve, (iv) age trend removal by calculating ratios between the raw MXD data and the (smoothed) regional curve, and (v) re-dating the detrended, now dimensionless, values back to calendar years (details in Esper et al. 2003). We here smoothed the mean of the age-aligned data using a 10-year spline filter (Cook and Peters 1981), and calculated chronologies of the detrended MXD data using the arithmetic mean. When aligning the MXD measurement series by biological age, the pith offset (the number of missing innermost rings of a sample) was considered to minimize distortion of the regional curve. RCS was applied to a combined dataset integrating S88 and M13, as well as S88 and E12 samples. In the first run, the effects of the mean and variance adjustments applied to M13 (Melvin et al. 2013) on post-1700 chronology levels were assessed. Then, using only the S88 and E12 samples, the final reconstruction was produced. Combining the S88 and E12 MXD measurements required an adjustment of the S88 data to compensate for a post-1988 change of the calibration wedge used to transfer X-ray film greyscales into values of g/cm^3, as well as the brand of analog film used (changed from Agfa to Kodak). These procedural changes required an adjustment of +0.053 g/cm^3 added to all S88 MXD measurement series (Fig. III-S2). The

adjustment appeared justified, as the S88 dataset integrates several successive tree generations covering the past 1.5 millennia, allowing a robust estimation of the average residual with the E12 data (covering 2 millennia). Additional treatment of the variance of the MXD series appeared unnecessary, as the measurement's standard deviations have not changed over the past 30 years (Fig. III-S3). For the final summer temperature reconstruction we only used tree rings of a certain biological age ranging from 31 to 306 years, i.e. removed the rings ≤ 30 years (here termed as the 'young rings') and > 306 (here termed as the 'old rings') from the combined, and adjusted S88+E12 dataset. Subsample chronologies integrating MXD data constrained to certain age-bands (e.g. 1-30, 31-306 and > 306 years) were calculated using the detrending program Spotty (Esper et al. 2009; Fig. III--S4). Removal of the old rings appeared useful, as these rings are relatively rare and clustered in the second millennium AD. Removal of the young data was also useful, as these rings contain a steep MXD increase from ~ 0.5 to 0.7 g/cm^3 and are clustered in the 20th century, thereby complicating proper proxy calibration and uncertainty estimation back in time (see below). All chronologies were truncated at a minimum replication of 5 MXD measurement series.

2.4 Calibration and error estimation

The MXD climate signal was estimated by calibrating the combined S88+E12 chronology against regional June-July-August (JJA) mean temperatures recorded at the Haparanda, Karasjok and Sodankyla meteorological stations over the 1876-2006 period. A split 1876-1940 calibration and 1941-2006 verification approach was considered for assessing the temporal robustness of the signal (Schneider et al. 2014), and the chronology transferred into JJA temperatures by scaling the record to the mean and variance of the instrumental climate data (Esper et al. 2005a). The resulting summer temperature reconstruction, integrating the adjusted and age-constrained MXD data from S88 and E12, is termed N-Eur.

Uncertainty estimates of N-Eur were calculated using a Monte Carlo approach that considered the declining replication of the MXD chronology back in time, together with the correlation of the less-replicated chronologies against regional JJA temperatures. The procedure involved producing pseudo-chronologies by randomly sampling n = 5, n = 10, ..., n = 75, n = 79 MXD series over the 1876-2006 period, and iteratively correlating these ´restricted´ chronologies with the instrumental climate data. The *n* = 79 chronology represents the (maximum) replication of the combined S88+E12 dataset during 1876-2006 after removing all trees younger than 100 years. The process was repeated 1000 times for each replication class (5, 10, ...79), and the mean correlation of each class used to calculate calibration model standard errors. The changing standard errors, from all Monte Carlo simulations, were added to N-Eur to provide an estimate of the increasing uncertainty associated with the decreasing MXD sample replication back in time. N-Eur replication falls below five MXD series before 17 BC.

3. Results and Discussion

3.1 Torn and N-Scan comparison

Comparison of the Torn and N-Scan temperature reconstructions reveals a significant fraction of shared variance over the past 1500 years ($r_{441–2006}$ = 0.65), although the correlation declines from r = 0.91 in the 20th century to r = 0.60 in the 6th century, and down to r = 0.43 in the first 100 years of overlap (AD 441-540; Fig. III-2A, B). Similar trends are found when comparing the first-differenced reconstructions, indicating this long-term correlation decay is unrelated to a decoupling of lower frequency variances. The changing coherency is probably a function of the changing replication through time. Both reconstructions have their greatest sample replication in the 20th century (N-Scan = 116, Torn = 61), but this quantity declines rapidly back over the past 1500 years (Fig. III-2D). The N-Scan reconstruction contains 49 MXD series during the 10th century, and only 12 series during the first 100 years of overlap with Torn. Torn replication is already down to 13 series in the 10th century and falls below five series before AD 517.

The influence of changing samples depths was confirmed by the stepwise reduction in replication of the N-Scan and Torn chronologies during the calibration period (1876–2006), re-developing chronologies using the reduced sub-samples (1000 times each), and iteratively calculating correlations between the sub-sample chronologies. Results show decreasing correlations as a function of sample replication. For example, sub-sample chronologies integrating 48 MXD samples correlate at 0.825, 30 samples at 0.815, 10 samples at 0.760 and five samples at 0.696. In addition to changes in sample size, a gradual shift in the intra-reconstruction coherence of both chronologies (Fig. III-2C) may also contribute to the reduced correlation between the reconstructions back in time. Yet the running 100-year Rbar values exhibit minor trend, decreasing from 0.41 and 0.43 over the recent ~ 800 years, to 0.38 and 0.39 over the first ~ 800 years, in N-Scan and Torn, respectively. Similarly, the changing geographical area represented by the chronologies might add to the temporally changing correlations, as the NScan reconstruction integrates living trees from both Finland and Sweden, plus sub-fossil trees from Finland only. However, since the different spatial pattern of the two reconstructions' constituent time series are not reflected in the intra-reconstruction's Rbar, it appears most likely that the shrinking replication is the main reason for the reduced agreement between N-Scan and Torn back in time. Despite the significant correlation between N-Scan and Torn, the reconstructions display demonstrably different millennial-scale temperature trends over the late Holocene (Fig. III-2E). While N-Scan temperature estimates decline by about 0.28 to 0.39 ˚C per millennium, the Torn reconstruction has a positive trend ranging from+0.09 to +0.23 ˚C per millennium. Esper et al. (2012b) suggested the elevated sample replication of the N-Scan chronology is a key reason for retaining an orbitally forced cooling trend in a dendrochronological time series. The opposite, and overall positive trend in Torn, particularly the maximum +0.23 ˚C per 1000 years warming rate recorded over the AD 517–2006 period, might additionally be influenced by the adjustments applied to the M13 ITRAX update series (see below).

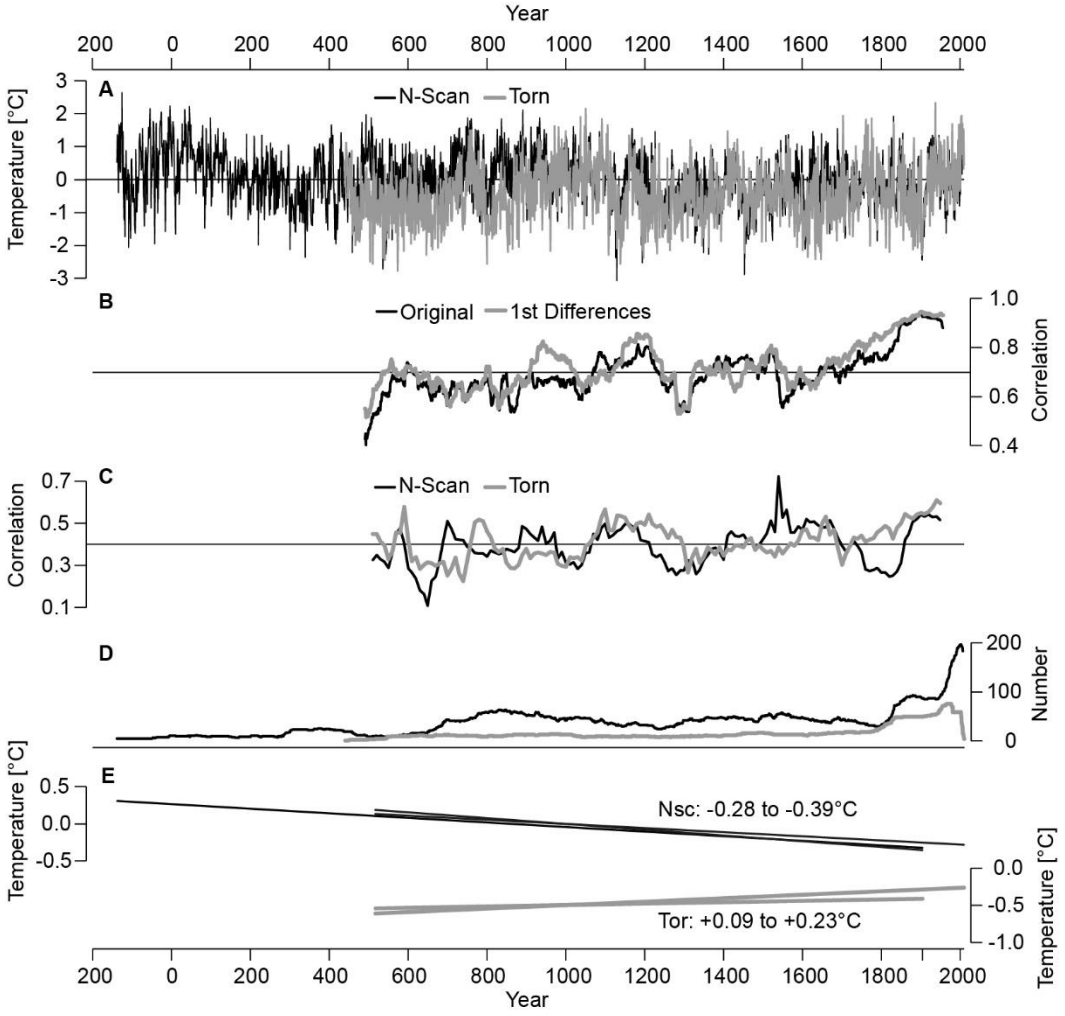

Figure III-2: Comparison of the N-Scan and Torn temperature reconstructions. (A) The N-Scan and Torn reconstructions as published in Esper et al. (2012a) and Melvin et al. (2013) expressed as anomalies with respect to a 1901-2000 reference period. (B) 100-year running correlations between the original reconstructions and between the first-differenced reconstructions. (C) 100-year running interseries correlations of the N-Scan and Torn chronologies. (D) Numbers of tree samples integrated in the N-Scan and Torn chronologies. (E) Linear regressions fit to the reconstructions over the common AD 517–2006, and the AD 517–1900 and 138 BC to AD 1900 (N-Scan only) periods.

3.2 MXD data selection

In the attempt to correct for the systematic differences between data developed on the ITRAX and Walesch instruments, Melvin et al. (2013) relied on an adjustment that ultimately reduced the variance and raised the mean of the ITRAX MXD series, thus producing the M13 dataset (Fig. III-3). While lifting the M13 update above the original S88 data during the post-1800 period of overlap might well be justified with regard to biological growth rates (the S88 data are a collection of much older trees than the M13 data), consideration of the adjusted M13 instead of the S88 living trees in an RCS run results in a substantial increase of recent chronology values (Fig. III-3D). Whether such effects are mitigated or even amplified by the use of split RCS standardization (Melvin et al. 2013) is beyond the scope of

this paper, although it appears preferable to use only the E12 living trees for extending N-Eur into the 21st century. Doing so reduces replication in the 19th and 20th centuries, which is, however, still larger than at any other time, and mitigates the millennial-scale trend differences advanced by the inclusion of the adjusted M13 data. Our decision not to join the adjusted ITRAX M13 data with the Walesch E12 data does not mean we consider M13 unreliable for reconstruction purposes (Torn and N-Scan correlate at 0.91 during the 20th century), but rather to avoid unnecessary complication when integrating data developed by different techniques.

To further restrain potential trend biases in the N-Eur reconstruction we removed tree rings older than 306 years and younger than 30 years from the combined S88+E12 dataset (Fig. III-4). Tree rings >306 years are relatively rare (3918 of 98 740 rings) and largely restricted to the S88 data, which include some of the oldest trees found in the Torneträsk region (up to 620 years). As these old rings are also concentrated in the second millennium AD, not meaningfully contributing to an assessment of long-term changes between the first and second millennium AD (but rather level off such variance in an RCS approach), the data were excluded from the final reconstruction. Truncation at a biological age of 306 years appeared reasonable as replication falls below 50 series beyond this age limit, and the regional curve becomes heteroscedastic (Fig. III-4A, B). Reasons for not considering tree rings ≤ 30 years result from the growing mismatch between the S88 and E12 regional curves towards younger ages, even after adjustment of the S88 data (Fig. III-S2A), as well as the documented sharp MXD increase in juvenile rings, from ~ 0.5 to 0.7 g/cm^3, in which climate signal age effects (Carrer and Urbinati 2004, Esper et al. 2008) are probably increased. The correlation between. The correlation between the central 31-306 age-band, and the young 1-30 age-band chronologies declines to r = 0.63 (n = 979 years; Fig. III-4C), and removing the young rings again balances replication as these data are culminating in the 20th century calibration period (79 series in 1992; the green curve in Fig. III-4D).

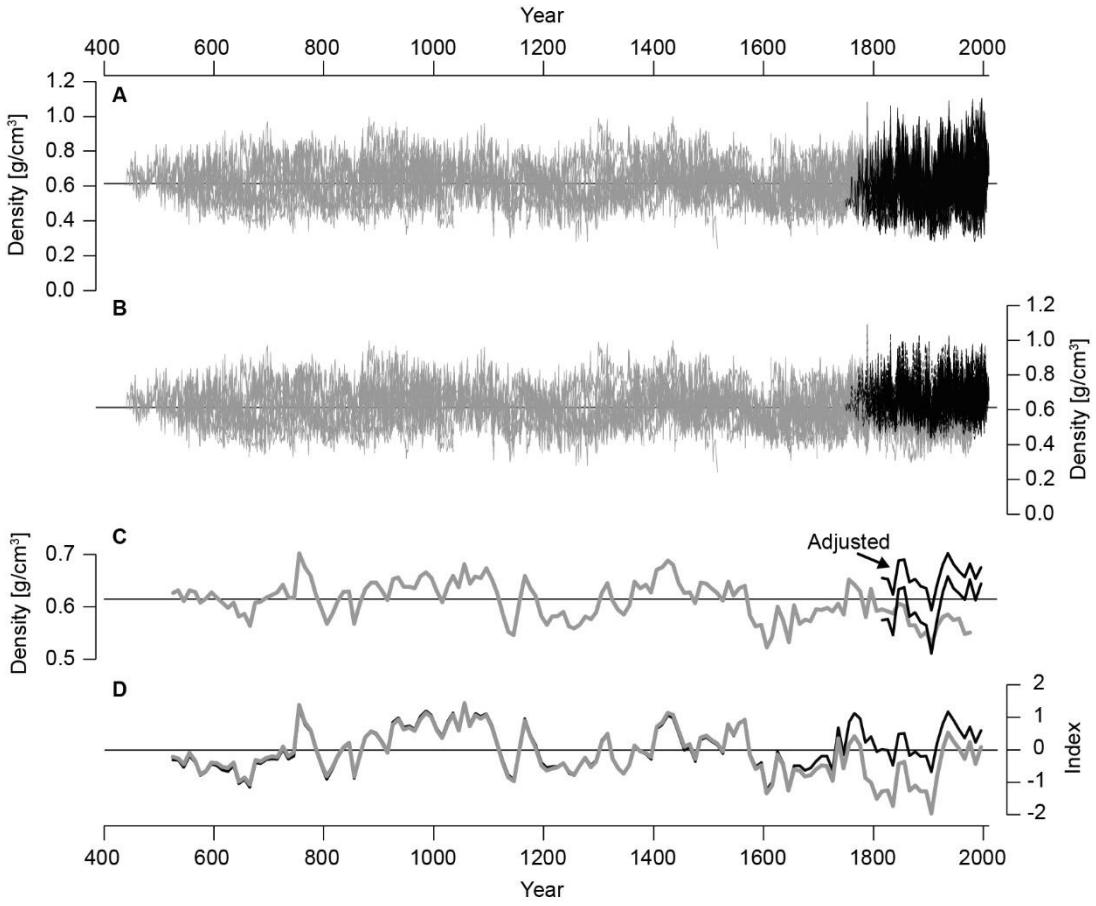

Figure III-3: Torneträsk original and update data. (A) Sixty-five original MXD series from living and relict pine samples (S88; grey curves) shown together with the 65 update MXD series from just living trees (M13; black curves). The original data were measured using a Walesch X-ray densitometer; the update data were measured using an ITRAX digital radiographic camera. (B) Same as in (A), but after adjustment of the mean and variance of the ITRAX data as detailed in Melvin et al. (2013). (C) Mean chronologies of the original (grey) and updated (black) MXD data at decadal resolution. Top back curve is the mean of the adjusted update data. (D) RCS detrended chronologies of a combined dataset integrating the 47 original relict series together with the 65 living tree update series (grey), as well as the same 47 relict series together with the 65 update series after adjustment of their means and variances (black). Chronologies were normalized over the AD 517–1700 period.

3.3 N-Eur summer temperature reconstruction

The 31–306 year age-band chronology correlates at 0.76 with 131 years of regional instrumental JJA temperatures (Fig. III-5A). Split calibration ($r_{1876\text{-}1940} = 0.78$) and verification ($r_{1941\text{-}2006} = 0.75$) indicates the climate signal is temporally robust with no sign of divergence (D'Arrigo et al. 2008, Esper et al. 2010). The correlation is slightly smaller than that obtained using all data of the Torn and N-Scan reconstructions ($r_{1876–2006} = 0.78$), which is likely a consequence of NEur's lower replication (93 series in the 20th century) compared with a non-constrained chronology (180 series in the 20th century). Nonetheless, the N-Eur correlation reported here is not representative of the pre-instrumental period, as the reconstruction's replication quickly decreases to 52 series in the 10th century and eight series in the 1st century AD. This decline in sample size is addressed by performing calibration experiments using

differently replicated chronologies. These Monte Carlo tests produced correlations ranging from 0.69 (±0.04) for chronologies integrating 79 MXD series to 0.63 (±0.14) for chronologies integrating five MXD series, and were used to add variable calibration model standard errors to the N-Eur reconstruction back in time (Fig. III-5B, C). The standard error increases from 0.76 ˚C in the 20th century to 0.92°C in the first 100 years of the reconstruction.

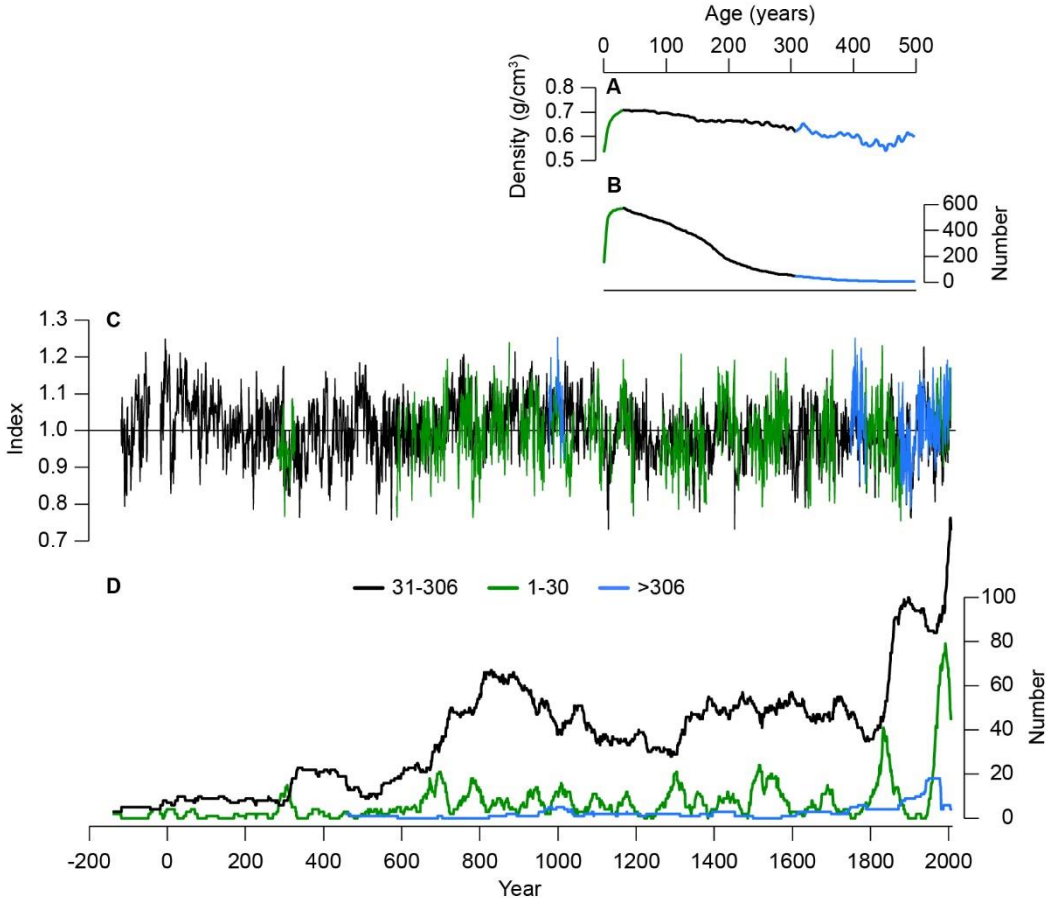

Figure III-4: N-Eur age-band chronologies. (A) Regional curves of the N-Eur MXD data of the age-bands 1-30 (green), 31-306 (black), and >306 years (blue). Bottom panel (B) shows the replication curves across all age-bands. (C) RCS detrended age-band chronologies, and (D) their replication over the past 2000 years. After truncation at n<5 MXD series, the chronologies cover 2097 years (age band 31–306), 979 years (age band 1–30) and 197 years (age band>306). Correlations with the 31–306 age-band chronology are 0.83 for the old chronology and 0.63 for the young chronology.

N-Eur indicates a long-term cooling trend of -0.30 ˚C per 1000 years over the 17 BC to AD 2006 period, in line with results detailed for the N-Scan reconstruction (Esper et al. 2012b), although the latter record has been transferred into temperatures using linear regression instead of scaling (Esper et al. 2005a). This overall negative trend is contrary to expectations based on the assumption that relict and subfossil wood, lying on the ground and in lakes for centuries, would lose density due to natural decaying processes. The assumption stems from the observation that older discs are lighter than younger ones. Superimposed on the long-term cooling trend are centennial-scale warm episodes, including the Roman

Warm Period until ~ AD 150, the Medieval Warm Period from ~ AD 700 to 1200, and the 20th century warm period (Kullman 2013). These warm phases are separated by cooler conditions during the Migration period and the Little Ice Age in the first and second millennium AD, respectively. Summer temperature variations at this temporal scale, i.e. after smoothing with a 100-year spline filter, reveal fluctuations that range by ~ 1.5 ˚C between warm and cold episodes.

Besides these lower frequency trends, N-Eur reveals extremely warm and cold summers deviating up to +3.2 ˚C (mean of 2 BC, 4 BC, AD 1937) and -3.4 ˚C (mean of AD 574, 1130, 1453) from the 1961–1990 reference period. Coincidently, one of the three coldest years (AD 1453, -3.47 ˚C) is synchronous with the large eruption of the Kuwae volcano in Vanuatu (Plummer et al. 2012), suggesting some of the earlier extremes might point to previously unknown eruptions. Given the good fit with instrumental climate data, the Common Era coverage and the good replication, exceeding all other MXD chronologies, the JJA temperature reconstruction presented here might be the most suitable proxy time series to estimate post volcanic cooling (Anchukaitis et al. 2012, D'Arrigo et al. 2013, Esper et al. 2013a, Esper et al. 2013b), and to compare with ice core-derived evidence of volcanic eruptions (Baillie 2008, Sigl et al. 2013).

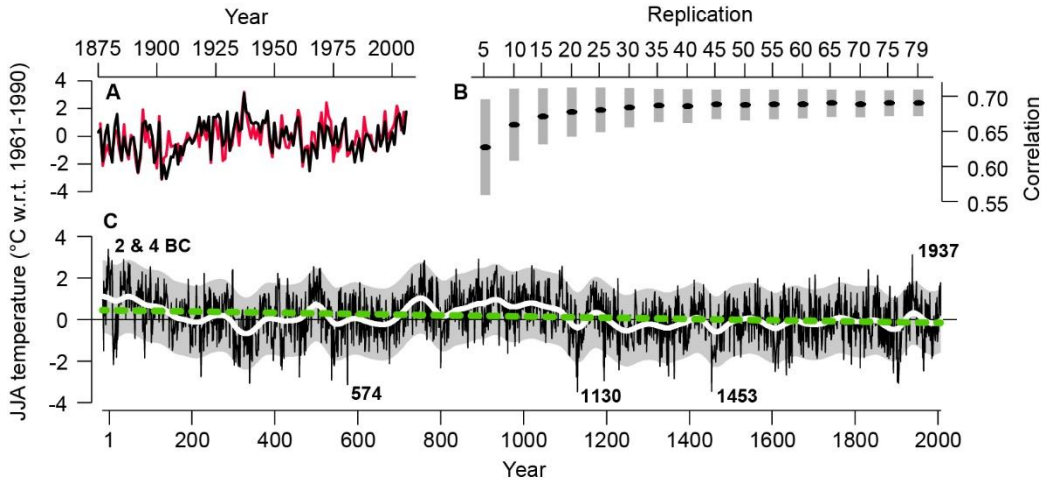

Figure III-5: N-Eur temperature reconstruction. (A) Calibration of the N-Eur chronology (black) against regional JJA temperatures (red) over the 1876-2006 period. (B) Mean correlations (black) of variously replicated (n = 5, n = 10, ..., n = 79) MXD chronologies against regional JJA temperatures. Grey bars indicate the standard deviation of correlations for each replication class 5–79 over 1000 iterations. (C) N-Eur temperature reconstruction at annual resolution (black) and after smoothing using a 100-year filter (white). Green curve is a linear regression fit to the annually resolved data over the 17 BC to AD 2006 period. Grey area indicates the smoothed standard error (2SE) of the calibration model, using variable chronology replicated error estimates (from B). Dates indicate the three coldest and warmest years over the past two millennia.

4. Conclusions

The world's two longest MXD chronologies were combined into one single reconstruction of summer temperature variability in northern Europe back to 17 BC. The reconstruction explains 58% of the variance in instrumental JJA temperature fluctuations, although climate signal strength decreases to ~ 47% in the 10th and ~ 40% in the 1st century AD. The signal decay is caused by a declining sample replication back in time, a reconstruction property evaluated here by iteratively calibrating differently replicated chronologies against the instrumental temperature data. The combination of MXD data from two independent reconstructions was challenged by changing laboratory procedures, established over the past 30 years, to measure high resolution wood density profiles. A recently completed update of MXD data from living trees was excluded from the reconstruction, as the necessary adjustment of the mean and variance, for the fraction of data covering the most recent centuries, appeared problematic. Excluding these data also reduced the sample replication during the 20th century, a period during which the number of MXD measurement series outnumbered pre-instrumental replication. Another data reduction was invoked by excluding MXD measurements from extremely young and old tree rings, as these data do not meaningfully contribute to the reconstruction's low-frequency variance but rather complicate the determination of uncertainty estimates over the past 2000 years.

The final product, a summer temperature reconstruction derived from a combined, adjusted and age-constrained MXD dataset from northern Sweden and Finland, shows a long-term cooling of -0.30 °C per 1000 years over the Common Era in northern Europe. The reconstruction has centennial-scale variations superimposed on this trend, indicating conditions during Medieval and Roman times were probably warmer than in the late 20th century. The record reveals several extreme summer temperature deviations exceeding -3 ˚C that might prove useful in the detection and dating of volcanic eruptions, and assessment of post-eruption cooling effects.

Acknowledgements

We thank Daniel Nievergelt for examining level differences between the 1980 and 2006 Walesch MXD data, Håkan Grudd for information on the Torn chronology development, and Lea Schneider for discussion of uncertainty estimation. Supported by the Mainz Geocycles Excellence Cluster.

References

Anchukaitis K.J., Breitenmoser P., Briffa K.R., Buchwal A., Büntgen U., Cook E.R., D'Arrigo R.D., Esper J. et al. (2012): Tree rings and volcanic cooling. *Nature Geoscience* 5: 836-837.

Baillie M.G.L. (2008): Proposed re-dating of the European ice core chronology by seven years prior to the 7th century AD. *Geophysical Research Letters* 35.

Bartholin T.S., Karlén W. (1983): Dendrokronologi i Lappland AD 436–1981. *Dendrokronologiska Sällskapets Meddelanden* 5: 3-16.

Bräker O.U. (1981): Der Alterstrend bei Jahrringdichten und Jahrringbreiten von Nadelhölzern und sein Ausgleich. *Mitteilungen der Forstlichen Bundesversuchsanstalt Wien* 142: 75-102.

Briffa K.R., Bartholin T.S., Eckstein D., Jones P.D., Karlen W., Schweingruber F.H., Zetterberg P. (1990): A 1,400-Year Tree-Ring Record of Summer Temperatures in Fennoscandia. *Nature* 346: 434-439.

Briffa K.R., Jones P.D., Bartholin T.S., Eckstein D., Schweingruber F.H., Karlen W., Zetterberg P., Eronen M. (1992): Fennoscandian Summers from Ad-500 - Temperature-Changes on Short and Long Timescales. *Climate Dynamics* 7: 111-119.

Bunde A., Büntgen U., Ludescher J., Luterbacher J., von Storch H. (2013): Is there memory in precipitation? *Nature Climate Change* 3: 174-175.

Büntgen U., Frank D., Neuenschwander T., Esper J. (2012): Fading temperature sensitivity of Alpine tree growth at its Mediterranean margin and associated effects on large-scale climate reconstructions. *Climatic Change* 114: 651-666.

Büntgen U., Raible C.C., Frank D., Helama S., Cunningham L., Hofer D., Nievergelt D., Verstege A. et al. (2011): Causes and Consequences of Past and Projected Scandinavian Summer Temperatures, 500-2100 AD. *Plos One* 6.

Carrer M., Urbinati C. (2004): Age-dependent tree-ring growth responses to climate in Larix decidua and Pinus cembra. *Ecology* 85: 730-740.

Cook E.R., Kairiukstis L.A. (1990): Methods of dendrochronology. Kluwer Academic Publishers.

Cook E.R., Peters K. (1981): The smoothing spline: a new approach to standardizing forest interior tree-ring width series for dendroclimatic studies. *Tree-Ring Bulletin* 41: 45-53.

D'Arrigo R., Wilson R., Anchukaitis K.J. (2013): Volcanic cooling signal in tree ring temperature records for the past millennium. *Journal of Geophysical Research-Atmospheres* 118: 9000-9010.

D'Arrigo R., Wilson R., Jacoby G. (2006): On the long-term context for late twentieth century warming. *Journal of Geophysical Research-Atmospheres* 111.

D'Arrigo R., Wilson R., Liepert B., Cherubini P. (2008): On the 'Divergence Problem' in Northern Forests: A review of the tree-ring evidence and possible causes. *Global and Planetary Change* 60: 289-305.

Düthorn E., Holzkämper S., Timonen M., Esper J. (2013): Influence of micro-site conditions on tree-ring climate signals and trends in central and northern Sweden. *Trees* 27: 1395-1404.

Eronen M., Zetterberg P., Briffa K.R., Lindholm M., Merilainen J., Timonen M. (2002): The supra-long Scots pine tree-ring record for Finnish Lapland: Part 1, chronology construction and initial inferences. *Holocene* 12: 673-680.

Esper J., Büntgen U., Luterbacher J., Krusic P.J. (2013a): Testing the hypothesis of post-volcanic missing rings in temperature sensitive dendrochronological data. *Dendrochronologia* 31: 216-222.

Esper J., Büntgen U., Timonen M., Frank D.C. (2012b): Variability and extremes of northern Scandinavian summer temperatures over the past two millennia. *Global and Planetary Change* 88-89: 1-9.

Esper J., Cook E.R., Krusic P.J., Peters K., Schweingruber F.H. (2003): Tests of the RCS method for preserving low-frequency variability in long tree-ring chronologies. *Tree-Ring Research* 59: 81-98.

Esper J., Cook E.R., Schweingruber F.H. (2002): Low-frequency signals in long tree-ring chronologies for reconstructing past temperature variability. *Science* 295: 2250-2253.

Esper J., Frank D., Büntgen U., Verstege A., Hantemirov R.M., Kirdyanov A.V. (2010): Trends and uncertainties in Siberian indicators of 20th century warming. *Global Change Biology* 16: 386-398.

Esper J., Frank D.C., Timonen M., Zorita E., Wilson R.J.S., Luterbacher J., Holzkamper S., Fischer N. et al. (2012c): Orbital forcing of tree-ring data. *Nature Climate Change* 2: 862-866.

Esper J., Frank D.C., Wilson R.J.S., Briffa K.R. (2005a): Effect of scaling and regression on reconstructed temperature amplitude for the past millennium. *Geophysical Research Letters* 32.

Esper J., Krusic P.J., Peters K., Frank D. (2009): Exploration of long-term growth changes using the tree-ring detrending program "Spotty". *Dendrochronologia* 27: 75-82.

Esper J., Niederer R., Bebi P., Frank D. (2008): Climate signal age effects - Evidence from young and old trees in the Swiss Engadin. *Forest Ecology and Management* 255: 3783-3789.

Esper J., Schneider L., Krusic P.J., Luterbacher J., Büntgen U., Timonen M., Sirocko F., Zorita E. (2013b): European summer temperature response to annually dated volcanic eruptions over the past nine centuries. *Bulletin of Volcanology* 75.

Franke J., Frank D., Raible C.C., Esper J., Bronnimann S. (2013): Spectral biases in tree-ring climate proxies. *Nature Climate Change* 3: 360-364.

Fritts H.C. (1976): Tree rings and climate. Academic Press.

Grudd H. (2008): Tornetrask tree-ring width and density AD 500-2004: a test of climatic sensitivity and a new 1500-year reconstruction of north Fennoscandian summers. *Climate Dynamics* 31: 843-857.

Kullman L. (2013): Ecological tree line history and palaeoclimate - review of megafossil evidence from the Swedish Scandes. *Boreas* 42: 555-567.

Ljungqvist F.C. (2010): A New Reconstruction of Temperature Variability in the Extra-Tropical Northern Hemisphere during the Last Two Millennia. *Geografiska Annaler Series a-Physical Geography* 92A: 339-351.

Ljungqvist F.C., Krusic P.J., Brattstrom G., Sundqvist H.S. (2012): Northern Hemisphere temperature patterns in the last 12 centuries. *Climate of the Past* 8: 227-249.

Mann M.E., Zhang Z.H., Hughes M.K., Bradley R.S., Miller S.K., Rutherford S., Ni F.B. (2008): Proxy-based reconstructions of hemispheric and global surface temperature variations over the past two millennia. *Proceedings of the National Academy of Sciences of the United States of America* 105: 13252-13257.

Melvin T.M., Briffa K.R. (2008): A "signal-free" approach to dendroclimatic standardisation. *Dendrochronologia* 26: 71-86.

Melvin T.M., Grudd H., Briffa K.R. (2013): Potential bias in 'updating' tree-ring chronologies using regional curve standardisation: Re-processing 1500 years of Tornetrask density and ring-width data. *Holocene* 23: 364-373.

Moser L., Fonti P., Büntgen U., Esper J., Luterbacher J., Franzen J., Frank D. (2010): Timing and duration of European larch growing season along altitudinal gradients in the Swiss Alps. *Tree Physiology* 30: 225-233.

Plummer C.T., Curran M.A.J., van Ommen T.D., Rasmussen S.O., Moy A.D., Vance T.R., Clausen H.B., Vinther B.M. et al. (2012): An independently dated 2000-yr volcanic record from Law Dome, East Antarctica, including a new perspective on the dating of the 1450s CE eruption of Kuwae, Vanuatu. *Climate of the Past* 8: 1929-1940.

Schneider L., Esper J., Timonen M., Büntgen U. (2014): Detection and evaluation of an early divergence problem in northern Fennoscandian tree-ring data. *Oikos* 123: 559-566.

Schweingruber F.H., Bartholin T., Schar E., Briffa K.R. (1988): Radiodensitometric-Dendroclimatological Conifer Chronologies from Lapland (Scandinavia) and the Alps (Switzerland). *Boreas* 17: 559-566.

Schweingruber F.H., Fritts H.C., Bräker O.U., Drew L.G., Schär E. (1978): The X-ray technique as applied to dendroclimatology. *Tree-Ring Bulletin* 38: 61-91.

Sigl M., McConnell J.R., Layman L., Maselli O., McGwire K., Pasteris D., Dahl-Jensen D., Steffensen J.P. et al. (2013): A new bipolar ice core record of volcanism from WAIS Divide and NEEM and implications for climate forcing of the last 2000 years. *Journal of Geophysical Research-Atmospheres* 118: 1151-1169.

Supplementary Material

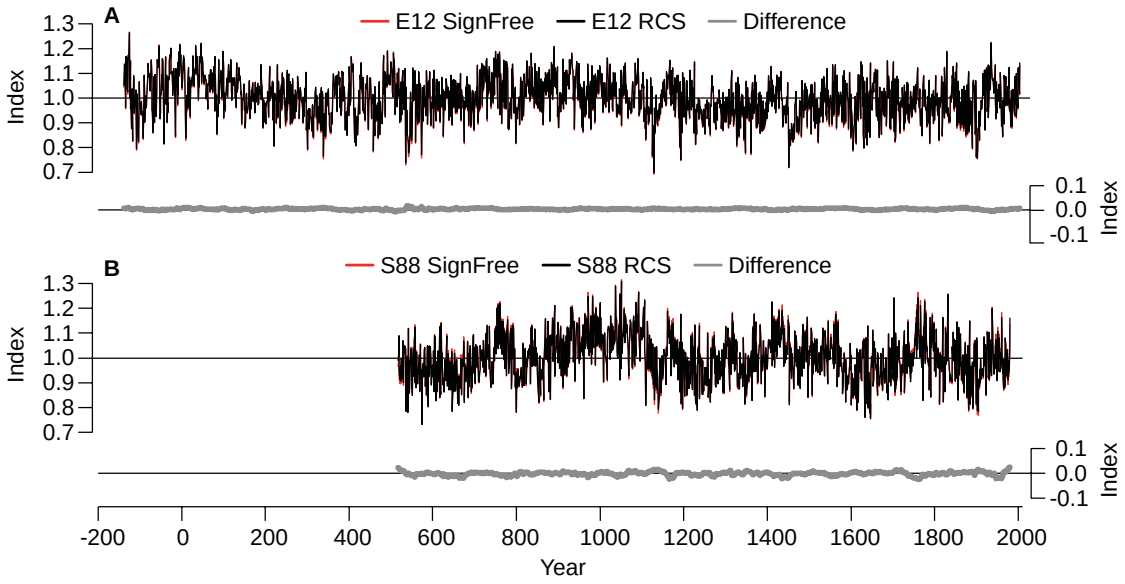

Supplement III-1: Comparison of RCS and Signal Free detrended chronologies. (A) RCS (black) and RCS plus Signal Free (red) detrended chronologies of the E12 dataset. Note the black curve is dawn on top of the red curve. Bottom panel shows the residual timeseries (grey) of the differently detrended chronologies. (B) Same as in (A), but for the S88 dataset.

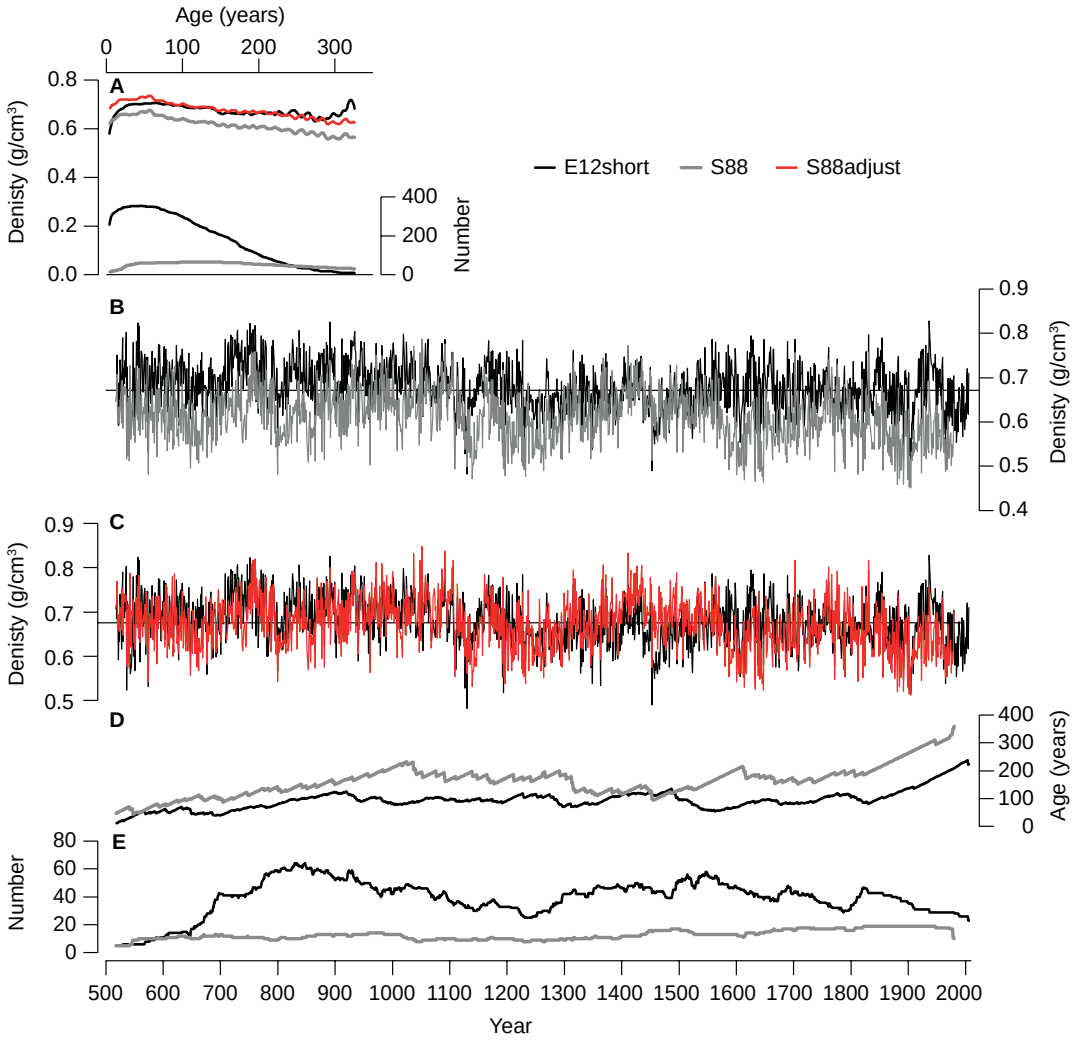

Supplement III-2: Adjustment of the S88 data. (A) Mean MXD timeseries (top) and replication curves (bottom) of the age-aligned E12short (black) and S88 (grey) datasets. E12short is a sub-sample of E12 approximating the temporal distribution of S88, i.e. living trees younger than AD 1822 (the age of the youngest living tree in S88) as well as pre-AD 500 sub-fossil trees (to match with the five samples of S88 in AD 517) were removed from E12. The E12short and S88 data are shown over the well-replicated ($n \geq 10$ series) age range from 5 to 326 years. The red curve is the mean timeseries of the adjusted S88 data, achieved by lifting each measurement series by 0.053 g/cm3. All regional curves were smoothed using a 10-year spline filter. (B) Mean chronologies of the raw E12short and S88 MXD data. (C) Same as in (B) but for the E12short and S88adjust data. (D) Mean age curves, and (E) replication curves of the E12short and S88 data.

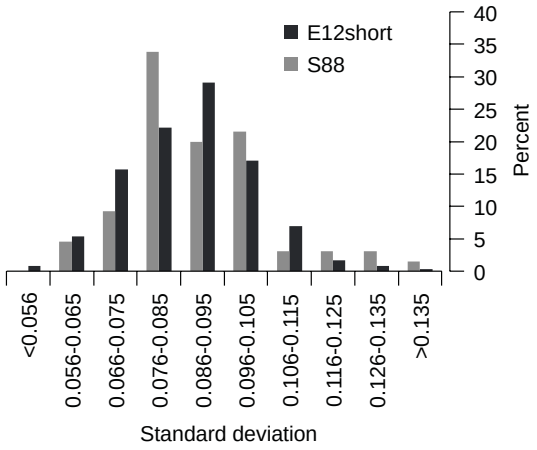

Supplement III-3: Variance of MXD timeseries. The number of individual MXD measurement series of the E12short and S88 datasets (in %) falling into distinct standard deviation classes ranging from < 0.056 to > 0.135 g/cm3.

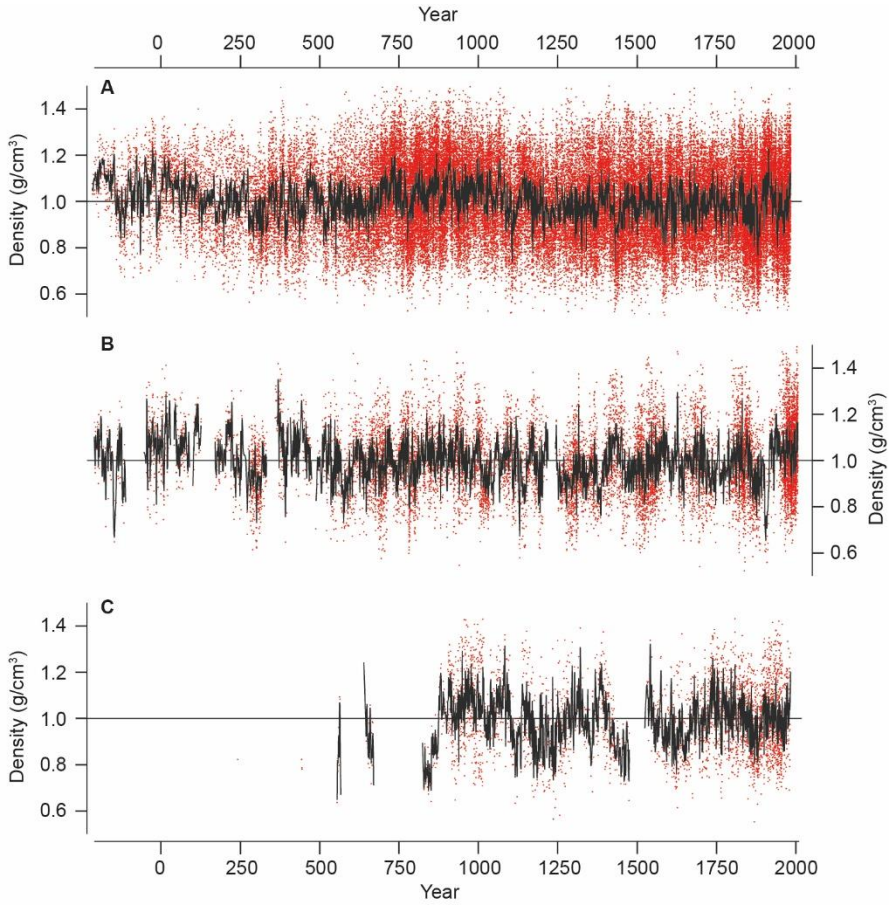

Supplement III-4: RCS detrended age-band chronologies. (A) RCS detrended chronology (black curve) of the 31-306 year age-band of the E12+S88adjust data. The red dots are the 98740 detrended MXD values in this age-band. (B and C) Same as in (A), but for the 1-30 year age-band containing 15202 values, and the 307-620 year age-band containing 3918 values.

Chapter IV: Ecological and climatological signals in tree-ring width and density chronologies along a latitudinal boreal transect

Düthorn[1], E., Schneider[1], L., Günther[2], B., Gläser[1], S., Esper[1], J.

[1] Department of Geography, Johannes Gutenberg University Mainz, 55099 Mainz, Germany

[2] Institute of Forest Utilization and Forest Technology, Technische Universität Dresden, 01735 Tharandt, Germany

(*Scandinavian Journal of Forest Research*, in review)

1. Introduction

The boreal forest system is highly sensible to external changes. In this ecosystem variations in tree growth are closely reflecting changes of the surrounding environment. Summer temperatures are the main driver and limiting factor for radial growth and wood density of conifer trees in northern latitudes (Fritts 1976). In particular tree growth close to the arctic treeline is very sensitive and respond to environmental variations. Hence, this region is in the focus of dendrochronological studies addressing climatological (Wilson and Luckman 2003, Kultti et al. 2006, McCarroll et al. 2013, Esper et al. 2014) and ecological (Schmitt et al. 2004, Seo et al. 2011, Düthorn et al. 2015b) questions. However, tree-ring studies also are carried further south, into more temperate zones of the boreal forest, out focusing on drought reconstructions and the influence of precipitation on tree growth (e.g. Helama and Lindholm 2003, Drobyshev et al. 2011, Düthorn et al. 2014). Most of this research is based on the analysis of tree-ring width (TRW) data (see previous references), and some studies additionally use maximum latewood density (MXD; Helama et al. 2014). In contrast to TRW, MXD has a stronger link to summer temperature (Briffa et al. 2002), a less pronounced age trend (Schweingruber 1983), reduced biological memory effects (Frank and Esper 2005), and the capability of preserving lowest frequency and millennial scale temperature variations (Esper et al. 2012c).

Transect studies are an important tool to detect drivers and limits of wood formation, to predict the influence of external factors on tree growth and to identify possible effects on future forest systems due to changing environments. Especially in the Alps altitudinal transects help to describe elevational dependent climate sensitivity patterns (Hartl-Meier et al. 2014a, Hartl-Meier et al. 2014b) and to identify sites and altitudes suitable for climate reconstructions (Kienast et al. 1987, Affolter et al. 2010). The alti-latitudinal transect of Rossi et al. (2015) considers the future forest management in relation to forest productivity. Martin-Benito and Pederson (2015) described the effects on trees in relation to latitude in eastern North America and defined precipitation or maximum temperature as main limiting factor according to the latitude. Similar effects are also described by Helama et al. (2005a) in Finland, where they analyzed TRW of Scots pine (*Pinus sylvestris* L.) along a latitudinal gradient. While trees in the north depend on July temperatures and moderate precipitation in May, this relationship weakens towards lower latitudes. An inconsistent connection of early summer precipitation and TRW chronologies in southern Finland was found by Düthorn et al. (2014). The more robust relationship of MXD and summer temperatures, however, suggests a limited influence of precipitation on tree growth in the more temperate southern Finland (Helama et al. 2014). Next to these large scale fingerprints also micro-site differences are important to understand the ecological needs and limits of tree growth (Düthorn et al. 2013).

We here are introducing a combined assessment of large and micro scale conditions. Next to the changing signals in TRW and MXD of *P. sylvetris* along a latitudinal transect in the Finish boreal forest, we additionally consider the influences of differing micro-site conditions on tree-ring formation and climate sensitivity.

2. Material and Methods

2.1 Study area and sampling design

Our study area covers a latitudinal transect of pine populations with each being representative for a subfield of the Finnish boreal forest ecosystem following the classification of Ahti et al. (1986) (Fig.IV-1). The northern site (Ailijärvi: 69.52°N, 28.56°E; hereafter: NB) is located close to the northern distribution limit of Scots pine. The central site (Sotkamo: 64.11°N, 28.34°E; hereafter: CB) is part of the middle boreal forest and has characteristics of a transition zone between the northern and southern sections of the coniferous forest. The southern boreal forest, as sub region of the northern coniferous woodland (Ahti et al. 1986), is represented by the southern site (Melkuttimet: 60.73°N, 24.05°E; hereafter: SB). Each site dataset consists of 40 tree-ring series subdivided in 20 series from the shoreline (wet micro-site) and 20 series from the inland (dry micro-site) according to (Düthorn et al. 2013). We sampled young and old trees at each site. The composition of the age structure was supposed to be similar along the transect to ease comparisons.

Table IV-1: Characteristics of the site and micro-site chronologies. Bold values represent MXD measurements.

Site	*Location*	*Lat (°N)*	*Lon (°E)*	*Elevation (m asl)*	*Series (wet/dry)*	*MSL (years)*	*July temperature (°C) 1961-1990*	*July precipitation (mm) 1961-1990*
NB	Ailijärvi	69.52	28.57	120	17/19	144.8	12.58	68.30
CB	Sotkamo	64.12	28.34	148	20/20	107.1	16.08	61.00
SB	Melkuttimet	60.73	24.06	120	18/20	91.1	16.00	71.08
	Standard deviation (wet/dry)*	***rbar (wet/dry)***	***Autocorrelation lag-1 (wet/dry)***	***Mean MXD [g/cm³] (wet/dry)****	*Standard deviation (wet/dry)**	*rbar (wet/dry)*	*Autocorrelation lag-1 (wet/dry)*	*Mean TRW [mm] (wet/dry)**
NB	**0.12/0.12**	**0.42/0.45**	**0.46/0.52**	**0.75/0.74**	0.29/0.34	0.54/0.46	0.74/0.79	0.67/0.77
CB	**0.11/0.11**	**0.1/0.21**	**0.6/0.58**	**0.85/0.94**	1.04/0.75	0.51/0.46	0.85/0.81	1.64/1.27
SB	**0.09/0.1**	**0.25/0.34**	**0.55/0.49**	**0.96/1**	0.58/0.49	0.45/0.53	0.74/0.67	1.47/1.32

*only tree-rings of an age of 5-120 years are included; NB: north boreal, CB: middle boreal, SB: south boreal; *MSL*: mean segment length

2.2 Tree-ring width and density measurements

Different tree-ring parameters were measured simultaneously considering TRW, MXD, earlywood width (EW), latewood width (LW), latewood density (LWD) and earlywood density (EWD). The measurements were performed using a common MXD setup according to Lenz et al. (1976) and Schweingruber et al. (1978). Increment cores were sawn into 1.2 ± 0.02 mm thick laths using a double bladed saw (DENDROCUT – WALESCH Electronics). Organic extractives from the laths, e.g. resin, were extracted using alcohol (95%) for 48 h. Before X-raying the samples were acclimated for 24 h at 65 % air humidity and 20 °C air temperature. X-ray films (AGFA-Microvision Ci) were exposed with a duration of 55 minutes using a "BALTOGRAPHE" devise by Balteau. Grey values from the films were measured with the WALESCH "DENDRO 2003" densitometer at a resolution of ~ 10 µm.

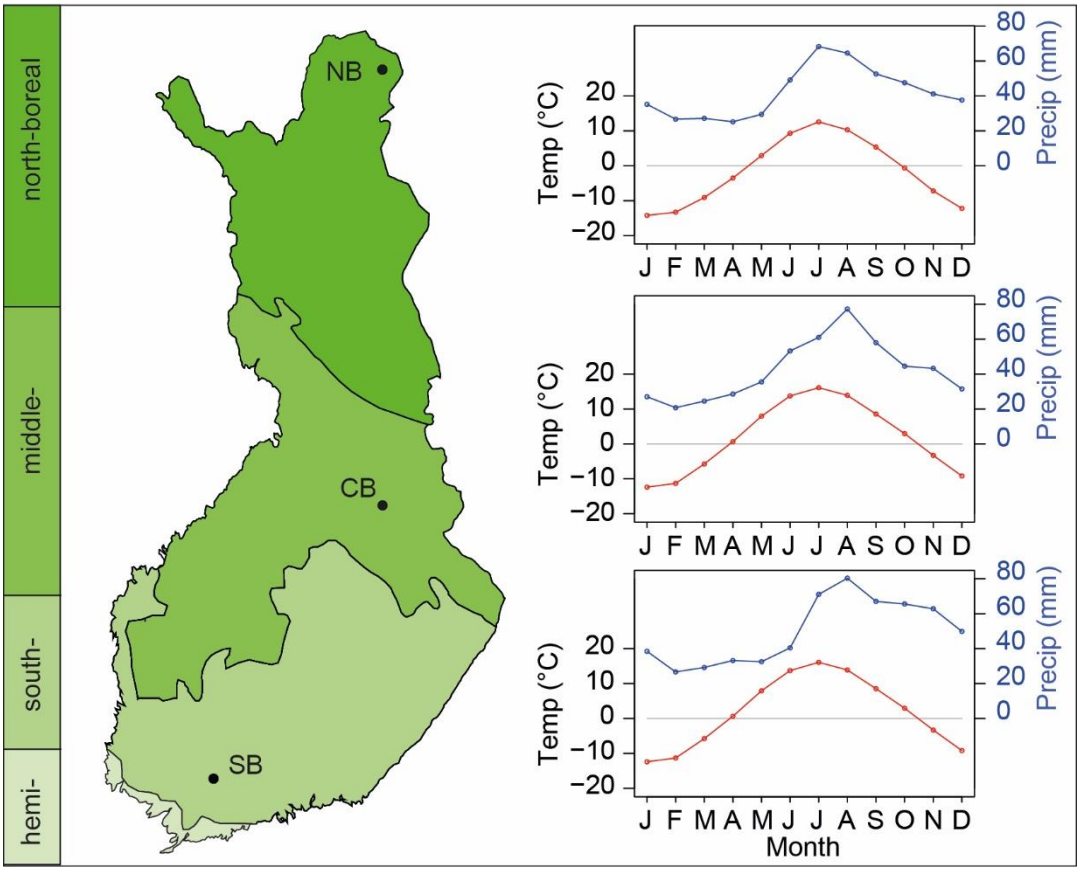

Figure IV-1: Map of Finland with the boreal forest zones defined by Ahti et al. (1986). Dots represent the sampling sites of the TRW and MXD transect. On the right climate diagrams with mean temperature and precipitation sums (1961-1990) from interpolated data of the four nearest grid points to the sampling site are plotted.

2.3 Data standardization and chronology characterization

Tree-ring age-effects were removed using Negative Exponential Curve Standardization with TRW, EW, and LW. Age trends in the density time series (MXD, LWD, EWD) were removed using Hugershoff Standardization enabling fit of initially increasing values typical to density data from juvenile rings (Bräker 1981, Cook and Kairiukstis 1990). Both standardization methods support emphasizing inter-annual to multi-decadal variability in mean chronologies. A data adaptive power transformation was applied to stabilize heteroscedastic variance, and residuals were calculated to obtain index time series (Cook and Peters 1997). Mean site and micro-site chronologies were produced using the biweight robust mean and the variance was stabilized using methods outlined in Frank et al. (2007). All chronologies were truncated at a minimum replication of three time series and, to avoid age related biases, only tree-rings of an age from 5-120 years were used for calculating the mean growth or mean density (Fig. IV-2). Growth behavior, independent of climate influences, was assessed using regional growth curves (RC) in which the single raw series are aligned by their cambial age considering pith offsets. The average of all series represents the typical regional growth for a certain site (details in Esper et al. (2003)). For chronology characterization mean series length (MSL), mean TRW and MXD as well as the standard deviation and first year autocorrelation (lag-1) were computed for raw tree-ring parameter (see Table IV-1). The coherency among series within a chronology was assessed using inter-series correlation (Rbar) based on raw data.

2.4 Climate data and response analysis

Climate-growth relationships were assessed by correlating monthly and seasonal climate data with the mean (TRW and MXD) site and micro-site chronologies. The relationship was calculated by computing bootstrapped Pearson´s correlation coefficients ($p \leq 0.01$) over the common period 1902 – 2011 with treeclim (Zang and Biondi 2014). We used interpolated temperature and precipitation data derived from the four nearest grid points to our sampling sites (see the climate diagrams in Fig. IV-1). The gridded data originate from the CRU TS 3.21 data set (Mitchell and Jones 2005, Harris et al. 2014). Besides this, a multi-scalar drought index was considered to assess changes in the hydrologic water balance, using the standardized precipitation evapotranspiration index (SPEI) with a memory of 12 month (Vicente-Serrano et al. 2010). In order to evaluate the temporal robustness of the growth-climate relationship, the MXD site chronologies were correlated against JA temperatures and precipitation over consecutive 37 year time periods (early: 1901 – 1937, middle: 1938 – 1974, recent: 1975 – 2011)

3. Results

3.1 Chronology characteristics

The common period (1902-2011) of the chronologies is limited by the relatively young trees in southern Finland (Fig. IV-2 and Table IV-1). Generally rbar values are similar between the micro-sites for TRW and MXD. In TRW data rbar is consistently high for all sites (0.45-0.53), meaning that there is high coherency among the series, independent of latitude. For MXD rbar values range from 0.10 to 0.45, indicating substantially changing internal coherence along latitude (Table IV-1). The inter-chronology correlation between wet and dry micro-sites is fairly high for the MXD chronologies (1902-2011: r_{NB} = 0.88, r_{CB} = 0.66, r_{SB} = 0.71) and the correlation between the TRW micro-sites is only slightly lower (1902-2011: r_{NB} = 0.85, r_{CB} = 0.37, r_{SB} = 0.66).

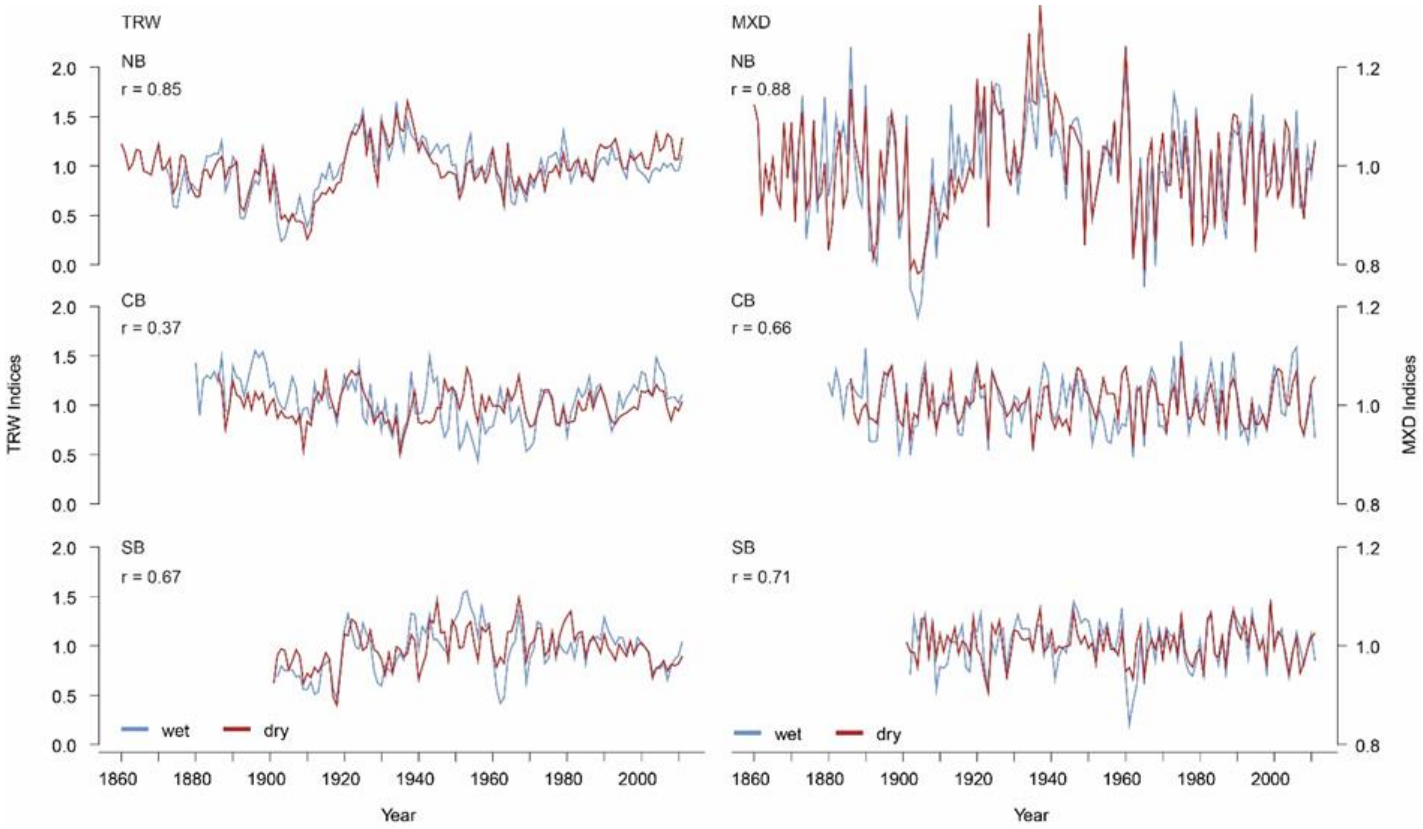

Figure IV-2: Maximum latewood density (left) and tree-ring width (right) micro-site chronologies for the northern, central and southern sampling site. Chronologies are truncated at n < 3.

3.2 Growth rates and tree-ring formation

The relative composition of the tree-ring shows latitude independent intra-annual wood formation processes and latitude dependent biomass production of the total tree-ring (Fig.IV-3a). The relative distribution of earlywood and latewood is very persistent throughout the transect reaching EW ~70% and LW ~ 30%. Similarly, mean earlywood density is fairly stable along the transect (~ 0.39 g/cm³), while latewood density decreases with increasing latitude. Furthermore, slightly higher EWD and LWD values are observed at the dry micro-sites. Mean TRW is higher at CB (1.45 mm) and SB (1.43 mm) compared to NB (0.69 mm). Best growth conditions among all six micro-sites are observed at the wet micro-site in central Finland (1.64 mm/year), and the harshest environment is found at the wet micro-site in the north with mean TRW of only 0.67 mm (Fig. IV-3b). At CB and SB, the lakeshore trees grow faster, whereas in the north the trees at the dry micro-site show higher growth rates.

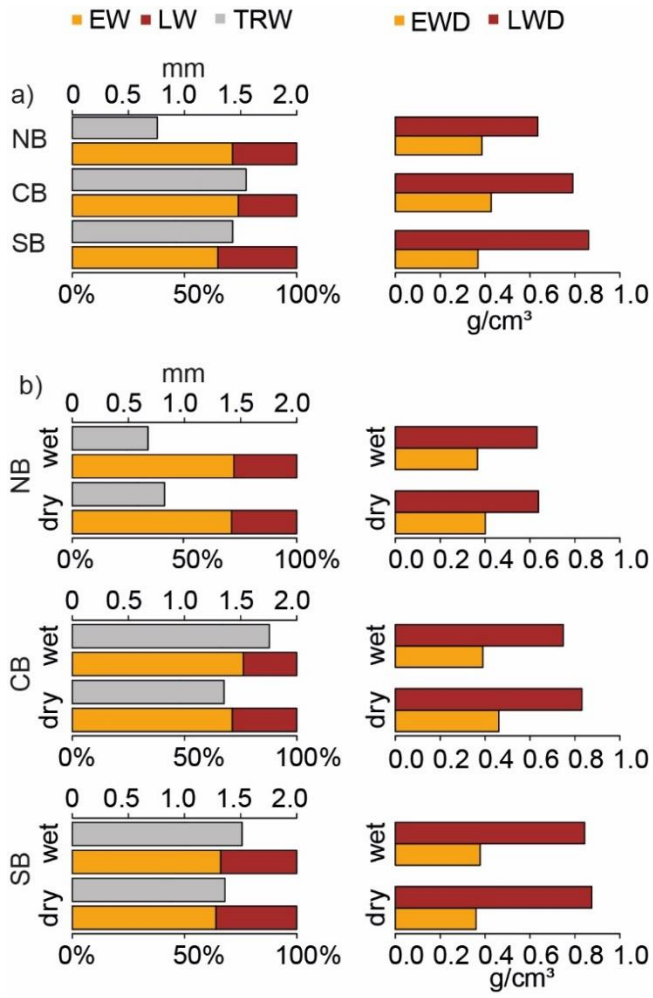

Figure IV-3: Comparison of the absolute and relative composition of the tree-rings for tree ages of 5-120 years. a) Left panel shows the mean growth in grey and the relative composition of earlywood (EW) and latewood (LW) in orange and brown, respectively. Means of earlywood density (EWD) and latewood density (LWD) are displayed in the right panel. b) Same as a) but the sites are grouped in "wet" and "dry" micro-sites.

The age aligned growth curves, which are representative for the typical growth behavior at each site, revealed no clear pattern, supporting more favorable growth conditions at the wet or dry micro-site (Fig. IV-4). In general, the growth curves of TRW data decrease with increasing cambial ages and the density values of MXD series show an increasing trend for the first 20-30 years and after this stage the values decrease slightly for the following years. Deviations of this models are found at SB for TRW and NB for MXD. The growth rate in SB is comparable with the typical MXD pattern and increases in the first 10-20 years before it decreases for the next 100 years. The anomalous age trend at NB for MXD is marked with continuous increasing density values with higher tree ages. In general, the growth rates, whether with a typical or anomalous run, are similar within the micro-sites. Wet trees grow faster and are less dense at CB and SB. The northern site does not point towards a more favorable and denser micro-site. The level of the density and TRW values increases with decreasing latitude.

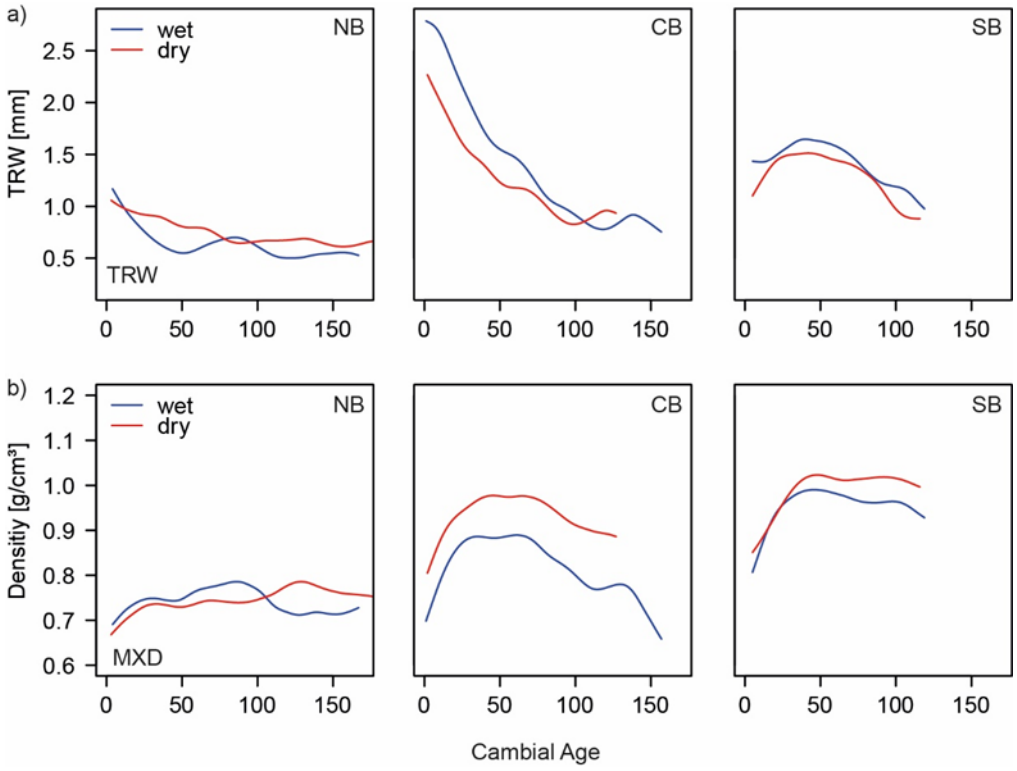

Figure IV-4: Smoothed (40-years) age-aligned regional growth curves of wet and dry micro-sites for a) TRW and b) MXD.

3.3 Climate growth relationship

Bootstrapped correlation coefficients with temperature, precipitation and the SPEI-12 index help identifying seasons with significant ($p \leq 0.01$) impact on tree growth (Fig.IV-5). Negative correlations with precipitation and the SPEI-12 index are linked with MXD. The negative relationship of tree growth and precipitation is strongest at SB, especially during mid-summer (June-August). For the early vegetation period in April and May the southern trees have a positive correlation with the drought index. July, JJA (June-August) and JA (July-August) precipitation is also important for CB. A negative link to July precipitation and to drought in summer (July-September) is visible at NB. Positive correlations with temperatures are characteristic to all density chronologies with a maximum response ($r_{JA} = 0.69$) at NB. Trees at all sites show a significant relationship to JJA mean temperatures and related seasons (August to September, JA, JAS). A link to early growing season temperatures (April and May) could only be detected at CB. In contrast, only the northern and central TRW chronologies respond positively to summer temperature ($r_{JA} = 0.49$). In general, the correlations of temperature with TRW chronologies are lower than with MXD time series. The micro-site chronologies are fairly similar and show no distinct differences between wet and dry sites. But there is a continuous trend towards stronger correlations in the dryer micro-sites, especially in northern and southern Finland. This trend exists in both tree-ring parameters.

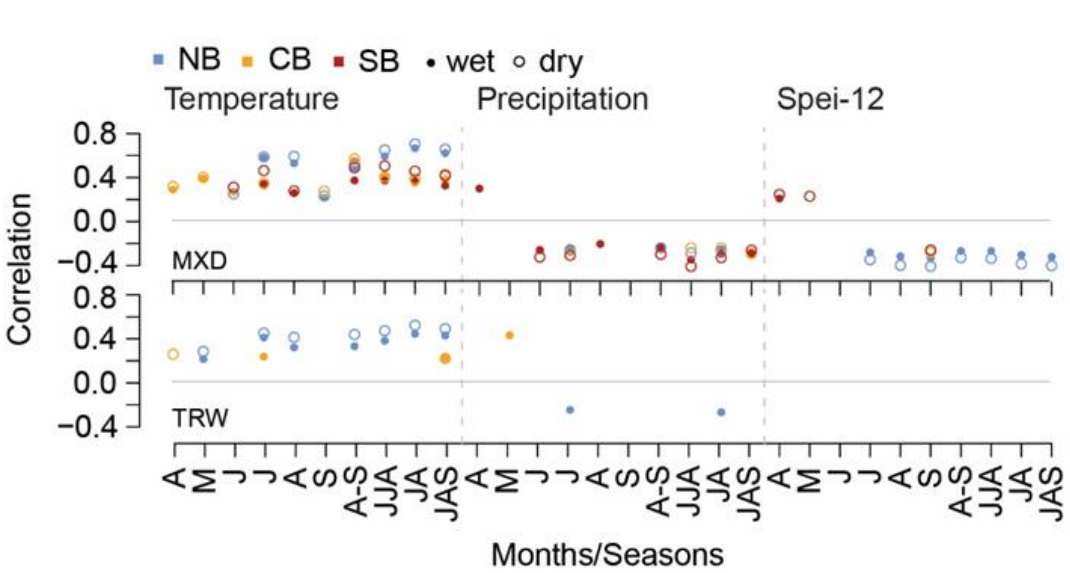

Figure IV-5: Significant correlations ($p \leq 0.01$) between micro-site chronologies and climate data over the 1902-2011 common period. Upper (lower) panel shows correlations with maximum latewood density (tree-ring width) series for single months and seasonal means (A-S: April to September, JJA: June, July and August, JA: July and August, JAS: July, August and September) of the growing season. On the left the relationship with temperature is plotted, the middle climate parameter is precipitation and on the right correlations with the 12 months SPEI index are computed. Blue dots represent NB, orange CB and red SB. Filled dots (circles) symbolize the wet (dry) sites.

The temporal relationship of summer temperatures and MXD is decreasing towards the most recent time, while in this period the negative precipitation signal is increasing (Fig. IV-6). NB reveals the highest correlations with temperature during all periods (Fig. IV-6a), while the lowest correlations are found during the most recent period at CB. At CB and SB the correlation decreases linear in the time frames, while highest correlation is attained during the middle period (r = 0.78). The link of tree growth and precipitation is constantly negative (Fig. IV-6b). In the early period, this link is weak however, particularly at SB (r < -0.2). This relationship decreases in the middle, and during the recent period the correlation coefficients of all sites are most negative.

4. Discussion

4.1 Tree-ring formation and growth characteristics

The boreal tree-ring growth-patterns assessed here, show that the composition of tree-rings with EW and LW is constant along a latitudinal gradient from 60-69°N and among ecologically differing micro-sites. Around 70% of the total tree-ring is formed by EW and the EW/LW relationship remains constant throughout latitudes and micro-sites. Schmitt et al. (2004) divide pine growth during the vegetation period in a slow initiation, faster growth in the middle and a decreasing activity of the cambium towards the end of the season. The length of these phases is adjusted to the duration of the vegetation period and therefore the relative composition of EW/LW is not influenced by latitude. In higher latitudes growing season temperatures are the limiting factor of cell enlargement and the number of days, with adequate temperatures for tree growth, decreases towards the arctic treeline. At the same time the day length, sunshine hours and photosynthesis rates increase. Positive correlations of TRW chronologies with summer temperatures reflect the dependence of growing season temperatures (Fig. IV-5). Due to the strong influence of EW on TRW (70 %), early and mid-growing season temperatures are dominating ring formation. In late summer, when secondary wall formation starts, the cell walls thicken, the lumen shrinks and the wood is getting denser (Butterfield 2003, Rossi et al. 2015). Besides the season of cell formation, the density of the cells depends also on the latitude and on the micro-habitat. The more south and moderate the sites, the denser the EW and LW. This coincides with the altitudinal studies of Schweingruber (1983), where more favorable conditions are directly associated with higher density values. More systematically the duration of the latewood cell formation is associated to the wall thickness of the cells (Rossi et al. 2006) and the longer the cells have time to form, the denser they are. This lead to the assumption that mainly late summer temperatures are responsible for the differences in the latewood density values.

4.2 Climate and tree-ring growth

As TRW is dominated by EW, formed in the beginning of the growing season, this tree-ring fragment is also influenced by carry-over effects of the previous year and harsh conditions during winter time (Fritts 1976). It has been argued that this memory, on top of the current year growing season influence,

causes a reduced climate sensitivity compared to MXD (Büntgen et al. 2010a). This theory is supported by the higher lag-1 autocorrelation for TRW as for MXD (Table IV-1). Ecotone tree growth in high latitudes and high elevations is mainly connected to one limiting factor (Fritts 1976). Next to the widely known temperature signal in high latitudes (Fritts 1976, Schweingruber et al. 1978, Büntgen et al. 2010a, McCarroll et al. 2013, Esper et al. 2014, Helama et al. 2014), some studies however, also point out that density data are related to precipitation sums as a secondary effect (Briffa et al. 2002). The relationship between drought or precipitation, and tree growth can be strong. But until now mainly TRW data are used as proxy for these climate parameters (Cook and Jacoby 1977, Casty et al. 2005, Wilson et al. 2005, Drobyshev et al. 2011).

Along our boreal tree-ring transect, highest correlations with summer temperature were found in the density data. Additionally, the MXD chronologies are significantly anti-correlated with summer precipitation and the SPEI-12 drought-index (Fig. IV-5), a finding that is less consistent in the TRW data throughout the boreal transect. The anti-correlation indicates that trees react with reduced growth and lower wood density to increasing precipitation sums. This effect seems to be more pronounced at NB as the SPEI-12 index also shows this negative relationship. A closer look at the micro-sites reveals no clear differences between the different habitats, but the slightly stronger correlations at the dry micro-sites might indicate an increased sensitivity to moist atmospheric conditions in this locally dryer "inland" environment. Briffa et al. (2002) already defined this signal as beside effect, as temperature and precipitation are coupled in some way. It seems that inland trees are slightly more stressed by moist atmospheric conditions. But the continuous run-off at the slopes and the porous soil do not allow backwater accumulations. Lower growth rates at the dry micro-sites in CB and SB also imply a more restricted tree growth. Depending on the prevailing atmospheric regime more or less cloud coverage impedes the passing of sunlight and also forces precipitation (Schneider et al. 2014). Messier et al. (1999) introduce the aspect of increasing competition for sunlight in closed canopy forests, especially during the growing season (Nemani et al. 2003). Competition for sunlight among trees at the dry site, where the forest has a closed canopy structure, is higher than at the wet site, where a more open canopy forest system dominates. An increased sensitivity to external factors might also indicate a higher vulnerability of the ecosystem to future climatic changes (Cook et al. 2014). The correlation pattern also points out that micro-site conditions are less important for the relationship of climate and MXD than for climate and TRW. With regard to climate reconstructions this is less substantial for MXD, as the climate signal at the wet site is almost as strong as at the dry site. Both sites offer significant responses to temperature and precipitation data, while this is not the case for TRW. TRW only shows a stable relationship to summer temperatures for NB and the precipitation signal appears only at the wet site of NB. This indicates that the lakeshore trees are stressed by high precipitation sums, while inland trees are less affected. Next to the benefits from a climatological point of view lakeshore trees are also important for long term chronologies with regard to ecological and statistical properties (Düthorn et al. 2015b).

Next to the ecological conditions, also the period of correlations with climate data matters. The splitting of the analyzed period in three equally long periods results in enhanced precipitation sensitivity in recent times (Fig. IV-6b). This rise is connected to higher precipitation sums (IV-S1) and thus more cloudy conditions in the last decades. Furthermore, projections of Cook et al. (2014) predict wetter conditions for the Scandinavian Peninsula whereas other parts, as the Mediterranean area, have to deal with drought. In combination with increasing precipitation sums also the cloud cover will increase in the next decades and finally the amount of direct sunlight will diminish.

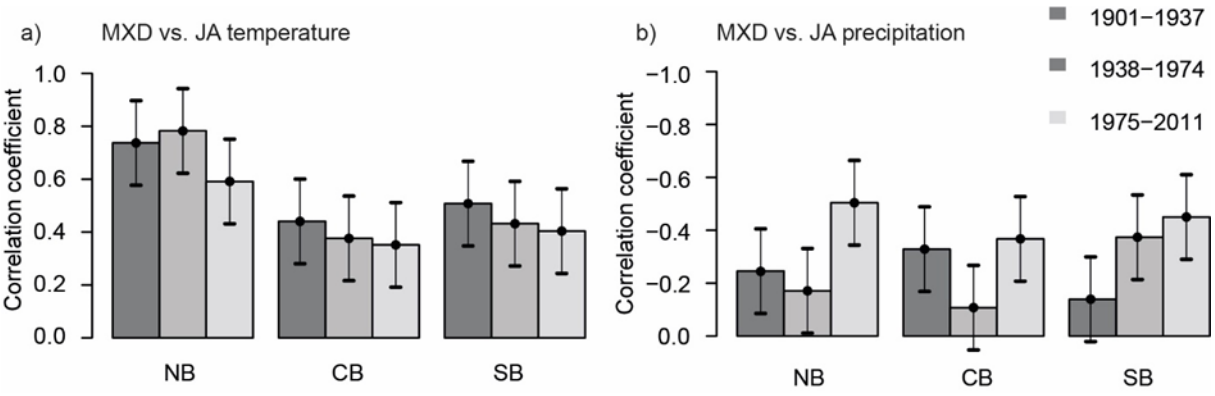

Figure IV-6: Correlation patterns with a) JA temperatures and b) JA precipitation over different time periods (1901-1937, 1938-1974, 1975-2011).

5. Conclusion

The boreal forest ecosystem is vulnerable to changing external conditions. During the growing season higher precipitation sums and more clouds negatively affects tree growth. In contrast to earlier studies (Düthorn et al. 2013), the micro-sites do not reveal a clear pattern of growth rates between wet and dry sites along a boreal gradient from 60°N to 69°N. Interestingly, the MXD variability is not affected by the separation in inland and lakeshore trees. This is in accordance to Wilson and Luckman (2003) as they also state that site specific factors are less important for the common signal of MXD time series. In contrast, micro-sites influence TRW. However, the inconsistent regional curves of TRW concerning micro-site effects, needs further research as the differentiation of micro-sites can produce statistical biases during the standardization process and lead to misinterpretations of long-term chronologies and climate reconstructions (Düthorn et al. 2015b).

In conclusion for absolute tree growth and the climate growth relationship the latitudinal effects are larger than micro-site effects. In general, micro-site effects are less pronounced in MXD compared to TRW. Though there are micro-site effects they decrease with increasing latitude. Indeed if the effects of the micro-sites are miner, the insights in ecological issues for assessing tree growth under future climatic conditions, as increasing precipitation sums (Cook et al. 2014), are substantial.

Acknowledgements

We thank Steffen Holzkämper, Mauri Timonen and Maria Mischel for fieldwork and Claudia Hartl-Meier for discussion.

References

Affolter P., Büntgen U., Esper J., Rigling A., Weber P., Luterbacher J., Frank D. (2010): Inner Alpine conifer response to 20th century drought swings. *European Journal of Forest Research* 129: 289-298.

Ahti T., Hämet-Ahti L., Jalas J. (1986): Vegetation zones and their sections in north western Europe. *Annales Botanici Fennici* 3: 169-2011.

Bräker O.U. (1981): Der Alterstrend bei Jahrringdichten und Jahrringbreiten von Nadelhölzern und sein Ausgleich. *Mitteilungen der Forstlichen Bundesversuchsanstalt Wien* 142: 75-102.

Briffa K.R., Osborn T.J., Schweingruber F.H., Jones P.D., Shiyatov S.G., Vaganov E.A. (2002): Tree-ring width and density data around the Northern Hemisphere: Part 1, local and regional climate signals. *Holocene* 12: 737-757.

Büntgen U., Frank D., Trouet V., Esper J. (2010a): Diverse climate sensitivity of Mediterranean tree-ring width and density. *Trees-Structure and Function* 24: 261-273.

Butterfield B. (2003): Wood anatomy in relation to wood quality. In: Barnett, J, Jeronimidis, G (eds): Wood quality and its biological basis. Blackwell. 30-52.

Casty C., Wanner H., Luterbacher J., Esper J., Bohm R. (2005): Temperature and precipitation variability in the european Alps since 1500. *International Journal of Climatology* 25: 1855-1880.

Cook B.I., Smerdon J.E., Seager R., Coats S. (2014): Global warming and 21st century drying. *Climate Dynamics* 43: 2607-2627.

Cook E.R., Jacoby G.C. (1977): Tree-Ring Drought Relationships in Hudson Valley, New-York. *Science* 198: 399-401.

Cook E.R., Kairiukstis L.A. (1990): Methods of dendrochronology. Kluwer Academic Publishers.

Cook E.R., Peters K. (1997): Calculating unbiased tree-ring indices for the study of climatic and environmental change. *Holocene* 7: 361-370.

Drobyshev I., Niklasson M., Linderholm H.W., Seftigen K., Hickler T., Eggertsson O. (2011): Reconstruction of a regional drought index in southern Sweden since AD 1750. *Holocene* 21: 667-679.

Düthorn E., Holzkämper S., Timonen M., Esper J. (2013): Influence of micro-site conditions on tree-ring climate signals and trends in central and northern Sweden. *Trees* 27: 1395-1404.

Düthorn E., Lindén J., Gläser S., Timonen M., Esper J. (2014) Heterogeneity in the climate signal strength of Pinus sylvestris tree-ring chronologies in Southern Finland. Paper presented at the TRACE, Viterbo,

Düthorn E., Schneider L., Konter O., Schön P., Timonen M., Esper J. (2015b): On the hidden significance of differing micro-sites on tree-ring based climate reconstructions. *Silva Fennica* 49.

Esper J., Cook E.R., Krusic P.J., Peters K., Schweingruber F.H. (2003): Tests of the RCS method for preserving low-frequency variability in long tree-ring chronologies. *Tree-Ring Research* 59: 81-98.

Esper J., Düthorn E., Krusic P.J., Timonen M., Büntgen U. (2014): Northern European summer temperature variations over the Common Era from integrated tree-ring density records. *Journal of Quaternary Science*.

Esper J., Frank D.C., Timonen M., Zorita E., Wilson R.J.S., Luterbacher J., Holzkamper S., Fischer N. et al. (2012c): Orbital forcing of tree-ring data. *Nature Climate Change* 2: 862-866.

Frank D., Esper J. (2005): Temperature reconstructions and comparisons with instrumental data from a tree-ring network for the European Alps. *International Journal of Climatology* 25: 1437-1454.

Frank D., Esper J., Cook E.R. (2007): Adjustment for proxy number and coherence in a large-scale temperature reconstruction. *Geophysical Research Letters* 34.

Fritts H.C. (1976): Tree rings and climate. Academic Press.

Harris I., Jones P.D., Osborn T.J., Lister D.H. (2014): Updated high-resolution grids of monthly climatic observations - the CRU TS3.10 Dataset. *International Journal of Climatology* 34: 623-642.

Hartl-Meier C., Dittmar C., Zang C., Rothe A. (2014a): Mountain forest growth response to climate change in the Northern Limestone Alps. *Trees-Structure and Function* 28: 819-829.

Hartl-Meier C., Zang C., Dittmar C., Esper J., Gottlein A., Rothe A. (2014b): Vulnerability of Norway spruce to climate change in mountain forests of the European Alps. *Climate Research* 60: 119-132.

Helama S., Lindholm M. (2003): Droughts and rainfall in south-eastern Finland since AD 874, inferred from Scots pine ring-widths. *Boreal Environment Research* 8: 171-183.

Helama S., Lindholm M., Merilainen J., Timonen M., Eronen M. (2005a): Multicentennial ring-width chronologies of Scots pine along a north-south gradient across Finland. *Tree-Ring Research* 61: 21-32.

Helama S., Vartiainen M., Holopainen J., Makela H.M., Kolstrom T., Merilainen J. (2014): A palaeotemperature record for the Finnish Lakeland based on microdensitometric variations in tree rings. *Geochronometria* 41: 265-277.

Kienast F., Schweingruber F.H., Bräker O.U., Schär E. (1987): Tree-ring studies on conifers along ecological gradients and the potential of single-year analyses. *Canadian Journal of Forest Research* 17: 683-696.

Kultti S., Mikkola K., Virtanen T., Timonen M., Eronen M. (2006): Past changes in the Scots pine forest line and climate in Finnish Lapland: a study based on megafossils, lake sediments, and GIS-based vegetation and climate data. *Holocene* 16: 381-391.

Lenz O., Schar E., Schweingruber F.H. (1976): Methodological Problems Relative to Measurement of Density and Width of Growth Rings by X-Ray Densitogrames of Wood. *Holzforschung* 30: 114-123.

Martin-Benito D., Pederson N. (2015): Convergence in drought stress, but a divergence of climatic drivers across a latitudinal gradient in a temperate broadleaf forest. *Journal of Biogeography* 42: 925-937.

McCarroll D., Loader N.J., Jalkanen R., Gagen M.H., Grudd H., Gunnarson B.E., Kirchhefer A.J., Friedrich M. et al. (2013): A 1200-year multiproxy record of tree growth and summer temperature at the northern pine forest limit of Europe. *Holocene* 23: 471-484.

Messier C., Doucet R., Ruel J.C., Claveau Y., Kelly C., Lechowicz M.J. (1999): Functional ecology of advance regeneration in relation to light in boreal forests. *Canadian Journal of Forest Research-Revue Canadienne De Recherche Forestiere* 29: 812-823.

Mitchell T.D., Jones P.D. (2005): An improved method of constructing a database of monthly climate observations and associated high-resolution grids. *International Journal of Climatology* 25: 693-712.

Nemani R.R., Keeling C.D., Hashimoto H., Jolly W.M., Piper S.C., Tucker C.J., Myneni R.B., Running S.W. (2003): Climate-driven increases in global terrestrial net primary production from 1982 to 1999. *Science* 300: 1560-1563.

Rossi S., Cairo E., Krause C., Deslauriers A. (2015): Growth and basic wood properties of black spruce along an alti-latitudinal gradient in Quebec, Canada. *Annals of Forest Science* 72: 77-87.

Rossi S., Deslauriers A., Anfodillo T. (2006): Assessment of cambial activity and xylogenesis by microsampling tree species: An example at the alpine timberline. *Iawa Journal* 27: 383-394.

Schmitt U., Jalkanen R., Eckstein D. (2004): Cambium dynamics of Pinus sylvestris and Betula spp. in the northern boreal forest in Finland. *Silva Fennica* 38: 167-178.

Schneider L., Esper J., Timonen M., Büntgen U. (2014): Detection and evaluation of an early divergence problem in northern Fennoscandian tree-ring data. *Oikos* 123: 559-566.

Schweingruber F.H. (1983): Der Jahrring: Standort, Methodik, Zeit und Klima in der Dendrochronologie. P. Haupt.

Schweingruber F.H., Fritts H.C., Bräker O.U., Drew L.G., Schär E. (1978): The X-ray technique as applied to dendroclimatology. *Tree-Ring Bulletin* 38: 61-91.

Seo J.W., Eckstein D., Jalkanen R., Schmitt U. (2011): Climatic control of intra- and inter-annual wood-formation dynamics of Scots pine in northern Finland. *Environmental and Experimental Botany* 72: 422-431.

Vicente-Serrano S.M., Beguería S., López-Moreno J.I., Angulo-Martínez M., El Kenawy A.M. (2010): A new global 0.5° gridded dataset (1901-2006) of a multiscalar drought index: comparison with current drought index datasets based on the Palmer Drought Severity Index. *Journal of Hydrometeorology* 11: 1033-1043.

Wilson R.J.S., Luckman B.H. (2003): Dendroclimatic reconstruction of maximum summer temperatures from upper treeline sites in Interior British Columbia, Canada. *Holocene* 13: 851-861.

Wilson R.J.S., Luckman B.H., Esper J. (2005): A 500 year dendroclimatic reconstruction of spring-summer precipitation from the lower Bavarian Forest region, Germany. *International Journal of Climatology* 25: 611-630.

Zang C., Biondi F. (2014): treeclim: an R package for the numerical calibration of proxy-climate relationships. *Ecography*: n/a-n/a.

Supplementary Material

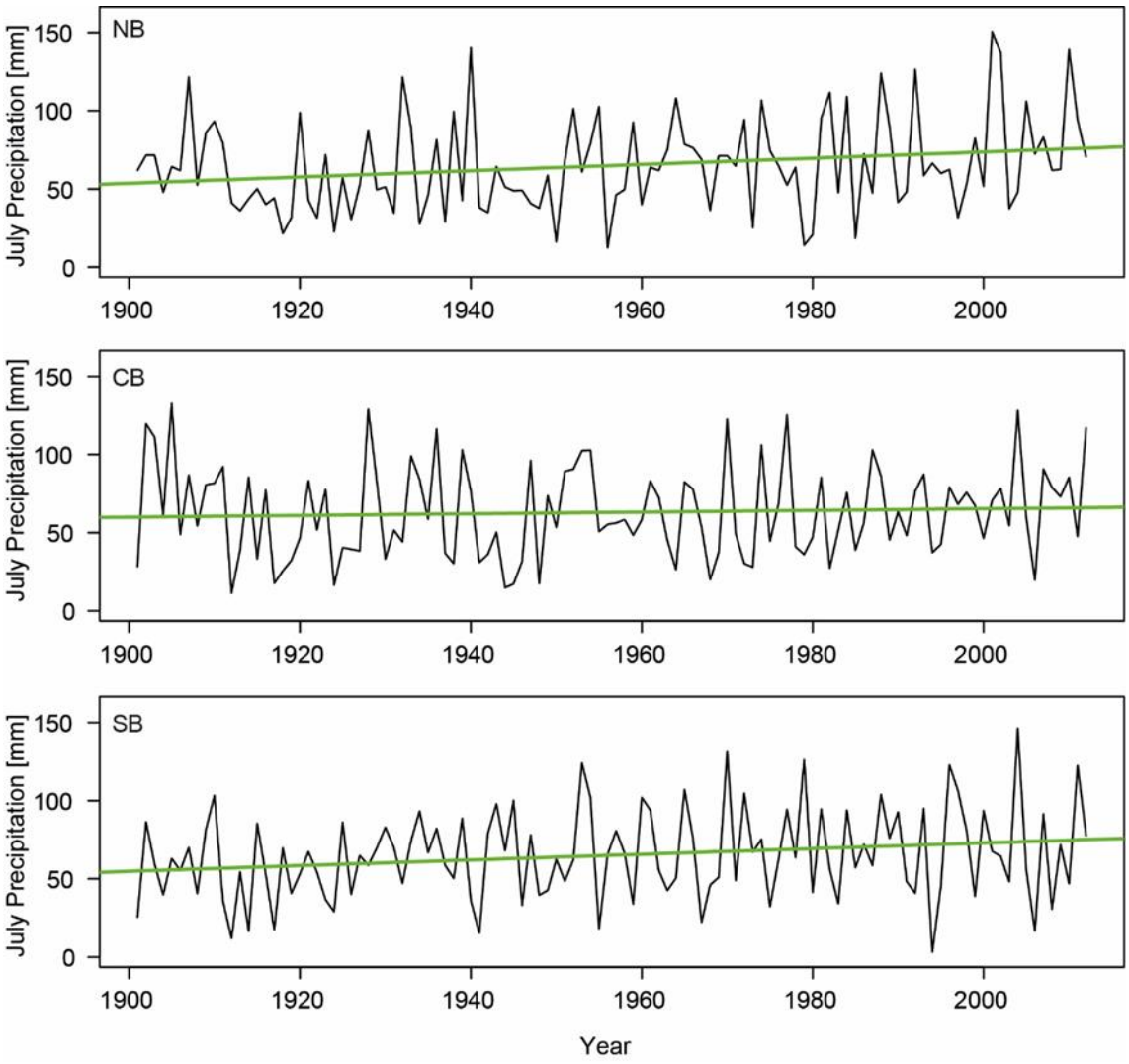

Supplement IV-1: July precipitation for NB, CB and SB with the liner trend (green) from 1901-2012. Precipitation data are based on interpolated CRU 3.21 TS from the four nearest grid points to the sampling sites.

Chapter V: Spatial patterns in a Fennoscandian micro-site tree-ring network

E. Düthorn[1], E. Tejedor Vargas[2], A. Kirchefer[3], M. Timonen[4], S. Holzkämper[5], J. Esper[1]

[1] Department of Geography, Johannes Gutenberg University, 55099 Mainz, Germany

[2] Environmental Sciences Institute (IUCA), University of Zaragoza, 50009 Zaragoza, Spain

[3] Dendroøkologen A.J. Kirchhefer, NO-9011 Tromsø, Norway

[4] Natural Ressources Institute Finland, Eteläranta 55, 96301 Rovaniemi, Finland

[5] Department of Physical Geography, Stockholm University, 10691 Stockholm, Sweden

(*Applied Vegetation Science*, submitted)

1. Introduction

The boreal forest provides a unique continuous ecosystem and forms one of the main industrial pillars for the Fennoscandian countries (FAO 2010). Next to its economic significance, the boreal forest is also interesting for paleoclimatic studies. Due to the unchanged woodlands, reduced anthropogenic influences, and marginal geographical location, the boreal ecosystem forms an important archive to study vegetation dynamics and evaluate the impact of external factors on tree growth (Swetnam et al. 1999). Beside dendroclimatological studies (Gouirand et al. 2008, Grudd 2008, Büntgen et al. 2011, Gunnarson et al. 2011, Esper et al. 2012c, McCarroll et al. 2013) also dendroecological studies (Schmitt et al. 2004, Holtmeier and Broll 2005, Kultti et al. 2006, Düthorn et al. 2013) are carried out in these areas.

While maximum latewood density (MXD) measurements achieve a higher temperature signal, tree-ring width (TRW) data might provide more detailed information on the processes that force radial growth (Fritts 1976). TRW series from northern and central Sweden were shown to display differences between trees directly standing at the lakeshore, and trees some meters away from the lakeshore in a dryer ecological habitat (Düthorn et al. 2013). The differences between these lakeshore (here also named: wet) and inland (dry) habitats are described as micro-site effects (Düthorn et al. 2013). Further studies on micro-sites revealed a heterogeneous picture on the characterization and possible influences of this ecological phenomenon (Düthorn et al. 2013; Düthorn et al. 2015a; Düthorn et al. 2015b). While a statistical bias on long-term chronologies and the potential of misinterpretation of temperature reconstructions has been shown (Düthorn et al. 2015b), it is unclear whether the occurrence and characteristics of micro-site effects are a general phenomenon, but appear to depend on changing external factors, e.g. latitude and soil conditions.

Beside these locally variable effects, it is important to understand the drivers of tree growth at larger scales to assess spatial patterns, detect potential provenances of coherent micro-site characteristics and evaluate underlying mechanisms. The micro-site network also helps to detect areas with possible outliers in the micro-site pattern and to avoid statistical biases by obtaining low-frequency in composite time-series. The preservation of low-frequency variability will improve temperature reconstructions from higher latitudes.

In this study we introduce a network of 20 tree-ring sites in Fennoscandia where at each location a well-replicated wet and dry micro-site was sampled. We identify common growth patterns in different regions of the boreal forest, and use cluster analysis to develop chronologies and assess macro-scale influences with regard to longitude and latitude. As the climate-growth relationship is an important component of dendrochronology we also focus on differences in the climate signal with regard to wet and dry micro-site habitats.

2. Material and Methods

2.1 Species

Pinus sylvestris L. (Scots pine) is a coniferous tree species, which can cope with extreme environmental situations (Schmitt et al. 2004, Mátyás et al. 2004). It grows in regions with predominantly poorer and sandy soils, peatlands or close to a forest limit (Mátyás et al. 2004). At the forest limit it can manage less than 100 frost-free days/year and less than 300 mm precipitation. Scots pine is distributed in dense stands over Fennoscandia ranging up to 70°N. In high latitudes, the combination of high content of resin and low temperatures allow good conservation of dead wood on the ground (hereafter: snag material) and in lakes (subfossil material). Many dendroclimatological studies showed that the species is sensitive to summer temperatures in high latitudes and altitudes (e.g.: Gunnarson et al. 2011, Esper et al. 2012c, McCarroll et al. 2013), whereas in more southern and central areas of Fennoscandia tree growth is coupled with drought stress (Drobyshev et al. 2011).

Table V-1: Chronology characteristics

Site	Lat °N	Lon °E	Elevation (m asl)	First Year	Last Year	Chrono length (n≥5)	Mean (mm)	Number of series	rbar	Cluster
Ail	69.52	28.57	120	1688	2011	294	0.58	190	0.302	N-East
Nik	69.36	18.73	90	1788	2014	180	0.83	132	0.397	N-West
Ski	69.35	20.32	72	1801	2013	194	0.54	202	0.344	N-West
Jou	69.26	27.40	200	1700	2011	303	0.87	316	0.314	N-East
Fis	69.06	19.34	151	1680	2014	272	0.78	139	0.265	N-West
Div	68.86	19.59	320	1742	2013	221	1.04	182	0.193	N-West
Kar	68.83	27.31	258	1511	2011	455	0.53	200	0.253	N-East
Nes	68.57	16.06	345	1701	2013	273	1.17	164	0.206	N-West
Kuu	68.45	27.36	302	1710	2011	164	1.16	175	0.174	N-East
Ket*	68.22	24.05	300	1569	2006	417	0.55	115	0.298	N-East
Tor*	68.20	19.80	390	1796	2006	205	1.08	176	0.281	N-East
Kir12*	67.95	20.03	430	1656	2006	200	0.84	191	0.303	N-East
Kir**	67.90	20.10	451	1800	2009	231	0.98	128	0.37	N-East
Jok	66.65	20.11	302	1715	2013	275	0.85	212	0.167	C-Scan
Hos	65.49	29.40	229	1729	2011	257	0.65	200	0.311	C-Scan
Sot	64.12	28.34	148	1840	2011	163	0.91	191	0.192	C-Scan
Mek	62.73	31.01	147	1830	2011	162	1.17	213	0.297	C-Scan
Pun	61.81	29.31	78	1824	2011	173	1.23	186	0.403	C-Scan
Mel	60.73	24.06	120	1875	2011	129	1.21	209	0.251	C-Scan
Sto**	59.44	17.99	20	1804	2009	197	1.24	127	0.235	C-Scan

* Esper et al. (2012); ** Düthorn et al. (2013)

2.2 Micro-site network

The boreal micro-site tree-ring network consists of 20 sites located 59°-69°N and 15°-29°E (Fig. V-1). Our sampling design distinguishes between trees growing directly at the lakeshore (hereafter: wet micro-site) and more than 5 meters away in the upland (dry micro-site; see Düthorn et al. 2013).

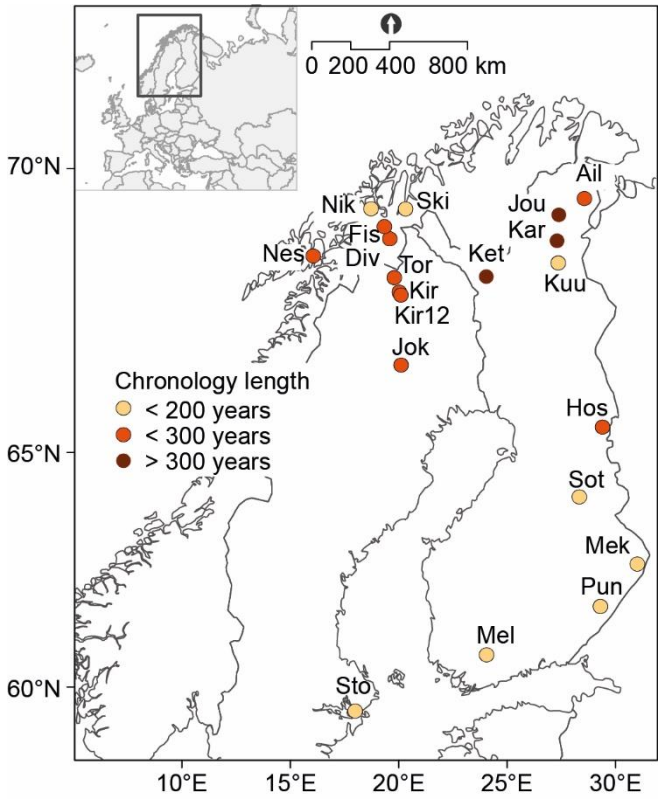

Figure V-1: Map showing the Scandinavian micro-site tree-ring network. All 20 sites are sampled considering the lakeshore (wet) and inland (dry) micro-site sampling design detailed in Düthorn et al. (2013). The colors of the dots indicate chronology lengths after truncating at a minimum replication of 5 series.

For longitudinal and latitudinal comparisons the network can be divided into two main transects: 13 sites north of 67°N are arranged in a clear west-east pattern indeed capturing Luv and Lee effects from the Scandes as the main orographic barrier. A distinct north-south transect is represented by nine sites in Finland capturing tree growth in different types of the boreal forest (Ahti et al. 1986). While the northern boreal zone is characterized by the dominance of conifers and sub-alpine birch forest at the tree line, the middle boreal, southern boreal and hemiboreal zone include a larger number of deciduous tree species.

Data were collected during several field campaigns between 2012 and 2014 and complemented by five sites from previous studies of micro-site effects on tree-ring density data (Kir, Sto, Ket, Kir12, Tor; Esper et al. 2012c, Düthorn et al. 2013) (Table V-1). We here combine this micro-site network with another 40 Fennoscandian pine TRW sites, downloaded from the International Tree-Ring Data Bank

(ITRDB; Grissino-Mayer and Fritts 1997), to place the micro-site tree-ring network into a full Fennoscandian perspective and represent its spatial expansion. The oldest downloaded pine dataset was sampled in 1982; all datasets exceed a minimum of 10 TRW series, and are located between 58.9°-69.5°N and 8°-32°E (Fig. V-S1). The common period for all 60 site chronologies is 1882-1981.

2.3 Data analysis

The micro-site tree-ring network consist of 3648 TRW series (Fig. V-2). Each series was standardized by applying a Negative Exponential Curve Standardization to remove non-climatic information and to preserve inter-annual to multi-decadal variability in the mean chronologies. Before calculating residuals a data adaptive power transformation was applied to stabilize heteroscedastic variance (Cook and Peters 1997). The variance was stabilized using a 100-year spline, and all chronologies were truncated at a minimum replication of five TRW series. Moreover, the single raw series were aligned by their cambial age, considering the pith-offset, to calculate regional growth curves (RC) and assess the growth behavior typical to each micro-site in our network (Esper et al. 2003).

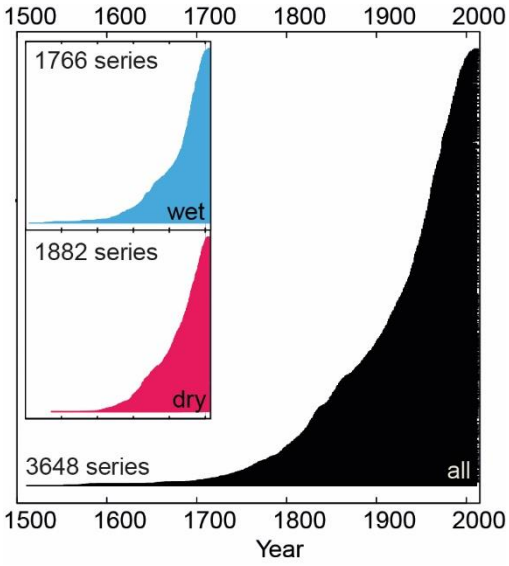

Figure V-2: Summary plot displaying all 3648 TRW measurement series of the Scandinavian micro-site network (black). Insert diagrams show the sample replication of the wet (blue) and dry (red) micro-sites.

Site chronologies were averaged considering a hierarchical cluster analysis of variables (HCAv). Thereby strongly correlated chronologies are arranged to clusters. Albeit, not simple intersite correlations are used, rather tree-ring data are grouped by the correlation with the first principal component of a PCAmix (Chavent et al. 2012b). This central and synthetic variable performs as neutral indication to combine homogeneous sites. The correlation coefficient with this generated parameter allocates cluster membership (Chavent et al. 2012a). In that way the clusters combine tree-ring time series with a statistically defined common signal.

For the "tail test" (Düthorn et al. 2013) subfossil data are combined with living-tree data from wet and dry micro-sites. Crucial for this test is that the most recent part of the chronology only consists of material from one specific micro-site (wet or dry). The relict material originates from three different long-term chronologies representing different areas in Fennoscandia and corresponding to the clusters defined above: Nscan (Esper et al. 2012c) ; Torn (swed021w; Schweingruber et al. 1988); c_fos (finl029, finl030, finl031, finl032, finl033, finl034, finl035, finl036, and finl037; Lindholm et al. 1999). After merging the material (subfossil + recent) the composite chronologies can be classified into three periods: the period only covered by relict data, the overlapping period, and the period covered by only living-tree data (wet or dry). As the cluster micro-site chronologies at least reach back to 1750 (5 series minimum replication), we truncated the subfossil records to not extend beyond the maximum period of 540 AD-1800 AD. For the recent material, we only proceeded with TRW data of an age 1-40 years, as this is the period where maximum differences between wet and dry micro-sites are detected. After combining the relict (truncated), and the living-tree material (age-banded; 1-40 years), RCS detrending was applied (Esper et al. 2003). The resulting chronologies were z-transformed over the 568-1670 AD period to support comparison of the different material and to emphasize differences.

To evaluate the climate signal in the micro-site and pine networks, the mean of the four nearest grid points of the CRU TS 3.22 gridded temperature and precipitation datasets were used (Mitchell and Jones 2005, Harris et al. 2014). Monthly and seasonal climate responses were calculated by computing bootstrapped Pearson´s correlation coefficients ($p \leq 0.01$) over the common period (pine network: 1901 – 1981, micro-site network: 1931-2006) with treeclim (Zang and Biondi 2014).

For the base map we interpolated 1431 CRU grid points with the Kriging method in order to generate the spatial climatic pattern. The main focus is on the climatic performance of July for the 1901-2013 period. Additionally, the SPEI-6 data (Vicente-Serrano et al. 2010) and topsoil data from the Land Use/Cover Area frame Statistical Survey (LUCAS; Toth et al. 2013) were spatially interpolated. The interpolated SPEI-index index defines relative moist areas in the western and central part of the Scandes and in central Finland and relatively drier conditions in low elevation zones of Sweden and northern as well as southern Finland.

3. Results

3.1 Characteristics of the tree-ring network

The Fennoscandian micro-site network consists of 1766 TRW series from lakeshore and 1882 TRW series from dry habitats, and covers the last 500 years (1511-2014 AD) (Fig. V-2). Every tree was cored twice to simplify crossdating. The maximum length of site chronologies provides a first-order impression of the age-structure in the boreal forest (Table V-1). Sites with tree ages of maximum 200 years occur mainly in the southern areas, whereas most sites provide information up to 300 years. Some sites in the north also comprise very old trees with tree ages up to 500 years.

The 20 sites of the micro-site network are not equally distributed over Fennoscandia, but concentrated in northwest Norway, northern Sweden, and in Finland with distances round about 200km between the sites (Fig. V-1). An assessment of the network using cluster analysis revealed also three main collections of site-chronologies with a clear division into two clusters north of 67°N (N-West and N-East) and one cluster combining sites south of the Arctic Circle (C-Scan; Fig. V-3a). N-West represents five sites in the Scandinavian mountain range, N-East combines five chronologies in north Finland as well as three sites near Lake Torneträsk in northern Sweden. The remaining seven sites, all below the Arctic Circle, are part of the third cluster (C-Scan). The validity of the HCAv with the micro-site network appears to be robust, as the addition of 40 pine sites re-validates the spatial patterns of chronologies, albeit an additional fourth cluster (SW-Scan) is introduced covering the south eastern part of Norway and central Sweden, an area where only few datasets are available in the micro-site network. The mean cluster chronologies representing major regions in Fennoscandia are dissimilar in length, variance, low-frequency variation and also differ extremely with regard to inter-site correlations (Fig. V-3b).

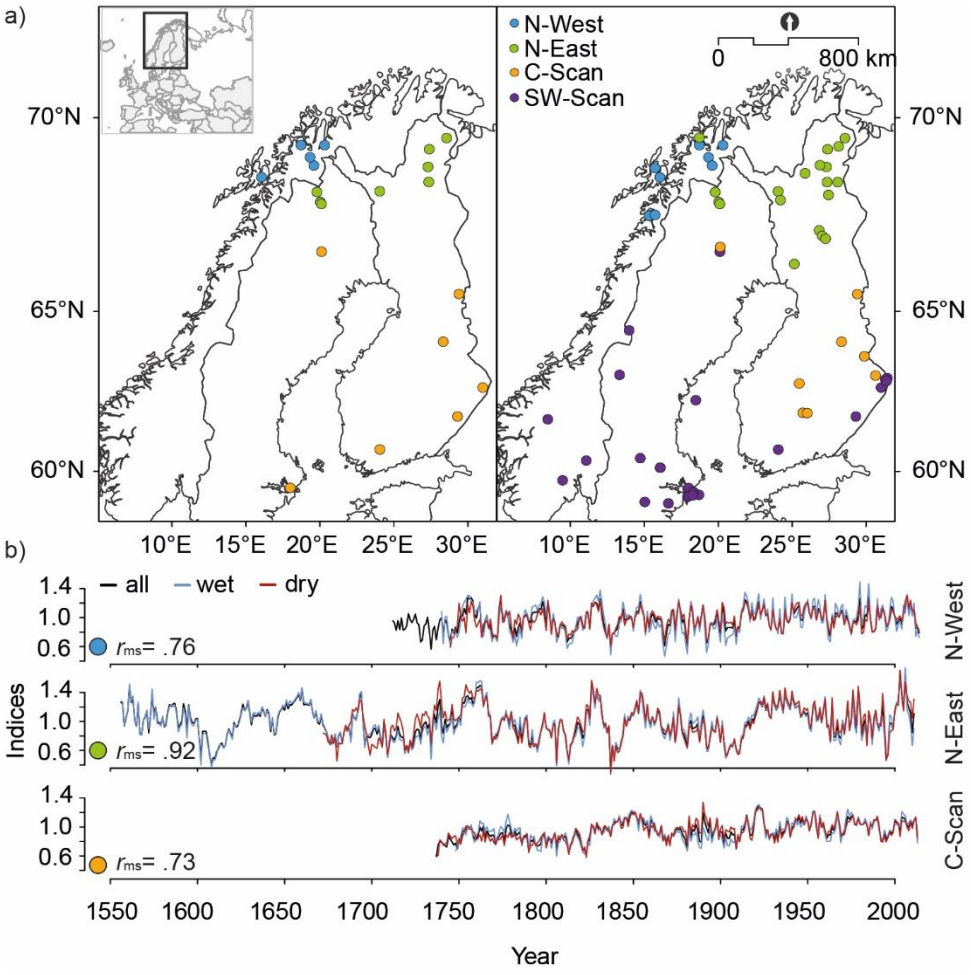

Figure V-3: Hierarchical cluster analysis of variables applied to the micro-site and Scandinavian pine networks. a) Spatial distribution of the first three clusters of the chronologies of the micro-site network (left), and the larger pine network including 40 additional TRW sites (right). b) Mean chronologies the N-West, middle (top), N-East (middle), C-Scan (bottom) clusters considering the lakeshore (blue), inland (red), and all data (black). Chronologies truncated at a minimum replication of 5 TRW series.

The cluster chronologies show high correlations between the wet and dry micro-sites (r_{NE}= 0.92, r_{NW}= 0.76, r_{SC}= 0.73; 1750-2011). The replication for these chronologies is quite substantial due to the merging of a number of site chronologies (N-West: 819 series; N-East: 1491 series; C-Scan: 1338 series). The inter-site correlations within the clusters decreases from north-to-south (r_{NE}= 0.72, r_{NW}= 0.54, r_{SC}= 0.34). This effect appears to be partly connected with the changes in inter-series correlation within the clusters ($rbar_{NE}$= 0.17, $rbar_{NW}$= 0.18, $rbar_{SC}$= 0.13), which also seems to affect the variance of the mean time series, i.e. less variance in chronologies from lower correlating TRW series (Fig. V-3b). As a consequence, N-East shows considerably higher inter-annual and decadal scale variations than N-West, and variability is lowest in the C-Scan chronologies.

3.2 Climate signals

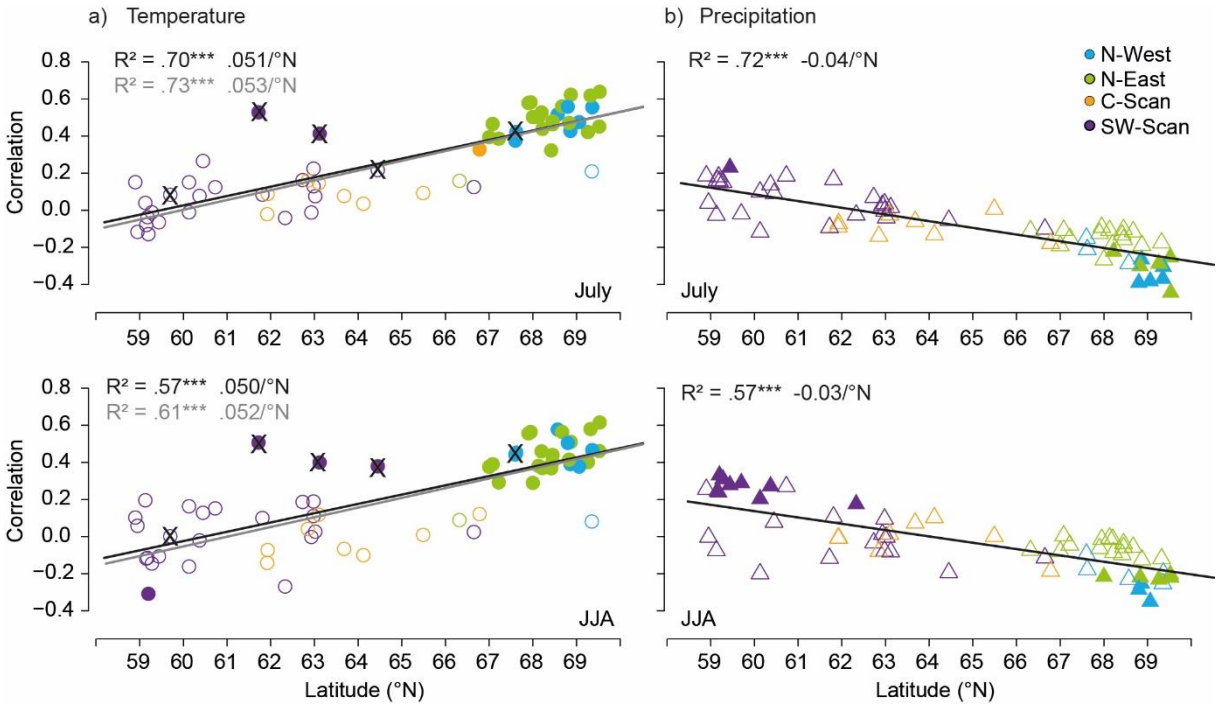

Figure V-4: Climate-growth analysis. a) Correlation coefficients of 60 Scandinavian pine chronologies ordered by latitude (x-axis) against July (top) and June-August (bottom) temperatures over the 1901-1981 common period. Filled symbols are sites reaching significant ($p \leq 0.01$) correlations. Different colors indicate the clusters from figure 3. The black X highlights five sites at elevation > 460 m asl. The black straight line is the linear regression from using all 60 sites, the grey line results from the fit of only 55 sites after excluding the 5 high-elevation sites (see Table 2). *** indicates $p \leq 0.01$. b) As in (a) but for correlations with June and June-August precipitation.

The correlations of the tree-ring data with precipitation and temperature reveal July temperatures as the most important driver for tree growth throughout the network. When evaluating the highest monthly and seasonal correlation coefficients over the 1901-1981 common period, in 16 out of 20 sites July ranks highest. The influence of July temperatures increases towards higher latitudes with correlation coefficients increasing by about 0.05 per degree latitude (Fig. 4a). All tree-ring chronologies north of

66.5° reveal a significant climate-growth relationship with summer temperature. Longitudinal effects on the climate signal appear to be of minor importance as N-West and N-East clusters of the same latitude correlate on a similar level. Besides latitude, also elevation impacts the network signal strength, as sites above 460 m asl also show a significant response in spite of their location in lower latitudes (Fig V-4a; Fig. V-S1). The influence of precipitation is changing from a slightly positive July precipitation signal in the southern part of the network towards significantly negative correlations in the north (Fig. V-4b). Both gradients, temperature and precipitation, are highly significant and display the intensifying sensitivity of trees to climate with increasing latitude. When considering seasonal temperatures (June-August), instead of only one month (July), the spread of the correlation coefficients in central latitudes increases. The relationship of latitude and tree growth slightly gets lost by considering not only the most important month for tree growth. This also results in decreasing R^2 values. In contrast, the number of sites with significant positive response for precipitation increases when using the seasonal (summer) mean instead of single months.

3.3 Regional curves

The single Regional Curves of all micro-sites represent the site specific growth behavior for each site sampled for this network analysis (Fig. V-S1). In general, the growth rate depends on the latitudinal position with higher growth rates in lower latitudes. The shape of the growth rates matches with the typical run that was stated at the beginning with decreasing growth levels with increasing age. Nevertheless, there are differences in growth between trees growing at the lakeshore or upslope at the dry site. Two main patterns with the focus on the first couple of decades could be identified because at this time period the largest differences between the micro-sites are present.

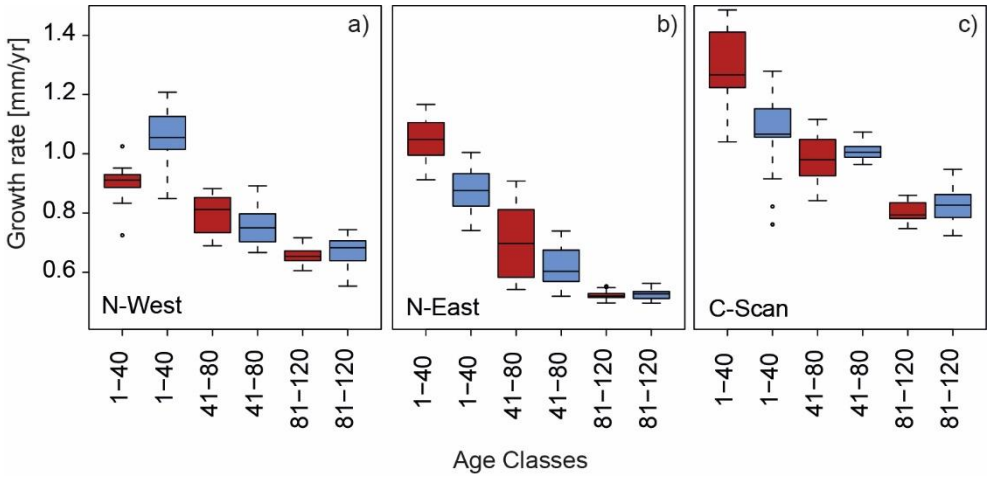

Figure V-5: Growth rate differences between wet (blue) and dry (red) micro-sites in the N-West (a), N-East (b), and C-Scan (c) clusters. Boxplots show the results for the innermost (youngest) 40 rings, and the two subsequent 40-year sections (41-80 and 81-120 years).

As the cluster analysis combines similar tree-ring sites also the growth behavior within clusters should be comparable. The mean pattern becomes clearer by concentrating on the aggregated time series of one cluster, especially when site specific outliers are removed. Highest growth rates are found for C-Fin and the rates for N-West and N-East are quite similar. Age classes based on 40 year long time periods show that the differences between wet and dry micro-sites are most pronounced and significant in the first age class, whereas in the second and third age class the wet and dry sites have similar growth levels (Fig. V-5). When examining the first age class in N-East and C-Scan the dry sites show considerably higher growth rates compared to the wet sites. The micro-sites present themselves vice versa in N-West, where the wet site surpasses the dry site in the first 40 years.

3.4 Tail Test

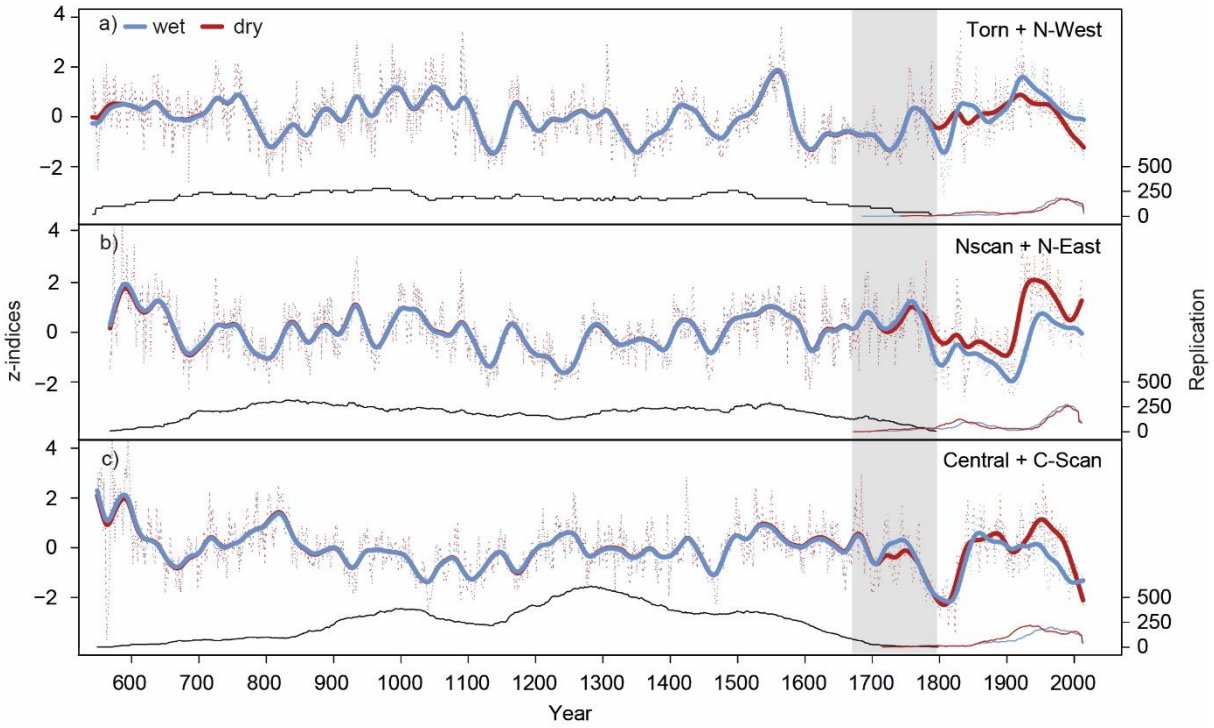

Figure V-6: Tail test displaying the influence of combining different micro-site chronologies with fossil and subfossil material. Long-term TRW data from fossil and subfossil samples from Torneträsk (Torn), northern Scandinavia (NScan) and central Scandinavia (central) are combined with TRW data from wet and dry micro-sites from N-West (a), N-East (b) and C-Scan (c). 50-year low pass filtered composite chronologies including lakeshore trees are shown in blue, the resulting chronology from integrating inland trees is shown in red. Curves at the bottom display the replication for the fossil and subfossil data (black) as well as the living tree data (wet: blue; dry: red) data. The grey box highlights the maximal overlapping period of fossil/subfossil and living tree data (1670-1800 AD).

The combination of snag and subfossil material with living-tree data is a commonly used approach to extend tree-ring chronologies back in time. Here we compiled three long-term chronologies for different areas in Fennoscandia to assess potential effects of including living-tee data from different micro-sites. TRW data of the N-West cluster were attached to relict data from Lake Torneträsk, N-East data were attached to the subfossil data of the N-Scan record, and C-Scan data were attached to the subfossil

dataset from southern Finland (Fig. V-6). These combinations reveal that the resulting RCS detrended chronologies deviate in the most recent periods (the "tails", Düthorn et al. 2013), showing partly substantial differences between wet and dry variants. The 50 year smoothed time series show that in northwestern Fennoscandia the dry chronology variant appears below the wet chronology after 1910. The differences are, however, most considerable in the N-Scan plus N-East chronologies, with the dry chronology variant showing substantially higher values throughout the past 200 years, reaching the highest chronology values (in the 1950s) over the past 1000+ years (red curve in Fig. V-6b). In contrast, the wet chronology variant in the 20th century stays all along under the mean of the previous centuries with deviations up to -2 around 1900. The alternative chronologies in southern Finland again show reduced differences and a similar run of wet and dry tails, though the dry variant is slightly higher around 1920-2005.

3.5 Spatial distribution of micro-sites

Since the difference between wet and dry micro-site is most substantial during the first 40 years (Fig. V-5 and V-S1), we calculated residuals for juvenile periods to assess the spatial patterns of wet/dry differences and evaluate potential underlying causes of these micro-site differences (wet RC > dry RC: wet+; dry RC > wet RC: dry+). The maps in Figure 7 distinguish between sites in the northwest with higher growth rates at the lakeshores, and sites in the eastern part of Fennoscandia with higher growth rates in the dry site compared to the other micro-site. There is also a mixing zone characterized by similar growth rates among micro-sites, located roughly between the other areas in the central part of Fennoscandia.

The dominating east-west pattern is related to regional July temperature, precipitation, and drought variability, as well as spatially changing soil carbon content (Fig. V-7). Of these variables, the SPEI-6 July index seems to fit closest with the spatial micro-site patterns as the "wet+" type is mainly persistent in relatively moist areas while the relative dry areas correspond with the "dry+" type.

The Scandes, as an orographical barrier, have a great influence on the climate of Fennoscandian. The stepwise increase of temperature from the west towards the southeast of Finland and thereby the decrease of precipitation towards the eastern regions is related to the mountain range and to distance from the Atlantic (Fig. V-7). Responsible for this gradient are atmospheric Luv and Lee effects forcing highest precipitation sums west of or in the mountain areas (Fig. V-7b). With increasing distance to the North Sea the continental influence is increasing and explains higher temperatures in the eastern parts. As the conditions for tree growth in the middle and southern boreal forest are less extreme here a mixed signal is expected. Therefore, the SPEI-6 index was added to see the spatial relationship of temperature and precipitation (Figure V-7c). Additionally, the carbon content of the organic layer is of interest as the distribution shows a strong east-west gradient (de Brogniez et al. 2015). In Norway the topsoil contains less than 1% carbon, whereas in Finland there are wide areas with more than 6% carbon content (Fig. V-7d).

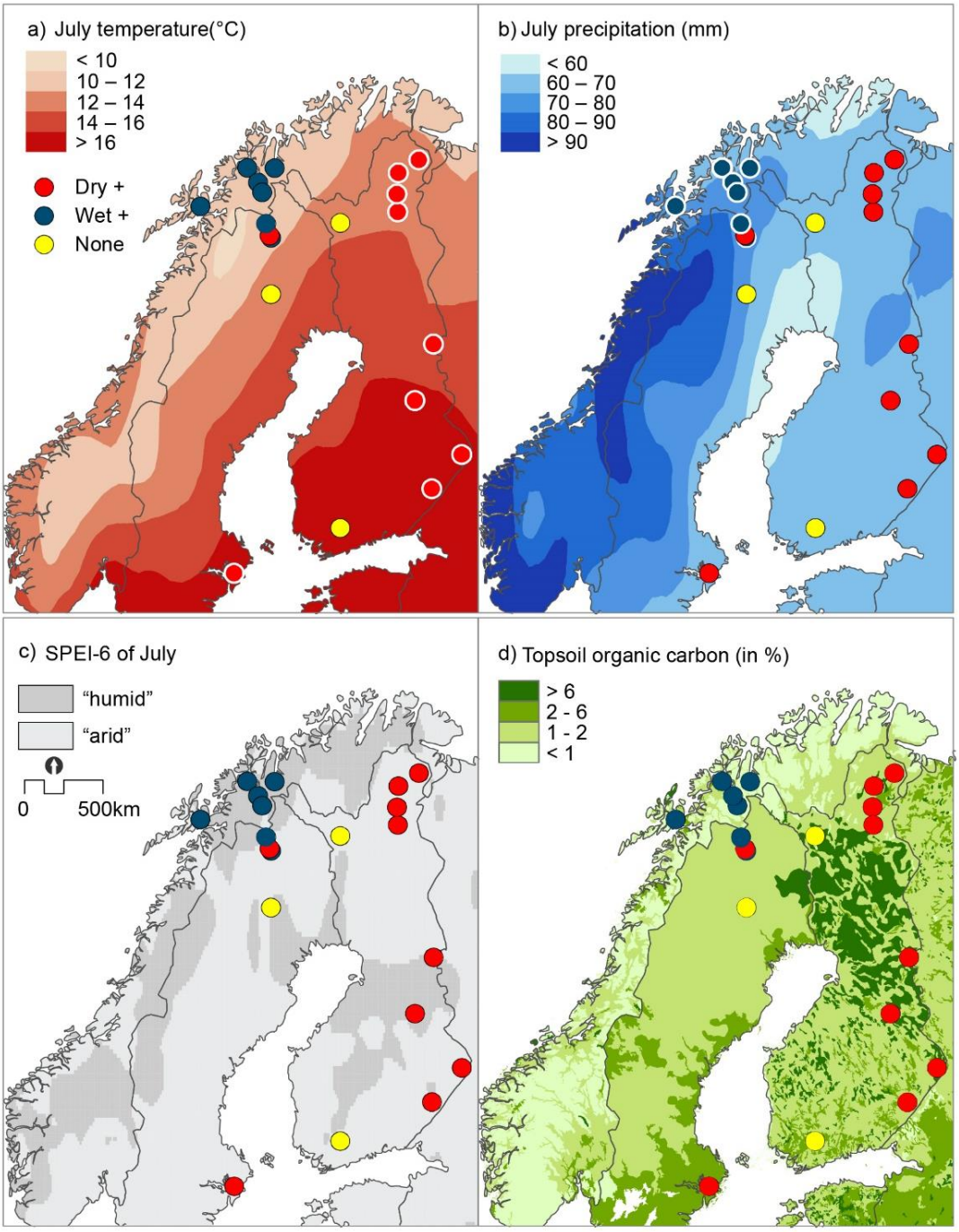

Figure V-7: Distribution maps of the different types of micro-site growth behavior. Types are defined of the residuals of wet and dry Regional Curves with a cambial age up to 40 years. Three micro-site patterns could be defined: blue (red) dots indicate higher mean growth rates in the juvenile phase for the wet (dry) site, relative to the counterpart micro-site, yellow dots show no distinction between the growth rates of the micro-sites. Different map layers are plotted: a) July mean temperatures (1901-2013), b) July mean precipitation sums (1901-2013), c) SPEI-6 index (1901-2013) and d) organic carbon content of the topsoil. Climate data in a) to c) are obtained from the CRU TS 3.22, soil data in d) are from the Topsoil Soil Organic Carbon Project (LUCAS).

3.6 Micro-site climate signals

The increasing temperature signal towards higher latitudes, as shown in the full 60-site pine network (Fig. V-4), is also revealed in the much smaller micro-site network (Fig. V-8). Separated by micro-sites, we found a linear increase of 0.04 per latitude of the correlation coefficients for both micro-sites. Differences appear by testing the significance of the linear relationship, with a slightly higher level of significance for the wet sites ($R^2 = 0.48$, $p \leq 0.001$) as for the dry sites ($R^2 = 0.45$, $p \leq 0.01$) over the 1931-2006 common period. In 17 out of 20 sites, the wet micro-sites correlate stronger with July temperatures, compared to the dry micro-sites. The mean deviation between the wet and the dry sites is about 0.11. Differences in the maximum correlation (r_{wet}= 0.56, r_{dry}=0.46) is also about 0.1, while the differences in the minimum correlation (r_{wet}= -0.14, r_{dry}=-0.27) are more pronounced and reach 0.13 (Fig. V-8c). If we focus on only the high latitude sites north of 67°N, the relationship between latitude and July correlation seems to switch, i.e. the correlations become weaker with increasing latitude (Fig. V-8b). The level of the coefficients for dry sites stays at a similar level (≈ 0.4) whereas the signal in trees from the lakeshore decreases linearly ($R^2 = 0.37$, $p \leq 0.05$). This effect could be related to poorer soil conditions combined with impermanent lake levels and frozen surfaces at high latitudes.

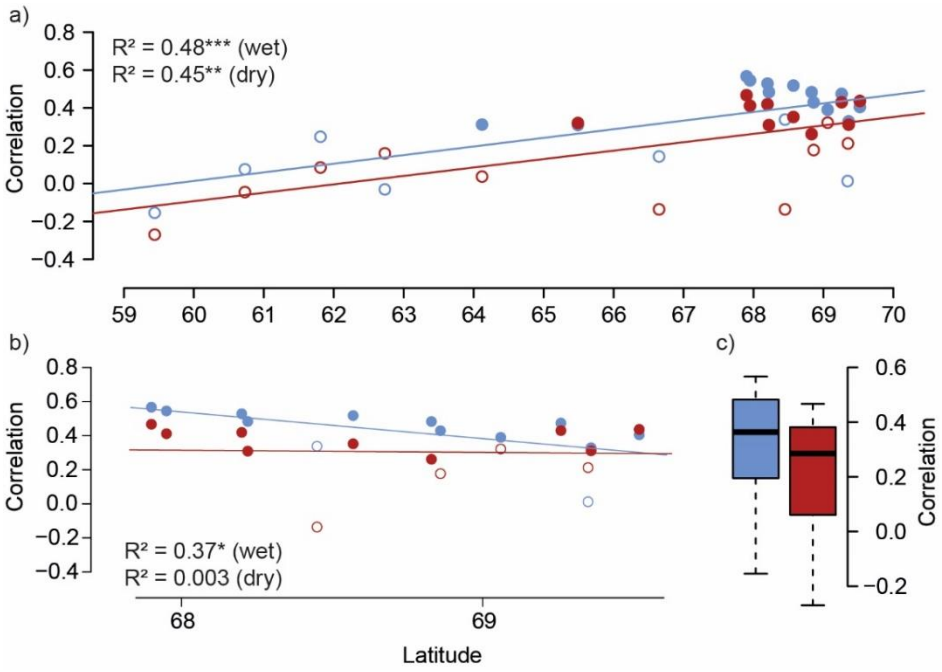

Figure V-8: Climate-growth relationship of micro-site chronologies and July temperature over the 1931-2006 common period. a) Correlation coefficients of the micro-site network against latitude. Dots (wet: blue; dry: red) symbolize significant ($p \leq 0.01$) coefficients, whereas sites plotted as circles do not reach significance. Straight lines are linear regression curves fitted to the wet (blue) and dry (red) coefficients. b) Same as in a) but only for sites north of 67°N. c) Boxplot of the correlation coefficients of 20 wet (blue) and dry (red) micro-sites.

4. Discussion

The micro-site network presented here is a unique dataset with regard to the differentiation into wet and dry habitats, the large number of sites (20 wet and 20 dry), high sample replication (on average 91 samples per micro-site), and his spatial representativeness for large areas in Fennoscandia. Recently published studies did not show a systematic or spatial link between tree growth and micro-sites effects (Düthorn et al. 2013, Düthorn et al. 2015a, Düthorn et al. 2015b), a shortcoming that may now be overcome by analyzing this large and exclusive network.

4.1 Local micro-site effects

For the first time the spatial regulation of micro-site patterns is detected. Trees in northwestern Fennoscandia seem to have higher growth rates at wet sites, whereas trees in the East show higher growth rates at the dry sites. Detailed analyses of the Regional Curves showed that this divergence effect is concentrated on the first 40 years, the juvenile phase of tree growth. The distinct east-west pattern is related to regional climate patterns. Trees which have belong to the provenance where the wet type dominates could deal better with colder mean July temperatures and manage higher precipitation sums in July, whereas trees situated in the area of the dry type benefit from warmer and dryer climatic conditions (Fig. V-7). The SPEI-6 index supports the hypothesis of a transition zone as the sites with no differences between wet and dry sites are located in areas with a mixed moisture pattern (Fig. V-3c) at the border between relative moist and relative dry areas.

Another reason for the occurrence of the observed growth performance of trees are varying soil properties along a longitudinal gradient. In general, Fennoscandia is characterized by sandy and nutrient-poor podzols. Due to the Westerlies and higher soil erosion rates in the west there are differences in the composition of the topsoil layer. The topsoil layer is characterized by a gradient with very poor organic carbon content in the west of the mountain range and increasing fertilizing carbon towards Finland. The higher inter-series and inter-site correlations in the northeastern area is an indicator for better growing conditions, as the growth is more synchronized, and displays the importance of the soil properties. Ryan and Yoder (1997) state that trees grow faster in moist and fertile sites whereas in dry and nutrient poor sites they grow more slowly. The harsh climatic conditions, together with the poor soils in the northwest characterize this part of Fennoscandia as disfavored area for tree growth. The topsoil layer at the slopes is eroded and washed out so that growing conditions for trees at the dry site are more difficult and that the trees at the lakeshore benefit from the accumulated nutrients. In contrast, in areas where the soil conditions are more favorable for tree growth, like in N-East, other factors limit tree growth. Here, the trees on the slopes benefit from the dryer and warmer conditions.

4.2 Climate signals

The vegetation period at high elevations and high latitudes coincides with short, cool and moist summers (Gouirand et al. 2008). The sensitivity of trees to summer temperature increases towards the northern latitudes (Fig. V-4) (Fritts 1976). Lower mean temperatures with increasing latitudes complicate physiological processes that are necessary for tree growth and this dependence of adequate summer temperatures synchronizes tree growth. This linear relationship is displayed by 60 tree-ring sites of the pine network where an increase of the correlation coefficient of 0.05 per degree latitude is discovered. The stability of this relationship is also present in the wet and dry latitudinal transect.

Besides the differences in latitude the temperature signal also varies with respect to the micro-sites (Fig. V-8). In general, lakeshore trees show persistently more positive response to July temperatures than inland trees. Assuming that subfossil trees in former times also grew at the lakeshore, the higher temperature signal and comparable growth rates indicates a good compatibility of subfossil and lakeshore trees. While trees at the lakeshore have a permanent water availability, trees at the slopes are struggling in some years with water stress. In extreme warm or dry Julys trees at the drier micro-sites react with slightly lower radial growth compared to trees at the lakeshore. Tests on extreme dry and warm years with superposed Epoch Analysis (SEA; Lough and Fritts 1987) display this phenomenon for most sites (not shown here). Therefore, we assume that trees at the dry site have an additional limiting factor in dry years resulting in reduced growth and a breakdown of the stored temperature signal for the inland chronologies.

4.3 Growth rate differences

Düthorn et al. (2013) presented differences between the growth rates as main distinction of lakeshore and inland trees. Variations in the annual growth are related to site depended disturbances in tree physiology, e.g. photosynthetic rates, water transport and vertical growth (Ryan and Yoder 1997, Bond 2000). Increasing competition and tree age are further aspects for reduced growth as the sensitivity of a tree to external factors and biological reactions changes with tree-age (Cook and Kairiukstis 1990, Carrer and Urbinati 2004). These effects are known as climate signal age effect (CSAE) and controversially discussed in literature (Carrer and Urbinati 2004, Esper et al. 2008, Liñan et al. 2012). Kobe et al. (1995) stated that especially young trees underlie an extreme stress situation due to competition and that survivorship increases the faster the tree is growing. The differences in growth during the juvenile phase between the micro-sites is related to the higher vulnerability of young plants. Main influencing factors are the carbon content in the top layer as well as extreme climatic conditions.

Even if the differences are more pronounced in the juvenile phase they could have a strong influence on long-term chronologies (Fig. V-6). Depending on the region where material (relict and recent) for long-term chronologies comes from the dimension of the potential error in long-term trends varies. While in N-West and C-Scan the gap between both recent tails is minor (Fig. V- 6a and c) the divergence of wet

and dry endings is relatively strong in N-East (Fig. V-6b). This means that especially temperature reconstructions could have large errors and underestimate past climate variations. These effects are directly connected to the detrending method that is applied. If a collective detrending method, such as Regional Curve Standardization, is used to remove unwanted biological noise, the offset in the Regional Curves causes statistically biased mean chronologies (Düthorn et al. 2013, Düthorn et al. 2015b). It is impossible to avoid this detrending method as RCS is an important statistical tool to preserve low-frequency variability in tree-ring time series (Esper et al. 2003).

The existence of subfossil material and the potential for long-term chronologies along with the strong temperature signal in the northern chronologies form the basis for the development of long temperature reconstructions for this area (Briffa et al. 1992, Eronen et al. 2002, Grudd 2008, Esper et al. 2012c, McCarroll et al. 2013). However, Düthorn et al. (2015b) pointed out that the effects of micro-sites in the living material are not negligible, and might cause misinterpretations of past climate variations particularly when relating 20th century warming trends with pre-instrumental climate variability.

5. Conclusion

Our results imply concrete recommendations for a sampling design adjusted to the needs when samples from living trees are combined with subfossil material. Based on the detailed analysis of a large micro-site pine network the cluster analysis of variables is proven to be a useful tool to group chronologies with similar characteristics. It is possible to define different ecological subsystems (N-West and N-East) of the boreal forest in addition to the sections defined by Ahti et al. (1986). Related to the different sections of the cluster analysis also the provenances of the micro-site patterns indicate a clear west-east pattern. By focusing on the juvenile phase with tree ages up to 40 years a clear detection of the micro-site type is possible. While lakeshore trees in the western part of the network exceed tree growth at the dry site, trees of the eastern part of the network conduct vice versa. This effect has to be taken into account when relict and recent material is combined (see also Helama et al. 2002). Even if the differences are pronounced only in the juvenile period choosing the "wrong" micro-site has large effects on trends of long-term chronologies. This easily leads to misinterpretations or overestimating of the warming in the 20th century and complicates comparisons of today's warming with past climate variability, i.e. the Medieval Climate Anomaly. Finally, site specific correlations with summer temperatures reveal consistently higher correlations at the lakeshore micro-site habitat. The definition as a distinct ecological setting, higher climate-growth relationships and the better comparability with subfossil material results in a recommendation to include lakeshore trees as living material in high latitude temperature reconstructions.

References

Ahti T., Hämet-Ahti L., Jalas J. (1986): Vegetation zones and their sections in north western Europe. *Annales Botanici Fennici* 3: 169-2011.

Bond B.J. (2000): Age-related changes in photosynthesis of woody plants. *Trends in Plant Science* 5: 349-353.

Briffa K.R., Jones P.D., Bartholin T.S., Eckstein D., Schweingruber F.H., Karlen W., Zetterberg P., Eronen M. (1992): Fennoscandian Summers from Ad-500 - Temperature-Changes on Short and Long Timescales. *Climate Dynamics* 7: 111-119.

Büntgen U., Raible C.C., Frank D., Helama S., Cunningham L., Hofer D., Nievergelt D., Verstege A. et al. (2011): Causes and Consequences of Past and Projected Scandinavian Summer Temperatures, 500-2100 AD. *Plos One* 6.

Carrer M., Urbinati C. (2004): Age-dependent tree-ring growth responses to climate in Larix decidua and Pinus cembra. *Ecology* 85: 730-740.

Chavent M., -Simonet V.K., Liquet B., Saracco J. (2012a): ClustOfVar: An R Package for the Clustering of Variables. *Journal of Statistical Software* 50: 1-16.

Chavent M., Kuentz-Simonet V., Saracco J. (2012b): Orthogonal rotation in PCAMIX. *Advances in Data Analysis and Classification* 6: 131-146.

Cook E.R., Kairiukstis L.A. (1990): Methods of dendrochronology. Kluwer Academic Publishers.

Cook E.R., Peters K. (1997): Calculating unbiased tree-ring indices for the study of climatic and environmental change. *Holocene* 7: 361-370.

de Brogniez D., Ballabio C., Stevens A., Jones R.J.A., Montanarella L., van Wesemael B. (2015): A map of the topsoil organic carbon content of Europe generated by a generalized additive model. *European Journal of Soil Science* 66: 121-134.

Drobyshev I., Niklasson M., Linderholm H.W., Seftigen K., Hickler T., Eggertsson O. (2011): Reconstruction of a regional drought index in southern Sweden since AD 1750. *Holocene* 21: 667-679.

Düthorn E., Holzkämper S., Timonen M., Esper J. (2013): Influence of micro-site conditions on tree-ring climate signals and trends in central and northern Sweden. *Trees* 27: 1395-1404.

Düthorn E., Schneider L., Günther B., Gläser S., Esper J. (2015a): Ecological and climatological signals in tree-ring width and density chronologies along a latitudinal boreal transect. *Scandinavian Journal of Forest Research*: in press.

Düthorn E., Schneider L., Konter O., Schön P., Timonen M., Esper J. (2015b): On the hidden significance of differing micro-sites on tree-ring based climate reconstructions. *Silva Fennica* 49.

Eronen M., Zetterberg P., Briffa K.R., Lindholm M., Merilainen J., Timonen M. (2002): The supra-long Scots pine tree-ring record for Finnish Lapland: Part 1, chronology construction and initial inferences. *Holocene* 12: 673-680.

Esper J., Cook E.R., Krusic P.J., Peters K., Schweingruber F.H. (2003): Tests of the RCS method for preserving low-frequency variability in long tree-ring chronologies. *Tree-Ring Research* 59: 81-98.

Esper J., Frank D.C., Timonen M., Zorita E., Wilson R.J.S., Luterbacher J., Holzkamper S., Fischer N. et al. (2012c): Orbital forcing of tree-ring data. *Nature Climate Change* 2: 862-866.

Esper J., Niederer R., Bebi P., Frank D. (2008): Climate signal age effects - Evidence from young and old trees in the Swiss Engadin. *Forest Ecology and Management* 255: 3783-3789.

FAO (2010): Global Forest Resources Assessment 2010. *FAO Forestry Paper* 163.

Fritts H.C. (1976): Tree rings and climate. Academic Press.

Gouirand I., Linderholm H.W., Moberg A., Wohlfarth B. (2008): On the spatiotemporal characteristics of Fennoscandian tree-ring based summer temperature reconstructions. *Theoretical and Applied Climatology* 91: 1-25.

Grissino-Mayer H.D., Fritts H.C. (1997): The International Tree-Ring Data Bank: an enhanced global database serving the global scientific community. *The Holocene* 7: 235-238.

Grudd H. (2008): Tornetrask tree-ring width and density AD 500-2004: a test of climatic sensitivity and a new 1500-year reconstruction of north Fennoscandian summers. *Climate Dynamics* 31: 843-857.

Gunnarson B.E., Linderholm H.W., Moberg A. (2011): Improving a tree-ring reconstruction from west-central Scandinavia: 900 years of warm-season temperatures. *Climate Dynamics* 36: 97-108.

Harris I., Jones P.D., Osborn T.J., Lister D.H. (2014): Updated high-resolution grids of monthly climatic observations - the CRU TS3.10 Dataset. *International Journal of Climatology* 34: 623-642.

Helama S., Lindholm M., Timonen M., Merilainen J., Eronen M. (2002): The supra-long Scots pine tree-ring record for Finnish Lapland: Part 2, interannual to centennial variability in summer temperatures for 7500 years. *Holocene* 12: 681-687.

Holtmeier F.K., Broll G. (2005): Sensitivity and response of northern hemisphere altitudinal and polar treelines to environmental change at landscape and local scales. *Global Ecology and Biogeography* 14: 395-410.

Kobe R.K., Pacala S.W., Silander J.A., Canham C.D. (1995): Juvenile Tree Survivorship as a Component of Shade Tolerance. *Ecological Applications* 5: 517-532.

Kultti S., Mikkola K., Virtanen T., Timonen M., Eronen M. (2006): Past changes in the Scots pine forest line and climate in Finnish Lapland: a study based on megafossils, lake sediments, and GIS-based vegetation and climate data. *Holocene* 16: 381-391.

Liñan I.D., Gutierrez E., Heinrich I., Andreu-Hayles L., Muntan E., Campelo F., Helle G. (2012): Age effects and climate response in trees: a multi-proxy tree-ring test in old-growth life stages. *European Journal of Forest Research* 131: 933-944.

Lindholm M., Eronen M., Timonen M., Merilainen J. (1999): A ring-width chronology of Scots pine from northern Lapland covering the last two millennia. *Annales Botanici Fennici* 36: 119-126.

Lough J.M., Fritts H.C. (1987): An Assessment of the Possible Effects of Volcanic-Eruptions on North-American Climate Using Tree-Ring Data, 1602 to 1900 Ad. *Climatic Change* 10: 219-239.

Mátyás C., Ackzell L., Samuel C.J.A. (2004): Technical Guidelines for genetic conservation and use for Scots pine (Pinus sylvestris). *EUFORGEN Technical Guidelines for Genetic Conservation and Use*.

McCarroll D., Loader N.J., Jalkanen R., Gagen M.H., Grudd H., Gunnarson B.E., Kirchhefer A.J., Friedrich M. et al. (2013): A 1200-year multiproxy record of tree growth and summer temperature at the northern pine forest limit of Europe. *Holocene* 23: 471-484.

Mitchell T.D., Jones P.D. (2005): An improved method of constructing a database of monthly climate observations and associated high-resolution grids. *International Journal of Climatology* 25: 693-712.

Ryan M.G., Yoder B.J. (1997): Hydraulic limits to tree height and tree growth. *Bioscience* 47: 235-242.

Schmitt U., Jalkanen R., Eckstein D. (2004): Cambium dynamics of Pinus sylvestris and Betula spp. in the northern boreal forest in Finland. *Silva Fennica* 38: 167-178.

Schweingruber F.H., Bartholin T., Schar E., Briffa K.R. (1988): Radiodensitometric-Dendroclimatological Conifer Chronologies from Lapland (Scandinavia) and the Alps (Switzerland). *Boreas* 17: 559-566.

Swetnam T.W., Allen C.D., Betancourt J.L. (1999): Applied historical ecology: Using the past to manage for the future. *Ecological Applications* 9: 1189-1206.

Toth G., Jones A., Montanarella L. (2013): The LUCAS topsoil database and derived information on the regional variability of cropland topsoil properties in the European Union. *Environmental Monitoring and Assessment* 185: 7409-7425.

Vicente-Serrano S.M., Beguería S., López-Moreno J.I., Angulo-Martínez M., El Kenawy A.M. (2010): A new global 0.5° gridded dataset (1901-2006) of a multiscalar drought index: comparison with current drought index datasets based on the Palmer Drought Severity Index. *Journal of Hydrometeorology* 11: 1033-1043.

Zang C., Biondi F. (2014): treeclim: an R package for the numerical calibration of proxy-climate relationships. *Ecography*: n/a-n/a.

Supplementary Material

ITRDB-Code	Latitude °N	Longitude °E	Elevation (m asl)	First Year	Last Year	Length (years)
FINL001	62.98	31.3	190	1589	1983	394
FINL002	63.02	31.43	200	1784	1983	199
FINL003	62.98	31.3	190	1831	1983	152
FINL004	62.93	31.38	190	1809	1983	174
FINL005	63.68	29.88	156	1588	1983	395
FINL008	63.1	30.63	180	1683	1984	301
FINL054	67.22	26.82	201	1550	2000	450
FINL055	67.08	27.02	289	1550	2000	450
FINL056	61.93	25.72	98	1750	2000	250
FINL057	61.92	26.02	136	1750	2000	250
FINL058	68.13	27.45	282	1560	1983	423
FINL059	68.45	28.07	213	1562	1983	421
FINL060	68.67	25.87	275	1536	1983	447
FINL061	69.32	28.13	120	1532	1983	451
FINL062	68.87	26.88	202	1560	1983	423
FINL063	67	27.25	200	1655	1983	328
FINL064	68	24.2	344	1657	1983	326
FINL065	66.32	25.15	130	1578	1983	405
FINL066	62.85	25.48	152	1602	1983	381
NORW008	69.53	18.73	101	1599	1992	393
NORW010	68.8	15.73	339	877	1994	1117
NORW011	67.6	15.33	-10	1550	1997	447
NORW012	67.62	15.73	518*	1550	1997	447
NORW013	60.37	11.07	370	1781	1981	200
NORW014	59.7	9.48	468*	1605	1981	376
NORW015	61.72	8.47	1701*	1600	1983	383
SWED302	59.2	18.7	-1	1588	1995	407
SWED305	60.45	14.73	267	1450	2002	552
SWED306	66.78	20.13	280	1667	1983	316
SWED307	58.95	15.03	142	1778	2004	226
SWED308	59.28	18.3	15	1733	2003	270
SWED310	58.9	16.63	27	1661	1997	336
SWED315	59.13	17.92	50	1800	1996	196
SWED316	60.13	16.08	123	1789	1997	208
SWED320	59.15	18	50	1713	1996	283
SWED323	60.13	16.08	123	1723	1997	274
SWED324	62.33	18.48	-79	1448	1998	550
SWED326	63.12	13.33	766*	1471	1998	527
SWED327	64.45	13.97	486*	1500	2000	500
SWED328	59.18	18.27	0	1694	2000	306

Supplement V-1: Site characteristics of 40 additional pine sites from Scandinavia north of 58.9°N.

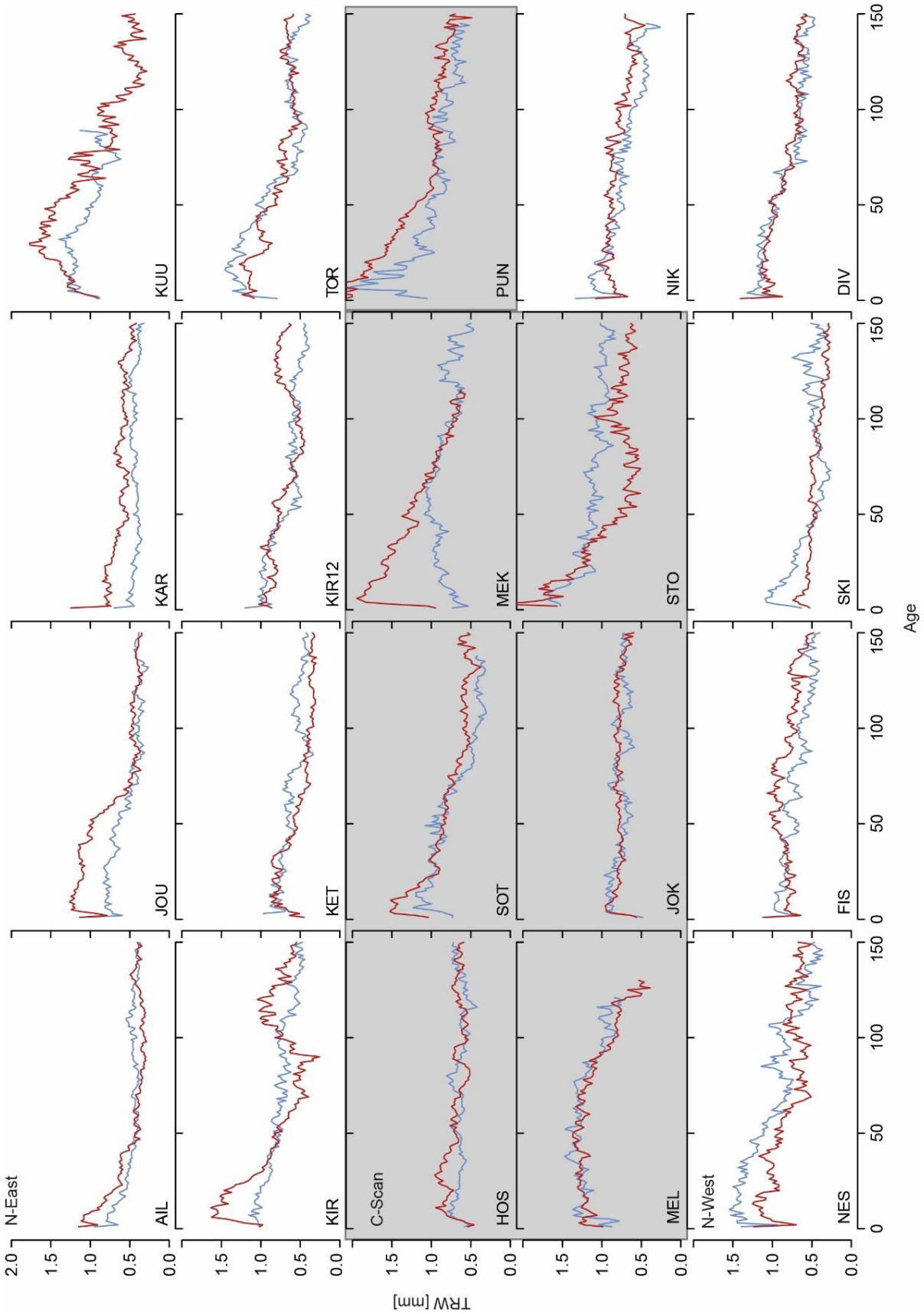

Supplement V-2: Mean growth rates of wet (blue) and dry (red) micro-sites. Data shown after aligning by cambial age.

Conclusion and Perspectives

The results of this thesis describe the influence of different ecological settings (lakeshore vs. inland) on long-term chronologies introduced by Esper et al. (2012c). In addition, this thesis improves the understanding of the climatic and hydrologic impact on tree growth at lakeshores, as demanded by Helama et al. (2013). The aim of this thesis was (i) to analyze whether lakeshore and inland trees belong to the same ecological background, (ii) what the outstanding differences to characterize micro-sites are, and (iii) how the potential bias of micro-site effects on long-term chronologies can be reduced.

Ecological fingerprints in trees could be miscellaneous and hard to identify. For the micro-site effects presented by Esper et al. (2012c) it is inevitable to investigate the ecological affinity of lakeshore and inland trees. After the appearance of the terms "wet" and "dry" micro-sites it became obvious that an additional site between the wet and dry one needs to be integrated to test the significance of their definition of being a proper ecological habitat. It became apparent that the third or "middle" site serves as transition zone with characteristics similar to the dry site (CHAPTER I). Also, for a clear separation of micro-site conditions and to avoid a mixing with the dry site, only trees growing directly at the lakeshores should represent the ecological setting "wet". In the remaining chapters (II, IV, V), therefore only wet and dry micro-sites were included. This ecological differentiation is applicable for different species, both Scots pine and Norway spruce are sensitive to this division with an even more pronounced gap between wet and dry growth rates for Norway spruce (CHAPTER II). This leads over to one of the main hypothesis of this studies. It is assumed that as subfossil trees normally are found in lake sediments or bogs, they grew close to the lakeshore. Eronen et al. (1999) argued that the position of the trees, that are now subfossil trunks, was at dry land and only due to lake level changes their trunks are located in the lakes. In contrast, Gunnarson et al. (2003) addressed the phenomenon of changing lake levels differently. They show that trees standing at the lakeshore are only a snapshot of a constantly changing environment. The subfossil material was thus subject to alternating conditions and has stored the same ecological information as the current lakeshore trees. The comparability of wet and subfossil material is therefore taken for granted. This hypothesis is also supported by results of CHAPTER I as the growth rates of Torneträsk (Schweingruber et al. 1988) and Kiruna_wet (Fig. I-8) are relatively similar. Also, there is a clear offset in the shape of the subfossil and dry material. The fact that chronologies from the lakeshore diverge from inland ones is not a disqualification for lakeshore trees, as more recent chronologies are based on inland trees, rather an indication of a clear division in two separate ecological milieus. Therefore, criticism on chronologies only based on lakeshore trees by Linderholm et al. (2014) is only partly justified as the comparability with subfossil material is inevitable (CHAPTER I, II).

In accordance to the definition of two isolated ecological settings the next part describes the differences between those habitats. The separation of the ecological setting is mainly based on growth variations at the specific sites. Age-aligned tree-ring series, the growth rates, visualize this key effect of variation for the ecological setting (CHAPTER I, II, V). Several studies showed that this effect is stable throughout latitudes (CHAPTER I, V) and also arises in other species (CHAPTER II). In general, the dissimilarity between wet and dry micro-sites is most pronounced in the first 40 years of tree growth (CHAPTER V). In addition to TRW, MXD data were included in the micro-site analysis showing that the growth differences between wet and dry micro-sites are more pronounced for TRW than for MXD (CHAPTER IV). The reason why lakeshore and inland trees show different growth rates in the juvenile phase is not yet fully understood (CHAPTER V). Helama et al. (2005a) discussed the influence of forest density (open vs. closed canopy) on the shape of Regional Curves. In particular, competition in dense forest structures matters. But it is not evident how to relate the idea of different forest types to the growth rates in the micro-site network. Here, the network displayed a dichotomy within the growth rates (wet+ and dry+; CHAPTER V). However, although the first approach in Sweden shows distinct micro-site effects at the northern site (CHAPTER I), the micro-site type does not fit in the east-west pattern exposed in CHAPTER V. According to this, higher growth rates at the lakeshore compared to the inland site would be expected. This exceptional growth behavior for KIR does not contradict the results of the network analysis (CHAPTER V), it rather supports the existence of a transition zone. The map layer of the SPEI-6 (Fig. V-7c) displays this areas of transition with wetter and dryer conditions and that sometimes even the signal gets indistinct (see Fig. V-7; none = sites with no differences between the growth rates). Additionally, more analyses on age structure, soil conditions, replication and the sampling design could clarify the picture of micro-site effects in this transition zones. To sum up the network analysis, CHAPTER V recapitulates the work that has been done on micro-sites so far, showing that micro-site effects are important and take place all over Fennoscandia. The network indicates a clear west-east pattern of micro-site effects. In the eastern part, faster growth at the dry site was identified, whereas in the western ranges the wet site offers higher growth rates compared to the dry site. This pattern is related to temperature and precipitation gradients as well as the carbon content of the organic layer.

As a final point, the effects of micro-sites on climate reconstructions has to be discussed. In CHAPTER II the focus is to describe the statistical bias in temperature reconstructions forced by micro-sites. The combination of inappropriate (i.e. dry) living, and subfossil (wet "fingerprint") material results in an overestimation of recent warming. Climate reconstructions integrating living material of the dry site show too cold reconstructed temperatures before 1800 AD. This bias in temperature reconstructions could have a great economic and political impact with respect to discussions about postindustrial warming. A pitfall in tree-ring standardization is responsible for the divergence as the offset only appears after applying a common detrending method (RCS) and no differences are distinguishable when using an individual detrending approach (here: Negative Exponential Curve Standardization; CHAPTER I).

Albeit, the method of RCS is important as it keeps low-frequency variability in the standardized data (Esper et al. 2002). A simple way to avoid or minimize this bias is to integrate MXD series as proxy data. As shown in CHAPTER VI micro-sites only have minor effects on density data. In combination with a higher response to summer temperatures in the north (CHAPTER IV), temperature reconstructions based on MXD are superior to those based on TRW data. However, if a temperature reconstruction based on TRW is calculated, ecological comparability between recent and subfossil material should be carefully considered. Another advantage of integrating trees from the lakeshore is that this site offers higher correlation coefficients with July temperatures (CHAPTER V). Consequently, more solid results in calibration and verification statistics could be achieved. CHAPTER III describes a case study of the merging of two of the longest MXD based temperature reconstructions that have been developed in northern Scandinavia (N-Scan and Torneträsk). N-Scan supplies the samples for the most recent part and these trees are sampled at the lakeshore (see Esper et al. 2012c). The new summer temperature reconstruction shows reliable warm periods during Roman, Medieval and recent times (N-Eur; CHAPTER III).

Although this thesis covers a key region of dendroclimatology, networks of micro-site samplings should be established in other parts of the world to confirm that results presented here are applicable on a global scale. The boreal forests, for instance, which extend far towards east forms a unique study area (Hellmann et al. in rev). Influence of micro-sites should also be expanded to cover other species, in order to see what kind of micro-site pattern will arise for example in the Russian part of the boreal ecosystem. This effects might also become important when subfossil or snag material is allocated (Hellmann et al. 2015, Hellmann et al. 2013).

Studying micro-sites contributes to two main research fields. First, it helps to understand ecological influences on tree growth and how the climate fingerprint is stored in trees from different ecological settings. This leads directly to the second topic, the climate reconstructions. Here, micro-site studies help to improve established procedures and to avoid statistical biases while keeping the important low frequency information. After elucidating the background of micro-site effects it is possible to adapt future studies by applying novel strategies, as sampling designs or detrending methods.

Bibliography

Affolter P., Büntgen U., Esper J., Rigling A., Weber P., Luterbacher J., Frank D. (2010): Inner Alpine conifer response to 20th century drought swings. *European Journal of Forest Research* 129: 289-298.

Ahti T., Hämet-Ahti L., Jalas J. (1986): Vegetation zones and their sections in north western Europe. *Annales Botanici Fennici* 3: 169-2011.

Anchukaitis K.J., Breitenmoser P., Briffa K.R., Buchwal A., Büntgen U., Cook E.R., D'Arrigo R.D., Esper J. et al. (2012): Tree rings and volcanic cooling. *Nature Geoscience* 5: 836-837.

Baillie M.G.L. (2008): Proposed re-dating of the European ice core chronology by seven years prior to the 7th century AD. *Geophysical Research Letters* 35.

Bartholin T.S., Karlén W. (1983): Dendrokronologi i Lappland AD 436–1981. *Dendrokronologiska Sällskapets Meddelanden* 5: 3-16.

Björklund J.A., Gunnarson B.E., Seftigen K., Esper J., Linderholm H.W. (2014): Blue intensity and density from northern Fennoscandian tree rings, exploring the potential to improve summer temperature reconstructions with earlywood information. *Climate of the Past* 10: 877-885.

Bond B.J. (2000): Age-related changes in photosynthesis of woody plants. *Trends in Plant Science* 5: 349-353.

Bradley R.S. (1999): Paleoclimatology : reconstructing climates of the quaternary. Academic Press.

Bräker O.U. (1981): Der Alterstrend bei Jahrringdichten und Jahrringbreiten von Nadelhölzern und sein Ausgleich. *Mitteilungen der Forstlichen Bundesversuchsanstalt Wien* 142: 75-102.

Briceno-Elizondo E., Garcia-Gonzalo J., Peltola H., Matala J., Kellomaki S. (2006): Sensitivity of growth of Scots pine, Norway spruce and silver birch to climate change and forest management in boreal conditions. *Forest Ecology and Management* 232: 152-167.

Briffa K., Jones P., Schweingruber F., Karlén W., Shiyatov S. (1996): Tree-ring variables as proxy-climate indicators: Problems with low-frequency signals. In: Jones, P, Bradley, R, Jouzel, J (eds): Climatic Variations and Forcing Mechanisms of the Last 2000 Years. Springer Berlin Heidelberg. 9-41.

Briffa K.R., Bartholin T.S., Eckstein D., Jones P.D., Karlen W., Schweingruber F.H., Zetterberg P. (1990): A 1,400-Year Tree-Ring Record of Summer Temperatures in Fennoscandia. *Nature* 346: 434-439.

Briffa K.R., Jones P.D., Bartholin T.S., Eckstein D., Schweingruber F.H., Karlen W., Zetterberg P., Eronen M. (1992): Fennoscandian Summers from Ad-500 - Temperature-Changes on Short and Long Timescales. *Climate Dynamics* 7: 111-119.

Briffa K.R., Jones P.D., Pilcher J.R., Hughes M.K. (1988): Reconstructing Summer Temperatures in Northern Fennoscandinavia Back to Ad 1700 Using Tree-Ring Data from Scots Pine. *Arctic and Alpine Research* 20: 385-394.

Briffa K.R., Jones P.D., Schweingruber F.H., Osborn T.J. (1998): Influence of volcanic eruptions on Northern Hemisphere summer temperature over the past 600 years. *Nature* 393: 450-455.

Briffa K.R., Melvin T.M. (2011): A Closer Look at Regional Curve Standardization of Tree-Ring Records: Justification of the Need, a Warning of Some Pitfalls, and Suggested Improvements in Its Application. In: Hughes, MK, Swetnam, TW, Diaz, HF (eds): Dendroclimatology. Springer Netherlands. 113-145.

Briffa K.R., Osborn T.J., Schweingruber F.H., Jones P.D., Shiyatov S.G., Vaganov E.A. (2002): Tree-ring width and density data around the Northern Hemisphere: Part 1, local and regional climate signals. *Holocene* 12: 737-757.

Brown R.D., Brasnett B., Robinson D. (2003): Gridded North American monthly snow depth and snow water equivalent for GCM evaluation. *Atmosphere-Ocean* 41: 1-14.

Bunde A., Büntgen U., Ludescher J., Luterbacher J., von Storch H. (2013): Is there memory in precipitation? *Nature Climate Change* 3: 174-175.

Büntgen U., Bellwald I., Kalbermatten H., Schmidhalter M., Frank D.C., Freund H., Bellwald W., Neuwirth B. et al. (2006): 700 years of settlement and building history in the Lotschental, Switzerland. *Erdkunde* 60: 96-112.

Büntgen U., Esper J., Frank D.C., Nicolussi K., Schmidhalter M. (2005a): A 1052-year tree-ring proxy for Alpine summer temperatures. *Climate Dynamics* 25: 141-153.

Büntgen U., Frank D., Grudd H., Esper J. (2008): Long-term summer temperature variations in the Pyrenees. *Climate Dynamics* 31: 615-631.

Büntgen U., Frank D., Liebhold A., Johnson D., Carrer M., Urbinati C., Grabner M., Nicolussi K. et al. (2009): Three centuries of insect outbreaks across the European Alps. *New Phytologist* 182: 929-941.

Büntgen U., Frank D., Neuenschwander T., Esper J. (2012): Fading temperature sensitivity of Alpine tree growth at its Mediterranean margin and associated effects on large-scale climate reconstructions. *Climatic Change* 114: 651-666.

Büntgen U., Frank D., Trouet V., Esper J. (2010a): Diverse climate sensitivity of Mediterranean tree-ring width and density. *Trees-Structure and Function* 24: 261-273.

Büntgen U., Frank D.C., Kaczka R.J., Verstege A., Zwijacz-Kozica T., Esper J. (2007): Growth responses to climate in a multi-species tree-ring network in the Western Carpathian Tatra Mountains, Poland and Slovakia. *Tree Physiology* 27: 689-702.

Büntgen U., Frank D.C., Schmidhalter M., Neuwirth B., Seifert M., Esper J. (2005b): Growth/climate response shift in a long subalpine spruce chronology. *Trees-Structure and Function* 20: 99-110.

Büntgen U., Franke J., Frank D., Wilson R., Gonzalez-Rouco F., Esper J. (2010b): Assessing the spatial signature of European climate reconstructions. *Climate Research* 41: 125-130.

Büntgen U., Raible C.C., Frank D., Helama S., Cunningham L., Hofer D., Nievergelt D., Verstege A. et al. (2011): Causes and Consequences of Past and Projected Scandinavian Summer Temperatures, 500-2100 AD. *Plos One* 6.

Butterfield B. (2003): Wood anatomy in relation to wood quality. In: Barnett, J, Jeronimidis, G (eds): Wood quality and its biological basis. Blackwell. 30-52.

Carrer M., Urbinati C. (2004): Age-dependent tree-ring growth responses to climate in Larix decidua and Pinus cembra. *Ecology* 85: 730-740.

Casty C., Wanner H., Luterbacher J., Esper J., Bohm R. (2005): Temperature and precipitation variability in the european Alps since 1500. *International Journal of Climatology* 25: 1855-1880.

Chavent M., -Simonet V.K., Liquet B., Saracco J. (2012a): ClustOfVar: An R Package for the Clustering of Variables. *Journal of Statistical Software* 50: 1-16.

Chavent M., Kuentz-Simonet V., Saracco J. (2012b): Orthogonal rotation in PCAMIX. *Advances in Data Analysis and Classification* 6: 131-146.

Christiansen B., Ljungqvist F.C. (2012): The extra-tropical Northern Hemisphere temperature in the last two millennia: reconstructions of low-frequency variability. *Climate of the Past* 8: 765-786.

Cook B.I., Smerdon J.E., Seager R., Coats S. (2014): Global warming and 21st century drying. *Climate Dynamics* 43: 2607-2627.

Cook E.R. (1987): The decomposition of tree-ring series for environmental studies. *Tree-Ring Bulletin* 47: 37-59.

Cook E.R., Briffa K.R., Meko D.M., Graybill D.A., Funkhouser G. (1995): The Segment Length Curse in Long Tree-Ring Chronology Development for Paleoclimatic Studies. *Holocene* 5: 229-237.

Cook E.R., Jacoby G.C. (1977): Tree-Ring Drought Relationships in Hudson Valley, New-York. *Science* 198: 399-401.

Cook E.R., Kairiukstis L.A. (1990): Methods of dendrochronology. Kluwer Academic Publishers.

Cook E.R., Peters K. (1981): The smoothing spline: a new approach to standardizing forest interior tree-ring width series for dendroclimatic studies. *Tree-Ring Bulletin* 41: 45-53.

Cook E.R., Peters K. (1997): Calculating unbiased tree-ring indices for the study of climatic and environmental change. *Holocene* 7: 361-370.

D'Arrigo R., Wilson R., Anchukaitis K.J. (2013): Volcanic cooling signal in tree ring temperature records for the past millennium. *Journal of Geophysical Research-Atmospheres* 118: 9000-9010.

D'Arrigo R., Wilson R., Jacoby G. (2006): On the long-term context for late twentieth century warming. *Journal of Geophysical Research-Atmospheres* 111.

D'Arrigo R., Wilson R., Liepert B., Cherubini P. (2008): On the 'Divergence Problem' in Northern Forests: A review of the tree-ring evidence and possible causes. *Global and Planetary Change* 60: 289-305.

de Brogniez D., Ballabio C., Stevens A., Jones R.J.A., Montanarella L., van Wesemael B. (2015): A map of the topsoil organic carbon content of Europe generated by a generalized additive model. *European Journal of Soil Science* 66: 121-134.

Drobyshev I., Niklasson M., Linderholm H.W., Seftigen K., Hickler T., Eggertsson O. (2011): Reconstruction of a regional drought index in southern Sweden since AD 1750. *Holocene* 21: 667-679.

Düthorn E., Holzkämper S., Timonen M., Esper J. (2013): Influence of micro-site conditions on tree-ring climate signals and trends in central and northern Sweden. *Trees* 27: 1395-1404.

Düthorn E., Lindén J., Gläser S., Timonen M., Esper J. (2014) Heterogeneity in the climate signal strength of Pinus sylvestris tree-ring chronologies in Southern Finland. Paper presented at the TRACE, Viterbo,

Düthorn E., Schneider L., Günther B., Gläser S., Esper J. (2015a): Ecological and climatological signals in tree-ring width and density chronologies along a latitudinal boreal transect. *Scandinavian Journal of Forest Research*: in press.

Düthorn E., Schneider L., Konter O., Schön P., Timonen M., Esper J. (2015b): On the hidden significance of differing micro-sites on tree-ring based climate reconstructions. *Silva Fennica* 49.

Erhart R.R. (1972): Climates of Northern and Western Europe - Wallen,Cc. *Professional Geographer* 24: 179-180.

Eronen M., Hyvarinen H., Zetterberg P. (1999): Holocene humidity changes in northern Finnish Lapland inferred from lake sediments and submerged Scots pines dated by tree-rings. *Holocene* 9: 569-580.

Eronen M., Zetterberg P., Briffa K.R., Lindholm M., Merilainen J., Timonen M. (2002): The supra-long Scots pine tree-ring record for Finnish Lapland: Part 1, chronology construction and initial inferences. *Holocene* 12: 673-680.

Esper J., Benz M., Pederson N. (2012a): Influence of wood harvest on tree-ring time-series of Picea abies in a temperate forest. *Forest Ecology and Management* 284: 86-92.

Esper J., Büntgen U., Luterbacher J., Krusic P.J. (2013a): Testing the hypothesis of post-volcanic missing rings in temperature sensitive dendrochronological data. *Dendrochronologia* 31: 216-222.

Esper J., Büntgen U., Timonen M., Frank D.C. (2012b): Variability and extremes of northern Scandinavian summer temperatures over the past two millennia. *Global and Planetary Change* 88-89: 1-9.

Esper J., Cook E.R., Krusic P.J., Peters K., Schweingruber F.H. (2003): Tests of the RCS method for preserving low-frequency variability in long tree-ring chronologies. *Tree-Ring Research* 59: 81-98.

Esper J., Cook E.R., Schweingruber F.H. (2002): Low-frequency signals in long tree-ring chronologies for reconstructing past temperature variability. *Science* 295: 2250-2253.

Esper J., Düthorn E., Krusic P.J., Timonen M., Büntgen U. (2014): Northern European summer temperature variations over the Common Era from integrated tree-ring density records. *Journal of Quaternary Science*.

Esper J., Frank D., Büntgen U., Verstege A., Hantemirov R.M., Kirdyanov A.V. (2010): Trends and uncertainties in Siberian indicators of 20th century warming. *Global Change Biology* 16: 386-398.

Esper J., Frank D.C., Timonen M., Zorita E., Wilson R.J.S., Luterbacher J., Holzkamper S., Fischer N. et al. (2012c): Orbital forcing of tree-ring data. *Nature Climate Change* 2: 862-866.

Esper J., Frank D.C., Wilson R.J.S., Briffa K.R. (2005a): Effect of scaling and regression on reconstructed temperature amplitude for the past millennium. *Geophysical Research Letters* 32.

Esper J., Krusic P.J., Peters K., Frank D. (2009): Exploration of long-term growth changes using the tree-ring detrending program "Spotty". *Dendrochronologia* 27: 75-82.

Esper J., Niederer R., Bebi P., Frank D. (2008): Climate signal age effects - Evidence from young and old trees in the Swiss Engadin. *Forest Ecology and Management* 255: 3783-3789.

Esper J., Schneider L., Krusic P.J., Luterbacher J., Büntgen U., Timonen M., Sirocko F., Zorita E. (2013b): European summer temperature response to annually dated volcanic eruptions over the past nine centuries. *Bulletin of Volcanology* 75.

Esper J., Wilson R.J.S., Frank D.C., Moberg A., Wanner H., Luterbacher J. (2005b): Climate: past ranges and future changes. *Quaternary Science Reviews* 24: 2164-2166.

FAO (2010): Global Forest Resources Assessment 2010. *FAO Forestry Paper* 163.

Frank D., Esper J. (2005): Temperature reconstructions and comparisons with instrumental data from a tree-ring network for the European Alps. *International Journal of Climatology* 25: 1437-1454.

Frank D., Esper J., Cook E.R. (2007): Adjustment for proxy number and coherence in a large-scale temperature reconstruction. *Geophysical Research Letters* 34.

Franke J., Frank D., Raible C.C., Esper J., Bronnimann S. (2013): Spectral biases in tree-ring climate proxies. *Nature Climate Change* 3: 360-364.

Fritts H.C. (1976): Tree rings and climate. Academic Press.

Glenz C., Schlaepfer R., Iorgulescu I., Kienast F. (2006): Flooding tolerance of Central European tree and shrub species. *Forest Ecology and Management* 235: 1-13.

Gouirand I., Linderholm H.W., Moberg A., Wohlfarth B. (2008): On the spatiotemporal characteristics of Fennoscandian tree-ring based summer temperature reconstructions. *Theoretical and Applied Climatology* 91: 1-25.

Grissino-Mayer H.D., Fritts H.C. (1997): The International Tree-Ring Data Bank: an enhanced global database serving the global scientific community. *The Holocene* 7: 235-238.

Grudd H. (2008): Tornetrask tree-ring width and density AD 500-2004: a test of climatic sensitivity and a new 1500-year reconstruction of north Fennoscandian summers. *Climate Dynamics* 31: 843-857.

Grudd H., Briffa K.R., Karlen W., Bartholin T.S., Jones P.D., Kromer B. (2002): A 7400-year tree-ring chronology in northern Swedish Lapland: natural climatic variability expressed on annual to millennial timescales. *Holocene* 12: 657-665.

Gunnarson B.E., Borgmark A., Wastegard S. (2003): Holocene humidity fluctuations in Sweden inferred from dendrochronology and peat stratigraphy. *Boreas* 32: 347-360.

Gunnarson B.E., Linderholm H.W., Moberg A. (2011): Improving a tree-ring reconstruction from west-central Scandinavia: 900 years of warm-season temperatures. *Climate Dynamics* 36: 97-108.

Harris I., Jones P.D., Osborn T.J., Lister D.H. (2014): Updated high-resolution grids of monthly climatic observations - the CRU TS3.10 Dataset. *International Journal of Climatology* 34: 623-642.

Hartl-Meier C., Dittmar C., Zang C., Rothe A. (2014a): Mountain forest growth response to climate change in the Northern Limestone Alps. *Trees-Structure and Function* 28: 819-829.

Hartl-Meier C., Zang C., Dittmar C., Esper J., Gottlein A., Rothe A. (2014b): Vulnerability of Norway spruce to climate change in mountain forests of the European Alps. *Climate Research* 60: 119-132.

Helama S., Arentoft B.W., Collin-Haubensak O., Hyslop M.D., Brandstrup C.K., Makela H.M., Tian Q.H., Wilson R. (2013): Dendroclimatic signals deduced from riparian versus upland forest interior pines in North Karelia, Finland. *Ecological Research* 28: 1019-1028.

Helama S., Lindholm M. (2003): Droughts and rainfall in south-eastern Finland since AD 874, inferred from Scots pine ring-widths. *Boreal Environment Research* 8: 171-183.

Helama S., Lindholm M., Merilainen J., Timonen M., Eronen M. (2005a): Multicentennial ring-width chronologies of Scots pine along a north-south gradient across Finland. *Tree-Ring Research* 61: 21-32.

Helama S., Lindholm M., Timonen M., Eronen M. (2004): Detection of climate signal in dendrochronological data analysis: a comparison of tree-ring standardization methods. *Theoretical and Applied Climatology* 79: 239-254.

Helama S., Lindholm M., Timonen M., Merilainen J., Eronen M. (2002): The supra-long Scots pine tree-ring record for Finnish Lapland: Part 2, interannual to centennial variability in summer temperatures for 7500 years. *Holocene* 12: 681-687.

Helama S., Timonen M., Lindholm M., Merilainen J., Eronen M. (2005b): Extracting long-period climate fluctuations from tree-ring chronologies over timescales of centuries to millennia. *International Journal of Climatology* 25: 1767-1779.

Helama S., Vartiainen M., Holopainen J., Makela H.M., Kolstrom T., Merilainen J. (2014): A palaeotemperature record for the Finnish Lakeland based on microdensitometric variations in tree rings. *Geochronometria* 41: 265-277.

Hellmann L., Agafonov L., Churakova O., Düthorn E., Esper J., Kirdyanov A., Knorre A.A., Matskovsky V.V. et al. (in rev): On the importance of boreal reference chronologies for provenancing Arctic driftwood. *Dendrochronologia*.

Hellmann L., Tegel W., Eggertsson O., Schweingruber F.H., Blanchette R., Kirdyanov A., Gartner H., Büntgen U. (2013): Tracing the origin of Arctic driftwood. *Journal of Geophysical Research-Biogeosciences* 118: 68-76.

Hellmann L., Tegel W., Kirdyanov A.V., Eggertsson O., Esper J., Agafonov L., Nikolaev A.N., Knorre A.A. et al. (2015): Timber logging in central Siberia is the main source for recent Arctic driftwood. *Arctic Antarctic and Alpine Research* 47: 449-460.

Holmes R.L. (1983): Computer-assisted quality control in tree-ring dating and measurement. *Tree-Ring Bulletin* 43: 69-78.

Holtmeier F.K., Broll G. (2005): Sensitivity and response of northern hemisphere altitudinal and polar treelines to environmental change at landscape and local scales. *Global Ecology and Biogeography* 14: 395-410.

Kellomaki S., Karjalainen T., Vaisanen H. (1997): More timber from boreal forests under changing climate? *Forest Ecology and Management* 94: 195-208.

Kienast F., Schweingruber F.H., Bräker O.U., Schär E. (1987): Tree-ring studies on conifers along ecological gradients and the potential of single-year analyses. *Canadian Journal of Forest Research* 17: 683-696.

Kirchhefer A.J. (2001): Reconstruction of summer temperatures from tree-rings of Scots pine (Pinus sylvestris L.) in coastal northern Norway. *Holocene* 11: 41-52.

Kobe R.K., Pacala S.W., Silander J.A., Canham C.D. (1995): Juvenile Tree Survivorship as a Component of Shade Tolerance. *Ecological Applications* 5: 517-532.

Konter O., Esper J., Liebhold A., Kyncl T., Schneider L., Düthorn E., Büntgen U. (2015): Tree-ring evidence for the historical absence of cyclic larch budmoth outbreaks in the Tatra Mountains. *Trees-Structure and Function* 29: 809-814.

Körner C. (2012): Alpine Treelines. Springer.

Kottek M., Grieser J., Beck C., Rudolf B., Rubel F. (2006): World map of the Koppen-Geiger climate classification updated. *Meteorologische Zeitschrift* 15: 259-263.

Kozlowski T.T., Pallardy S.G. (1996): Physiology of Woody Plants. Elsevier Science.

Kullman L. (2013): Ecological tree line history and palaeoclimate - review of megafossil evidence from the Swedish Scandes. *Boreas* 42: 555-567.

Kultti S., Mikkola K., Virtanen T., Timonen M., Eronen M. (2006): Past changes in the Scots pine forest line and climate in Finnish Lapland: a study based on megafossils, lake sediments, and GIS-based vegetation and climate data. *Holocene* 16: 381-391.

Lenz O., Schar E., Schweingruber F.H. (1976): Methodological Problems Relative to Measurement of Density and Width of Growth Rings by X-Ray Densitogrames of Wood. *Holzforschung* 30: 114-123.

Liang E.Y., Wang Y.F., Xu Y., Liu B.M., Shao X. (2010): Growth variation in Abies georgei var. smithii along altitudinal gradients in the Sygera Mountains, southeastern Tibetan Plateau. *Trees* 24: 363-373.

Liñan I.D., Gutierrez E., Heinrich I., Andreu-Hayles L., Muntan E., Campelo F., Helle G. (2012): Age effects and climate response in trees: a multi-proxy tree-ring test in old-growth life stages. *European Journal of Forest Research* 131: 933-944.

Linderholm H.W., Björklund J.A., Seftigen K., Gunnarson B.E., Grudd H., Jeong J.H., Drobyshev I., Liu Y. (2010): Dendroclimatology in Fennoscandia - from past accomplishments to future potential. *Climate of the Past* 6: 93-114.

Linderholm H.W., Zhang P., Gunnarson B.E., Björklund J., Farahat E., Fuentes M., Rocha E., Salo R. et al. (2014): Growth dynamics of tree-line and lake-shore Scots pine (Pinus sylvestris L.) in the central Scandinavian Mountains during the Medieval Climate Anomaly and the early Little Ice Age. *Frontiers in Ecology and Evolution* 2.

Lindholm M., Eronen M., Timonen M., Merilainen J. (1999): A ring-width chronology of Scots pine from northern Lapland covering the last two millennia. *Annales Botanici Fennici* 36: 119-126.

Lindner M., Maroschek M., Netherer S., Kremer A., Barbati A., Garcia-Gonzalo J., Seidl R., Delzon S. et al. (2010): Climate change impacts, adaptive capacity, and vulnerability of European forest ecosystems. *Forest Ecology and Management* 259: 698-709.

Ljungqvist F.C. (2010): A New Reconstruction of Temperature Variability in the Extra-Tropical Northern Hemisphere during the Last Two Millennia. *Geografiska Annaler Series a-Physical Geography* 92A: 339-351.

Ljungqvist F.C., Krusic P.J., Brattstrom G., Sundqvist H.S. (2012): Northern Hemisphere temperature patterns in the last 12 centuries. *Climate of the Past* 8: 227-249.

Lough J.M., Fritts H.C. (1987): An Assessment of the Possible Effects of Volcanic-Eruptions on North-American Climate Using Tree-Ring Data, 1602 to 1900 Ad. *Climatic Change* 10: 219-239.

Mann M.E., Zhang Z.H., Hughes M.K., Bradley R.S., Miller S.K., Rutherford S., Ni F.B. (2008): Proxy-based reconstructions of hemispheric and global surface temperature variations over the past two millennia. *Proceedings of the National Academy of Sciences of the United States of America* 105: 13252-13257.

Martin-Benito D., Pederson N. (2015): Convergence in drought stress, but a divergence of climatic drivers across a latitudinal gradient in a temperate broadleaf forest. *Journal of Biogeography* 42: 925-937.

Mátyás C., Ackzell L., Samuel C.J.A. (2004): Technical Guidelines for genetic conservation and use for Scots pine (Pinus sylvestris). *EUFORGEN Technical Guidelines for Genetic Conservation and Use*.

McCarroll D., Jalkanen R., Hicks S., Tuovinen M., Gagen M., Pawellek F., Eckstein D., Schmitt U. et al. (2003): Multiproxy dendroclimatology: a pilot study in northern Finland. *Holocene* 13: 829-838.

McCarroll D., Loader N.J., Jalkanen R., Gagen M.H., Grudd H., Gunnarson B.E., Kirchhefer A.J., Friedrich M. et al. (2013): A 1200-year multiproxy record of tree growth and summer temperature at the northern pine forest limit of Europe. *Holocene* 23: 471-484.

Melvin T.M., Briffa K.R. (2008): A "signal-free" approach to dendroclimatic standardisation. *Dendrochronologia* 26: 71-86.

Melvin T.M., Grudd H., Briffa K.R. (2013): Potential bias in 'updating' tree-ring chronologies using regional curve standardisation: Re-processing 1500 years of Tornetrask density and ring-width data. *Holocene* 23: 364-373.

Messier C., Doucet R., Ruel J.C., Claveau Y., Kelly C., Lechowicz M.J. (1999): Functional ecology of advance regeneration in relation to light in boreal forests. *Canadian Journal of Forest Research-Revue Canadienne De Recherche Forestiere* 29: 812-823.

Mitchell T.D., Jones P.D. (2005): An improved method of constructing a database of monthly climate observations and associated high-resolution grids. *International Journal of Climatology* 25: 693-712.

Moberg A., Sonechkin D.M., Holmgren K., Datsenko N.M., Karlen W., Lauritzen S.E. (2006): Highly variable Northern Hemisphere temperatures reconstructed from low- and high-resolution proxy data (vol 433, pg 613, 2005). *Nature* 439: 1014-1014.

Morgan P., Aplet G.H., Haufler J.B., Humphries H.C., Margaret M.M., Wilson W.D. (1994): Historical range of variability: a useful tool for evaluationg ecosystem change. In: Sampson, RL, Adams, DL (eds): Assessing Forest Ecosystem Health in the Inland West: Proceedings of the American Forest Scientific Workshop. Hawthorn Press. 87-111.

Moser L., Fonti P., Büntgen U., Esper J., Luterbacher J., Franzen J., Frank D. (2010): Timing and duration of European larch growing season along altitudinal gradients in the Swiss Alps. *Tree Physiology* 30: 225-233.

Naiman R.J., Décamps H. (1997): The ecology of interfaces: Riparian zones. *Annual Review of Ecology and Systematics* 28: 621-658.

Nehrbass-Ahles C., Babst F., Klesse S., Nötzli M., Bouriaud O., Neukom R., Dobbertin M., Frank D. (2014): The influence of sampling design on tree-ring based quantification of forest growth. *Global Change Biology*: n/a-n/a.

Nemani R.R., Keeling C.D., Hashimoto H., Jolly W.M., Piper S.C., Tucker C.J., Myneni R.B., Running S.W. (2003): Climate-driven increases in global terrestrial net primary production from 1982 to 1999. *Science* 300: 1560-1563.

Nicolussi K., Kaufmann M., Melvin T.M., van der Plicht J., Schiessling P., Thurner A. (2009): A 9111 year long conifer tree-ring chronology for the European Alps: a base for environmental and climatic investigations. *Holocene* 19: 909-920.

Plummer C.T., Curran M.A.J., van Ommen T.D., Rasmussen S.O., Moy A.D., Vance T.R., Clausen H.B., Vinther B.M. et al. (2012): An independently dated 2000-yr volcanic record from Law Dome, East Antarctica, including a new perspective on the dating of the 1450s CE eruption of Kuwae, Vanuatu. *Climate of the Past* 8: 1929-1940.

Rossi S., Cairo E., Krause C., Deslauriers A. (2015): Growth and basic wood properties of black spruce along an alti-latitudinal gradient in Quebec, Canada. *Annals of Forest Science* 72: 77-87.

Rossi S., Deslauriers A., Anfodillo T. (2006): Assessment of cambial activity and xylogenesis by microsampling tree species: An example at the alpine timberline. *Iawa Journal* 27: 383-394.

Ryan M.G., Yoder B.J. (1997): Hydraulic limits to tree height and tree growth. *Bioscience* 47: 235-242.

Rydval M., Larsson L.A., McGlynn L., Gunnarson B.E., Loader N.J., Young G.H.F., Wilson R. (2014): Blue intensity for dendroclimatology: Should we have the blues? Experiments from Scotland. *Dendrochronologia* 32: 191-204.

Schmitt U., Jalkanen R., Eckstein D. (2004): Cambium dynamics of Pinus sylvestris and Betula spp. in the northern boreal forest in Finland. *Silva Fennica* 38: 167-178.

Schneider L., Esper J., Timonen M., Büntgen U. (2014): Detection and evaluation of an early divergence problem in northern Fennoscandian tree-ring data. *Oikos* 123: 559-566.

Schweingruber F.H. (1983): Der Jahrring: Standort, Methodik, Zeit und Klima in der Dendrochronologie. P. Haupt.

Schweingruber F.H., Bartholin T., Schar E., Briffa K.R. (1988): Radiodensitometric-Dendroclimatological Conifer Chronologies from Lapland (Scandinavia) and the Alps (Switzerland). *Boreas* 17: 559-566.

Schweingruber F.H., Braker O.U., Schar E. (1979): Dendro-Climatic Studies on Conifers from Central-Europe and Great-Britain. *Boreas* 8: 427-452.

Schweingruber F.H., Fritts H.C., Bräker O.U., Drew L.G., Schär E. (1978): The X-ray technique as applied to dendroclimatology. *Tree-Ring Bulletin* 38: 61-91.

Seo J.W., Eckstein D., Jalkanen R., Schmitt U. (2011): Climatic control of intra- and inter-annual wood-formation dynamics of Scots pine in northern Finland. *Environmental and Experimental Botany* 72: 422-431.

Sigl M., McConnell J.R., Layman L., Maselli O., McGwire K., Pasteris D., Dahl-Jensen D., Steffensen J.P. et al. (2013): A new bipolar ice core record of volcanism from WAIS Divide and NEEM and implications for climate forcing of the last 2000 years. *Journal of Geophysical Research-Atmospheres* 118: 1151-1169.

Skrøppa T. (2003): Technical guidelines for genetic conservation and use for Norway spruce Picea abies. *EUFORGEN Technical Guidelines for Genetic Conservation and Use*.

Solomon S., Intergovernmental Panel on Climate Change., Intergovernmental Panel on Climate Change. Working Group I. (2007): Climate change 2007 : the physical science basis : contribution of Working Group I to the Fourth Assessment Report of the Intergovernmental Panel on Climate Change. Cambridge University Press.

Speer J.H. (2010): Fundamentals of tree-ring research. University of Arizona Press.

Swetnam T.W., Allen C.D., Betancourt J.L. (1999): Applied historical ecology: Using the past to manage for the future. *Ecological Applications* 9: 1189-1206.

Sykes M.T., Prentice I.C. (1996): Climate change, tree species distributions and forest dynamics: A case study in the mixed conifer northern hardwoods zone of northern Europe. *Climatic Change* 34: 161-177.

Tegel W., Vanmoerkerke J., Büntgen U. (2010): Updating historical tree-ring records for climate reconstruction. *Quaternary Science Reviews* 29: 1957-1959.

Tejedor E., de Luis M., Cuadrat J.M., Esper J., Saz M.A. (2015): Tree-ring based drought reconstruction in the Iberian Range (East of Spain) since 1694. *International Journal of Biometeorology*.

Tikkanen M. (2002): Long-term changes in lake and river systems in Finland. *Fennia* 180: 31-42.

Toth G., Jones A., Montanarella L. (2013): The LUCAS topsoil database and derived information on the regional variability of cropland topsoil properties in the European Union. *Environmental Monitoring and Assessment* 185: 7409-7425.

Trachsel M., Kamenik C., Grosjean M., McCarroll D., Moberg A., Brazdil R., Büntgen U., Dobrovolny P. et al. (2012): Multi-archive summer temperature reconstruction for the European Alps, AD 1053-1996. *Quaternary Science Reviews* 46: 66-79.

Trouet V., Esper J., Graham N.E., Baker A., Scourse J.D., Frank D.C. (2009): Persistent Positive North Atlantic Oscillation Mode Dominated the Medieval Climate Anomaly. *Science* 324: 78-80.

Vaganov E.A., Hughes M.K., Kirdyanov A.V., Schweingruber F.H., Silkin P.P. (1999): Influence of snowfall and melt timing on tree growth in subarctic Eurasia. *Nature* 400: 149-151.

Vicente-Serrano S.M., Beguería S., López-Moreno J.I., Angulo-Martínez M., El Kenawy A.M. (2010): A new global 0.5° gridded dataset (1901-2006) of a multiscalar drought index: comparison with current drought index datasets based on the Palmer Drought Severity Index. *Journal of Hydrometeorology* 11: 1033-1043.

Wigley T.M.L., Briffa K.R., Jones P.D. (1984): On the Average Value of Correlated Time-Series, with Applications in Dendroclimatology and Hydrometeorology. *Journal of Climate and Applied Meteorology* 23: 201-213.

Wilson R.J.S., Luckman B.H. (2003): Dendroclimatic reconstruction of maximum summer temperatures from upper treeline sites in Interior British Columbia, Canada. *Holocene* 13: 851-861.

Wilson R.J.S., Luckman B.H., Esper J. (2005): A 500 year dendroclimatic reconstruction of spring-summer precipitation from the lower Bavarian Forest region, Germany. *International Journal of Climatology* 25: 611-630.

Zang C., Biondi F. (2014): treeclim: an R package for the numerical calibration of proxy-climate relationships. *Ecography*: n/a-n/a.

List of Figures

Figures

Tables

Supplement material